ROLE OF HYPOXIA AND HYPOXIA-INDUCED FACTORS IN THE DEVELOPMENT OF BREAST CANCER BRAIN METASTASIS

A Dissertation

by

GINA FLORENTINA LUNGU

Submitted to the Office of Graduate Studies of
Texas A&M University
in partial fulfillment of the requirements for the degree of

DOCTOR OF PHILOSOPHY

August 2008

Major Subject: Veterinary Microbiology

ROLE OF HYPOXIA AND HYPOXIA-INDUCED FACTORS IN THE DEVELOPMENT OF BREAST CANCER BRAIN METASTASIS

A Dissertation

by

GINA FLORENTINA LUNGU

Submitted to the Office of Graduate Studies of
Texas A&M University
in partial fulfillment of the requirements for the degree of

DOCTOR OF PHILOSOPHY

Approved by:

Chair of Committee,	Gheorghe Stoica
Committee Members,	Louise Abbott
	Jane Welsh
	David Caldwell
Head of Department,	Gerald Bratton

August 2008

Major Subject: Veterinary Microbiology

ABSTRACT

Role of Hypoxia and Hypoxia-induced Factors in the Development of

Breast Cancer Brain Metastasis.

(August 2008)

Gina Florentina Lungu, B.S., University of Bucharest;

M.S., Texas Woman's University

Chair of Advisory Committee: Dr. Gheorghe Stoica

Here we studied the role of hypoxia and hypoxia-induced factors in the development of breast cancer brain metastasis by using ENU1564, a carcinogen-induced mammary adenocarcinoma cell line.

We detected hypoxia noninvasively by using a novel spectroscopic photoacoustic tomography technology (SPAT). Sprague-Dawley rats inoculated intracranially with ENU1564, a carcinogen-induced rat mammary adenocarcinoma cell line, were imaged with SPAT three weeks post inoculation. Proteins important for tumor angiogenesis and invasion were detected in hypoxic brain foci identified by SPAT and were elevated compared with control brain. We showed that HIF-1α, MMP-9, VEGF-A, and VEGFR2 (Fkl-1) protein and mRNA expression levels were higher ($P < 0.05$) in brain tumor tissues compared to normal brain. We also found an increased expression of HIF-1α proteins, MMP-9, VEGF-A and VEGFR2 mRNA and proteins in hypoxic ENU1564 cells *in vitro*. We also demonstrated the involvement of PI3K-Akt pathway in hypoxic regulation of MMP-9 and VEGF but not VEGFR2 by using specific PI3K inhibitor. Using MEK1/2

inhibitor we showed that hypoxic regulation of MMP-9, VEGF-A and VEGFR2 also involve MEK1/2-ERK pathway.

We also investigated the effect of fibroblast growth factor-1 (FGF-1), one of the factors known to be upregulated by hypoxia, on the expression of MMP-9 in ENU1564 cell line. We observed that FGF-1 induces an increase in MMP-9 mRNA, protein, and activity in ENU1564 cells. Next, we investigated the role of components of PI3K-Akt and MEK1/2-ERK signaling pathways in our system. We demonstrated that FGF-1 increases Akt phosphorylation, triggers nuclear translocation of NF-κBp65, and enhances degradation of cytoplasmic IκBα. Pretreatment of cells with LY294002, a PI3K inhibitor, significantly inhibited MMP-9 protein expression in FGF-1-treated cells. Conversely, our data showed that FGF-1 increases ERK phosphorylation in ENU1564 cells, increases c-jun and c-fos mRNA expression in a time-dependent manner, and triggers nuclear translocation of c-jun. Pretreatment of cells with PD98059, a MEK1/2 inhibitor significantly inhibited MMP-9 protein expression in FGF-1 treated cells. Finally, we observed increased DNA binding of NF-κB and AP-1 in FGF-1-treated cells and that mutation of either NF-κB or AP-1 response elements prevented MMP-9 promoter activation by FGF-1.

DEDICATION

To my family

ACKNOWLEDGEMENTS

This work was carried out at the Department of Veterinary Pathobiology, College of Veterinary Medicine at Texas A&M University from January 2005 to April 2008. This work was supported by a National Institute of Health grant (No. R01-N5046214-01), for which I express my gratitude.

I am most grateful to my committee chair, Dr. George Stoica, for his enthusiasm, his open-mindedness and his encouraging support, not to mention his vast knowledge which he shared whenever needed.

I would like to thank my committee members, Dr. Louise Abbott, Dr. Jane Welsh, and Dr. David Caldwell, for their guidance and support throughout the course of this research.

Thanks also to my friends and colleagues and the department faculty and staff for making my time at Texas A&M University a great experience.

Last, but not least, I am very grateful to my husband, Christian, and my son, Andrei, for their patience, love and support, and for filling my life with things more important than science.

TABLE OF CONTENTS

CHAPTER Page

LIST OF FIGURES

Page

Page

LIST OF TABLES

CHAPTER I

INTRODUCTION

Overview of tumor hypoxia

The metastatic process of breast cancer (BC) has been subjected to intense scrutiny. We know today that the brain is one of the most common organs affected in the spread of BC that ultimately results in fatal overcome of the disease. More than 30% of breast cancer patients develop brain metastasis [1]. Many theories have been developed to study and understand the metastatic behavior. Factors like neoplastic cells, molecular and genetic characteristics [2] and biologic environment are thought to be determinants in the metastatic process. The process of breast cancer progression is characterized by rapid cellular growth, accompanied by alteration of the microenvironment of the tumor cells. Alterations in the cellular microenvironment are due to an inadequate oxygen level, and the resultant hypoxia [3].

Hypoxia, or lack of oxygen to the tissues, plays a significant role in tumor biology by altering the pattern of gene expression. Under hypoxia, a number of important proteins are up-regulated, and many of these contribute to cancer invasion and metastasis.

This dissertation follows the style of Clinical & Experimental Metastasis.

The question is why there is an inadequate oxygen supply to the tumor? The answer lies in the fact that the newly formed tumor must form their own vascular network and blood supply either by the process called angiogenesis or by incorporating preexisting host vessels [4]. The fact is that the newly formed vascular network differs from the normal tissue and display lots of abnormalities including tortuous architecture, incomplete or absent endothelial lining and basement membranes which lead to irregular and sluggish blood flow [3, 5]. All this will diminish the delivery of oxygen (and nutrients) to the tumor cells, with the resultant development of hypoxia or even anoxia [5].

Hypoxia has been shown to provide an important prognostic value in clinical trials involving radiation and chemotherapy. It is usually associated with adverse clinical outcomes and reduced patient survival [6]. Tumor hypoxia has been recognized for many years as a potential therapeutic problem because of its adverse impact on the effectiveness of radiation therapy. According to previous studies, tumor hypoxia has emerged as a major factor that influences tumor proliferation and invasion [7], and malignant progression associated with tumor hypoxia appears to be mediated by several mechanisms, including changes in gene expression regulation and activation of oncogenes.

Although tissue hypoxia usually occurs very early in tumor development due to inadequate blood supply, hypoxia remains a constant feature of these tumors even after neovascularization [8]. A series of studies are currently underway targeting molecular processes related to tumor hypoxia in tumor cells. Since the molecular mechanisms are

becoming more clear, future therapies may find new target molecules in tumor cells, finally leading to more and more efficient treatment of aggressive and metastasizing tumors.

Animal model and cell lines

Different animal models have been used for *in vivo* study of the mechanisms of cancer metastasis and for the role of matrix metalloproteinases (MMPs) and other proteins in the development of cancer. Most of these studies describe lung, bone and/or lymph node metastasis and are usually concurrent with the studies conducted on human patients that correlated MMPs with increased tumor invasion and metastatic behavior [9, 10, 11].

In our laboratory we have developed a syngeneic model to study distant metastasis of breast cancer. Using this model Mendes et al., showed that MMP-2, -3, and -9 are involved in mammary adenocarcinoma metastasis to the brain [12]. Mendes, by using 40 day old BD-IV rats inoculated with $1x10^4$ ENU1564 cells via left ventricle, characterized the metastasis of breast cancer cells in numerous tissues such as bone, lung, kidney and brain.

The ENU1564 cell line used in our study is a highly metastatic breast cancer cell line originated from N-ethyl-N-nitrosourea (ENU)-induced mammary adenocarcinoma in a female Berlin-Druckrey IV (BD-IV) rat **(Figure 1).** This cell line is highly metastatic to brain and bone tissues [13].

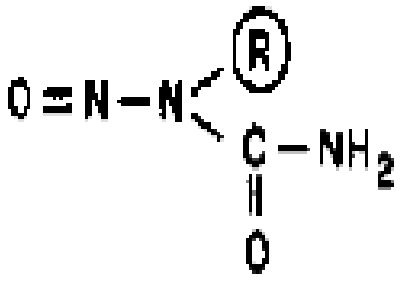

Figure 1. Chemical structure of N-ethyl N-Nitrosurea (ENU).

ENU is a carcinogenic substance that acts as a specific alkylating agent of DNA and RNA nucleotide bases [14]. It has high affinity for oxygen causing frequent alkylations of the 2'-O ring in DNA phosphodiesteres and 2'-O of RNA riboses. [15]. All 2'-O from DNA bases can react with ENU and ring OH is also susceptible to ENU ethylation [16]. Additionally, ethylation can also occur in a ring N position. Ethylation of 7'-N causes rapid depurination and subsequent DNA chain breakage. Alkylation of 4'-O of uridine or thymidine causes mispairing. Alkylation of 2'-O causes depyrimidiazation and possible deletion [17]. *In vivo* the bases that are more susceptible to ethylation are thymidine and guanidine, followed by cytosine [18, 19, 20] **(Figure 2).**

Throughout this study, we used three-week old Sprague-Dawley (SD) rats obtained from a colony maintained at Texas A& M University. All animal experiments were done in accordance with protocol approved by our Institutional Animal Care and Use Committee (IACHC) and following National Institute of Health (NIH) guidelines for animal welfare.

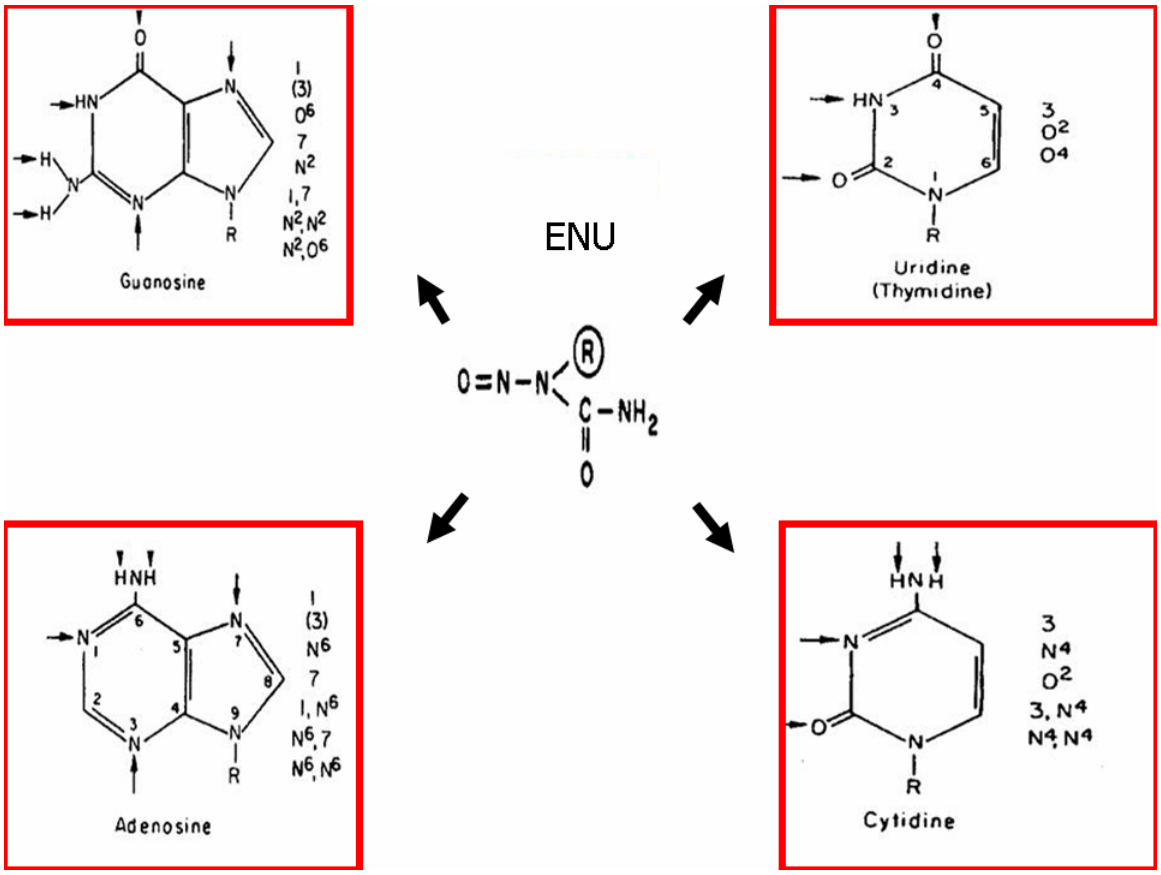

Figure 2. DNA and RNA base alkylation sites by N-ethyl N-Nitrosurea.

In our study, SD rats were inoculated with tumor cells (ENU1564) intracranially into the forebrain since we were mainly interested in locating tumor implant and detecting tumor hypoxia inside the brain using SPAT, as an assessment of this new technology. The mechanism of tumor invasion may apply to tumor metastasis because metastasis mediators are involved in both of these processes. In a pilot experiment we

also inoculated SD rats with ENU1564 ($1x10^4$) cells via the left ventricle and observed that they consistently produced brain metastasis **(Figure 3).**

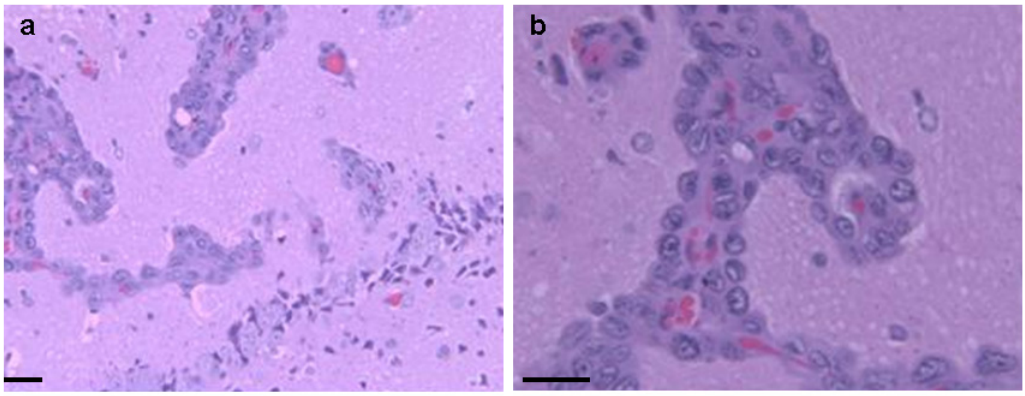

Figure 3. Histology of metastatic foci in ENU1564-SD rat. (**a, b**) H&E staining showing the presence of metastatic tumor in the rat brain which also shows increased tumor vascularization (red, blood vessels); Bars indicate 200 µm.

Overview of hypoxia-induced factors

Hypoxia areas are common features of rapidly growing malignant tumors and their metastasis. Due to an inadequate blood supply, tissue hypoxia is supposed to occur very early during tumor development beginning at a tumor diameter of a few millimeter [21]. Hypoxia not only accounts for cell necrosis but has also a strong impact on tumor cell biology [22]. The hypoxic tumor cell response is very important for the

understanding of tumor progression. A variety of proteins important in tumor cell progression and metastasis were found to be up-regulated under hypoxia.

The master regulator of hypoxic environment is hypoxia-inducible factor 1 α (HIF-1 α). In the presence of oxygen, HIF-1α protein is destroyed rapidly by the proteasome so the steady-state levels are very low [22]. In hypoxia, this process is suppressed, allowing activation of the transcriptional response. Under hypoxic conditions, the transcriptional activator HIF-1 α is stable and able to stimulate the expression of hypoxia-induced genes important in tumor migration and metastasis like metalloproteinases, vascular endothelial growth factor, fibroblast growth factors and others **(Figure 4).** HIF-1α expression is commonly observed at the invading margins of human cancers and tumor cells exposed to hypoxic conditions showed enhanced metastatic ability [23].

It is well established that local growth and metastasis of a large variety of malignant tumors are dependent on neovascularization. Several studies demonstrated that HIF-1α activity resulted in the transcriptional regulation of may angiogenic factors including VEGF-A, VEGFR's, IL-8, angiopoetin 2, and inducible nitric oxide synthase (iNOS) [23,24]. There are also several protein kinases that are activated by hypoxia and may contribute to tumor metastasis. Among those are mitogen activated protein kinases (MAPK) family members stress-activated protein kinases (SAPKs)/c-Jun N-terminal kinases (JNKs) and extracellular signal-regulated kinases 1 and 2 (ERK1/2) [25], but also phosphoinositide-3 kinase (PI3K-Akt) pathway. Several metalloproteinases as MMP-2, MMP-9 and MT1-MMP were found to be up-regulated under hypoxic

conditions [24] and those proteins play a crucial in tumor metastasis. MMPs play a key role in angiogenesis by degrading the extracellular matrix and permitting the migration and tube formation of endothelial cells.

Based on the current knowledge about its role in hypoxia-induced genes expression and the mechanisms of molecular regulation, HIF-1α might be an interesting target for future tumor therapy.

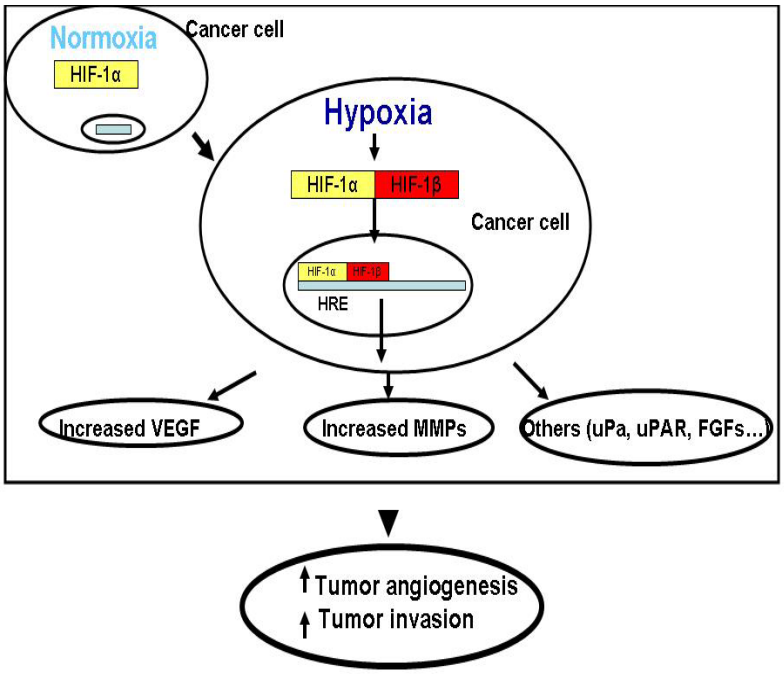

Figure 4. HIF-1α regulates several proteins important in tumor invasion and metastasis. Hypoxia-inducible factor 1 α (HIF-1α) can regulate several proteins important in tumor migration and metastasis. Under normoxia, HIF-1α is rapidly degraded but under hypoxic conditions HIF-1α is stable and forms heterodimer with the HIF-1β. The heterodimer translocates to the nucleus where it regulates the expression of hypoxia-induced genes.

Overview of matrix metalloproteinases

Matrix metalloproteinases (MMP) are structurally related endopeptidases that have multiple biological roles including the degradation of the extracellular matrix (ECM). There are 24 mammalian MMP members (MMP 1-28), each a product of a different gene which encode for zinc-dependent and calcium dependent proteases that are endopeptidases [26]. There are in fact 23 mouse MMPs and 24 human MMPs [27]. There are also two other large families of proteases that have major roles in extracellular proteolysis, the ADAM family (a disintegrin and metalloproteinase domain, with about 33 members in humans) and the ADAMTS family (a disintegrin-like and metalloproteinase domain (reprolysin type) with thrombospondin type I repeats, with about 19 members in humans).

Numerous classifications of MMPs can be made. Based on their solubility they can be divided in two major groups. Based on their substrates, they can be devided in several groups. They are known to degrade a large array of substrates such as Collagens (C), Fibronectin (FN), Cartilage oligomeric protein (COMP), Laminin (LN) and Proteoglycan (PG) [26] **(Table 1).**

They can also be classified according to their solubility. (A) Soluble type MMPs; include collagenases, stromelysins, gelatinases and matrilysins. (B) Membrane-anchored metalloproteinases; include Type II and type II types.

Table 1. MMP classification.

Protein	MMP	MW (kDa)	Substrate(s)
Soluble Type			
Collagenase			
Collagenase 1	MMP1	52/41	C-II, II, III, X
Collagenase 2	MMP8	5/64	C-I, II, III
Collagenase 3	MMP13	65/55	C-I, II, IV, X, XIV, FN, aggrecan, tenascin
Stromelysin			
Stromelysin 1	MMP3	57/45,28	PG, FN, C-III, IV, VII, IX, Gelatin, LN
Stromelysin 2	MMP10	56/47,24	C-III, IV, V, gelatin, PG, FN
Gelatinase			
Gelatinase A	MMP2	72/67	Gelatin, C-IV, FN, PG, LN
Gelatinase B	MMP9	92/67	Gelatin, C-III, IV, V, elastin
Matrylisin			
Matrylisin 1	MMP7	28/19	Gelatin, C-IV, FN, PG, LN
Matrylisin 2	MMP26	29/19	Gelatin, C-IV, FN, fibrinogen
Others			
Stromelysin 3	MMP11	58/28	Gelatin, PG, LN, FN
Epilysin	MMP28	56/45	Casein
Not named	MMP19	57	Gelatin, aggrecan, COMP, LN, nidogen, tenascin, C-IV, FN
Matalloelastase	MMP12	54/45,22	Elastin
Enamelysin	MMP20	54/43	Amelogenin, aggrecan, COMP, FN, CIV, LN
<u>Membrane-anchored</u>			
Type I transmem-brane-type			
MT1-MMP	MMP14	66/60	C I, II, III, gelatin, PG, FN
MT2-MMP	MMP15	68/62	FN, aggrecan, nidogen, tenascin, perlecan, LN
MT3-MMP	MMP16	64/55	C-III, FN, gelatin
MT5-MMP	MMP24	73/64	PG
GPI-type			
MT4-MMP	MMP14	71/67	Fibrin, fibrinogen
MT6-MMP	MMP25	62/58	Gelatin
Type II transmem-brane-type			

Metalloproteinases are composed by a pre-catalytic, a pro-catalytic domain, a fibronectin-like domain, a domain for binding to zinc and a homeopexin domain [28] **(Figure 5).**

Figure 5. Domain structure of MMP proteins.

The prodomain keeps the enzyme latent using the thiol group of a highly conserved cysteine at its carboxyl terminus. This conserved cysteine acts as an inactivating ligand for the catalytic zinc atom in the active state, resulting in the exclusion of water and rendering the enzyme inactive. In order to be activated a cystein residue that inactivates ligand binding to the zinc catalytic site must be removed **(Figure 6).**

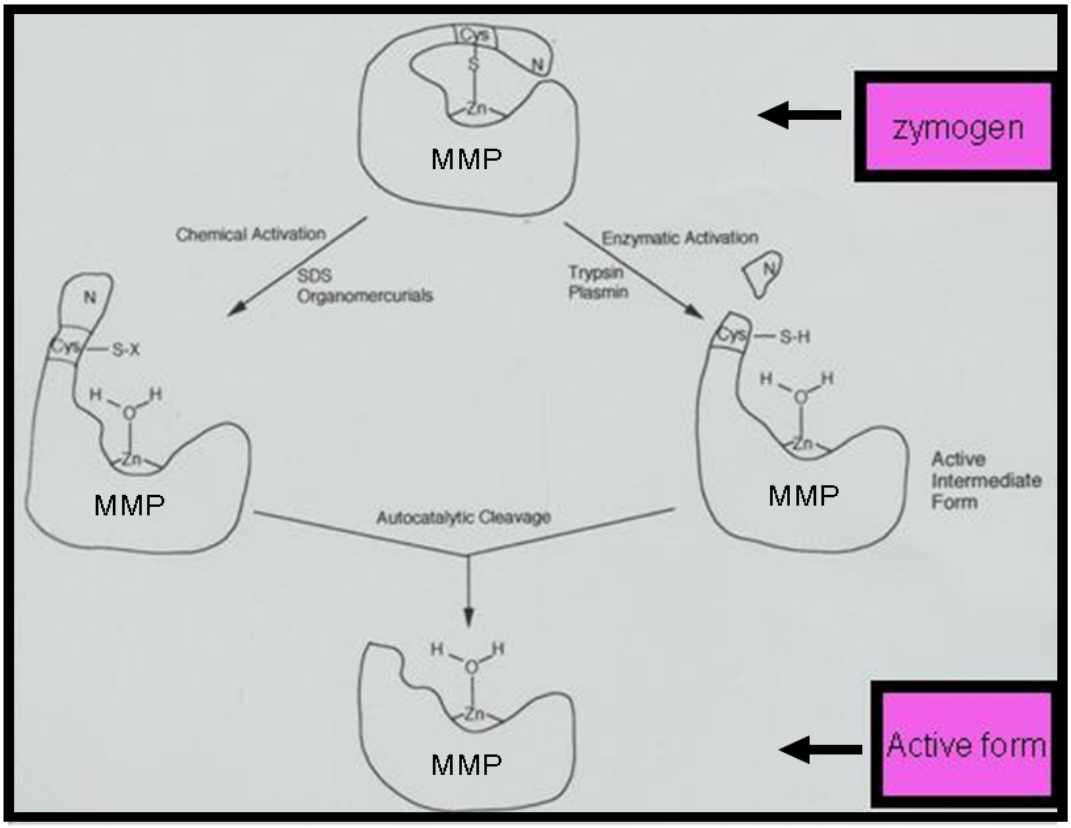

Figure 6. Mechanism of MMPs activation.

This can be done by conformational change or proteolysis accomplished by plasmin or other MMPs. MMPs are responsible for the turnover of the ECM that is rich in growth factors and other bioactive molecules and in this way contribute to numerous physiological and pathologic processes. Matrix metalloproteinases have multiple important roles in cancer development.

(A) MMPs are related to tumor angiogenesis;

(B) MMPs are crucial in degradation of basement membrane and extracellular matrix **(Figure 7);**

(C) MMPs are related to tumor invasion and metastasis;

(D) MMPs are correlated with cell proliferation.

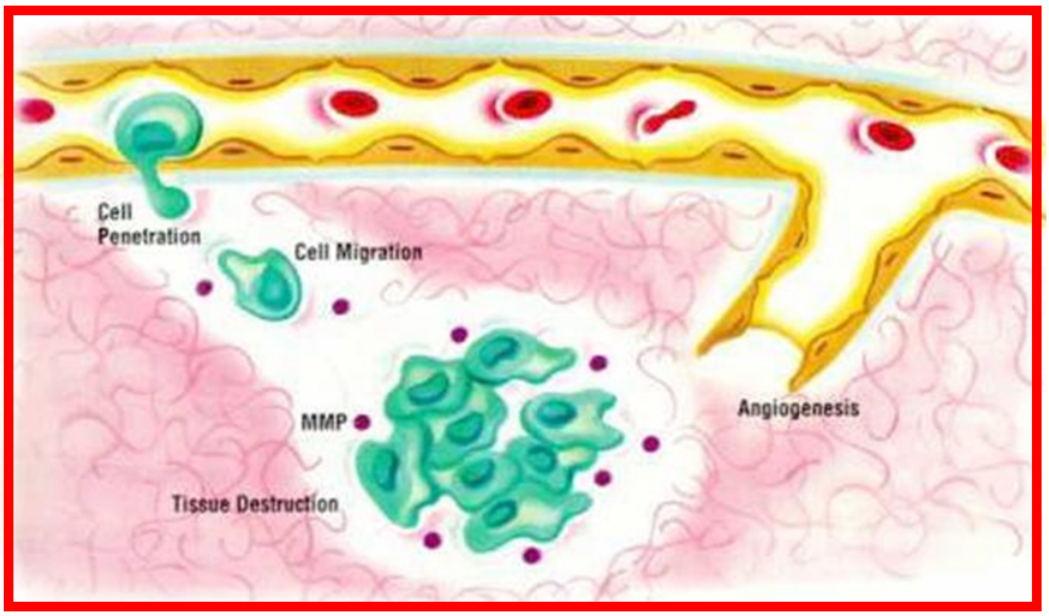

Figure 7. MMPs role in cancer cell extravasation from blood vessel, cancer cell migration and establishment of metastatic foci.

The morphological localization of MMPs intratumoral in breast cancer has been the subject of numerous studies. Different studies have generated-contradictory data on the location of MMPs. Some co-localize MMP with neoplastic epithelial cells whereas others associated them with different components of the neoplastic stroma. No matter where they localized, the tumor environment is very important for the expression and activities of MMPs. To date, few studies are available on the expression of MMPs within breast cancer metastasis [29, 30]. For example, MMP-9 has been associated with

the neoplastic cell plasma membrane, non-neoplastic ducts and acini, epithelial cells and macrophages, stromal fibroblasts and endothelial cells, tumor-infiltrating stromal cells, including neutrophils, macrophages, and vascular pericytes.

Overview of fibroblast growth factor 1 (FGF-1)

Fibroblast growth factors (FGFs) constitute a large family of structurally related polypeptide growth factors found in organs ranging from nematodes to humans. To date, the mammalian FGF proteins are encoded by twenty-three distinct genes [31]. FGFs differ significantly in both size (17-29 KDa) and sequence, but all contain a core region of homology encompassing 120-130 residues.

Fibroblast growth factor 1 or acidic (FGF-1) interact with a family of four distinct, high-affinity tyrosine kinase receptors, designated FGFR-1 to -4 [32]. FGF-1 also binds with a relative high affinity to heparan sulphates, which in general are present as covalently linked side chains on cell-surface proteoglycans. [33]. Upon binding to the ligand, it appears that the FGF receptor complexes dimerize, in conjunction with a heparan moiety, and the tyrosine kinase is activated through autophosphorylation [34, 35] **(Figure 8).** Ultimately, activation of FGF receptors leads to signal transduction through multiple pathways including mitogen-activated protein kinases (MAPK), phosphatidylinositol 3-kinase (PI3K), phospholipase Cγ (PLCγ) [36, 37], leading to cell proliferation, and survival in a variety of cells [36].

The multifunctional FGF-1 and its receptor may play a role in autocrine and paracrine growth control of malignant tumors, its overexpression or a constitutive activation of FGF-1 signaling is often associated with cancer [38]. FGF-1 have been shown to increase the mobility and invasiveness of a variety of cell types. Thus, FGF-1 has a broad range of biological activities that can play an important role in tumorigenesis.

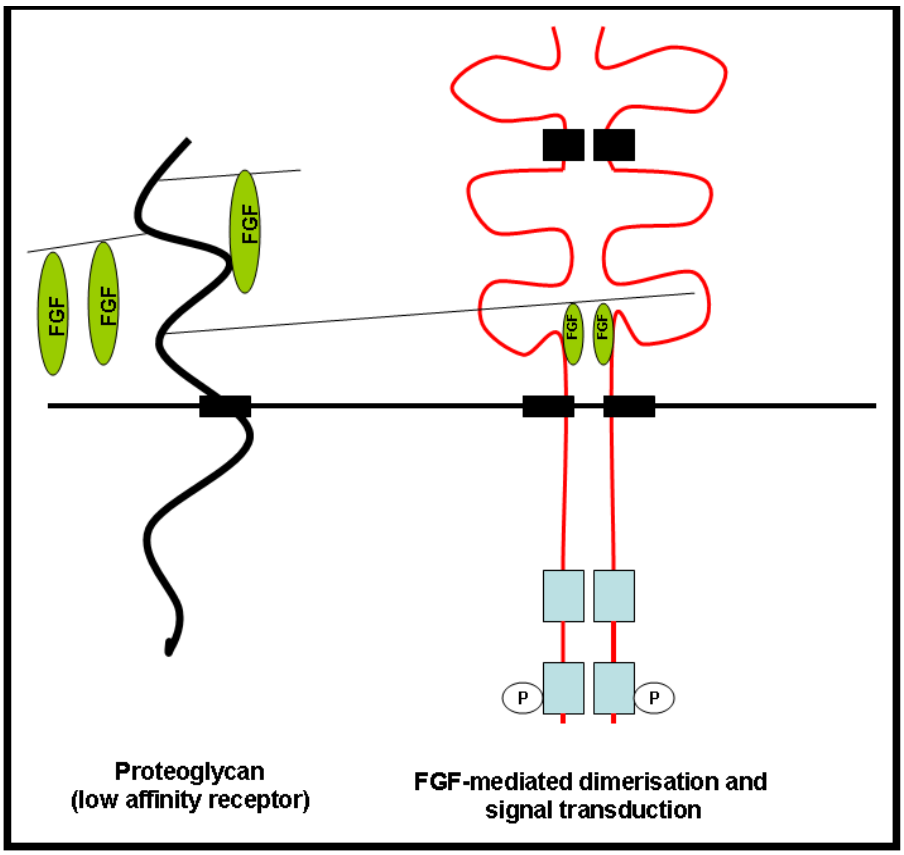

Figure 8. FGF receptor structure and FGF signaling.

In order to analyze the expression of FGF-1 in our breast cancer tumor, we inoculated three-week old Sprague–Dawley (SD) rats intracranially with ENU1564 tumor cell suspensions ($5x10^6$ cells). Three weeks post inoculation we sacrificed the animals and brain tumors were collected for semi-quantitative RT-PCR analysis and immunohistochemistry analysis. We showed that there is a significantLY higher level of FGF-1 mRNA in brain tumor foci than in normal brain tissues (control) from age-matched-non-inoculated rats **(Figure 9).** FGF-1 can be released from the tumor cells and can act as an autocrine or paracrine mitogenic factor to induce angiogenesis and tumor invasion.

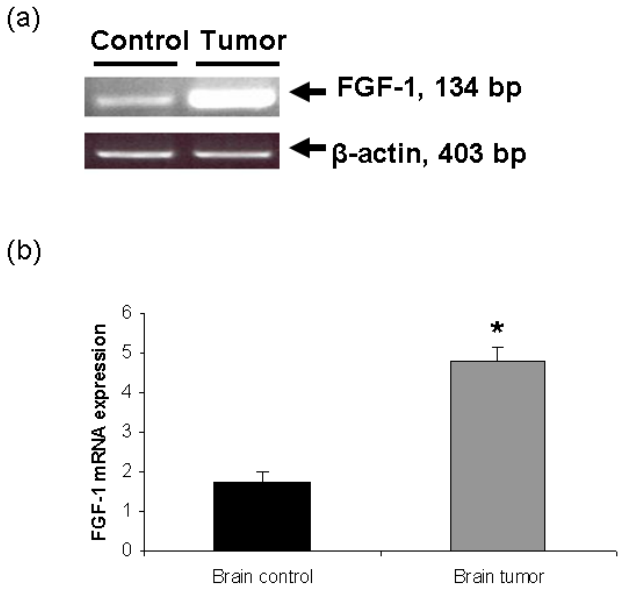

Figure 9. Increased expression of FGF-1 mRNA in the rat neoplastic brain foci. Semi-quantitative RT-PCR was used to detect FGF-1 in total RNAs from normal brain and neoplastic brain foci. β-actin was used as an internal control. Data are represented as mean ± standard deviation for three independent experiments and asterisks indicate statistically significant differences (*, $P < 0.05$).

Next we wanted to investigate if our cancer cells were expressing any of the four possible FGF-1 receptors, FGFR1-4. Using semi-quantitative RT-PCR we analyzed the expression of two of the FGF-1 receptors, FGFR1, and FGFR2 in the ENU1564 cell lines. We found that both receptors were expressed in ENU1564 cell lines **(Figure 10).** Because FGFR1 and FGFR2 are expressed in the cancer cells, FGF-1 can act as a mitogen on cancer cells and in turn, can activate many signal transduction cascades.

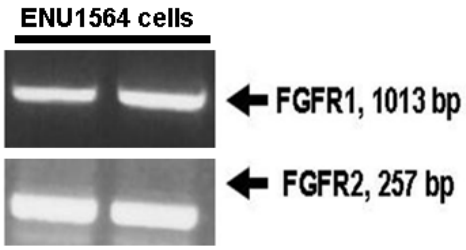

Figure 10. Expression of FGFR1 and FGFR2 mRNA in ENU1564 cell lines.

We also analyzed the expression of FGFR1 by IHC using SD rats brain tumor sections **(Figure 11)** and revealed that FGFR1 was highly expressed in the brain tumor foci.

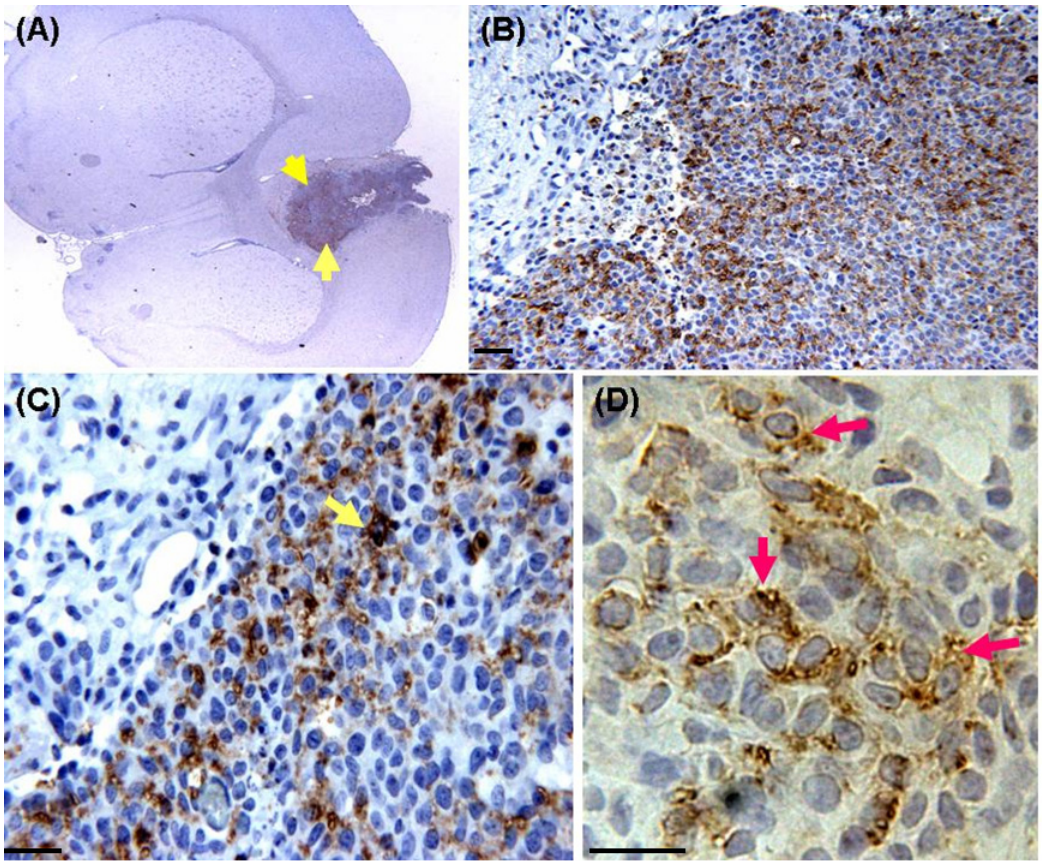

Figure 11. Expression of FGFR1 in the brain tumor foci. (**A, B, C, D)** Immunolocalization of FGFR1 in the brain tumor foci as indicated by red arrows. Yellow arrows indicate the tumor area. Bars indicate 200 µm.

Like FGF-2, FGF-1 does not have a signal peptide for channeling through the classical secretory pathway; however does possess a nuclear localization motif and has been found associated with the nucleus [39]. The presence of a nuclear localization motif appears to be important for FGF-1-induced mitogenesis. FGF-1 has also been shown to stimulate DNA synthesis without signaling through a cell-surface FGF receptor,

suggesting that the nuclear localization signal may allow FGF-1 to act through an intracrine mechanism [39]. Once FGF-1 is secreted can it bound to the extracellular matrix and can be released by the activity of degradative enzymes such as proteases **(Figure 12**). In addition, FGF-binding protein, a 17 KDa secreted polypeptide, can facililate release of FGFs from extracellular matrix and interaction of this growth factor with cellular receptors [40]. Following release from the extracellular environment FGF-1 binds cell surface receptors that, in turn, can activate many signal transduction cascades. These signal transduction pathways will then activate various genetic programs through the concerned regulation of transcription factors, stimulating cell growth by promoting cell cycle progression and inhibiting pathways of cell death. FGF-1 can be secreted from cancer cells and can act as an autocrine growth factor and/or paracrine angiogenic factor and this has been shown to occur in human gliomas [41]. It was found that FGF-1 is an important mitogen in prostate cancer due to the fact that it is mitogenic when it binds any type of isoform of FGF receptor [42]. Previous studies showed that FGF-1 is released in response to severe cellular injuries such as hypoxia [43] and serum starvation [44].

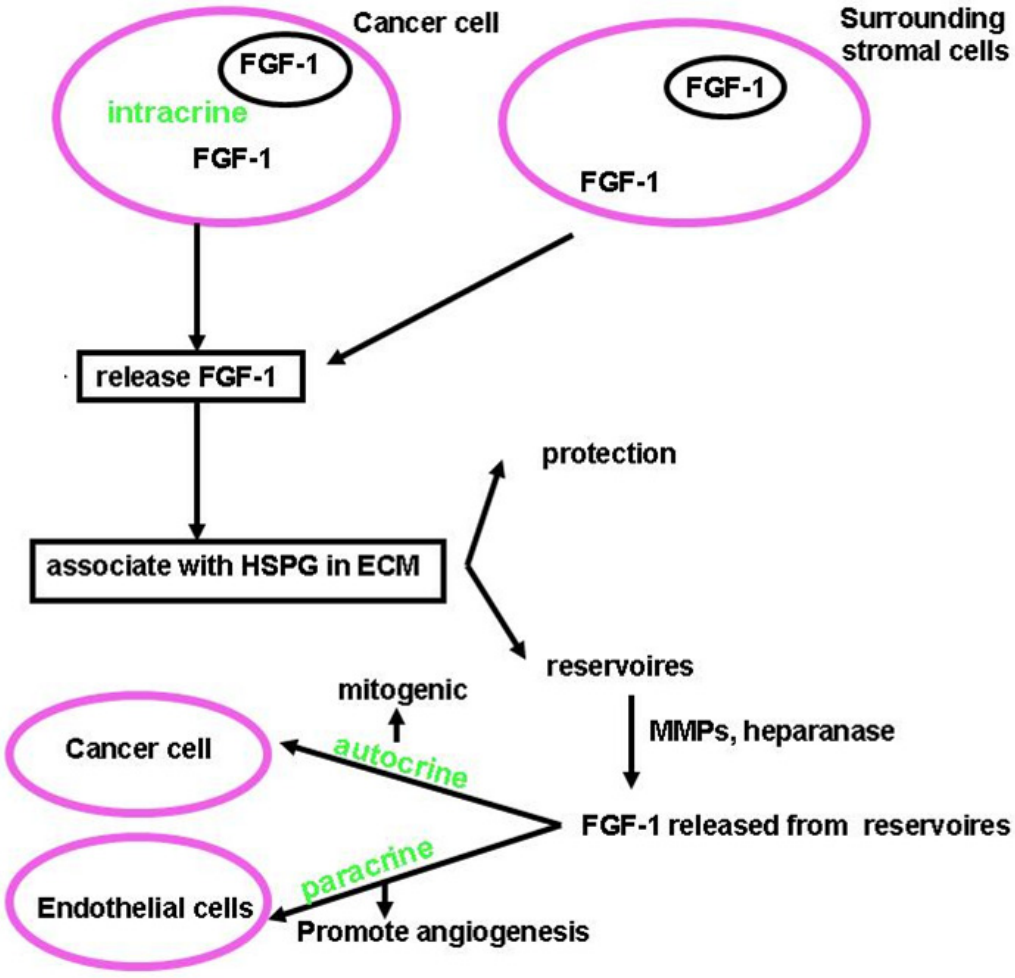

Figure 12. FGF-1 secretion and mechanism of action. Secreted FGF-1 can bound to the extracellular matrix (ECM) and can be released from ECM by the activity of degradative enzymes such as proteases. Once released from the matrix, FGF-1 is bounding to any of the four FGFRs on different cells in an autocrine or paracrine fashion (like endothelial cells, glial cells, cancer cells).

There are still a number of unresolved issues regarding of how FGF-1 is released from the cells that produce it and how it influences tumor progression. In this study we investigated the mechanism of MMP-9 regulation by FGF-1. Among MMPs, MMP-9 (gelatinase B) appears to play an important role in a wide array of patho-physiological processes including development, wound healing, angiogenesis, inflammation, invasion, and metastasis [39].

Specific objectives

Regulation of gene expression by oxygen is an important feature of many biological processes, and hypoxia is a powerful modulator of gene expression. The effect of hypoxia on malignant progression is mediated by a series of hypoxia- induced factors which contributes to angiogenesis and lysis of the extracellular matrix which enable tumor cells to escape their oxygen-deficient environment. Here we propose the use of a novel spectroscopic photoacoustic tomography technology (SPAT) for the detection of tumor hypoxia, an important parameter of tumor pathogenesis, by measuring the level of brain blood oxygenation. Validation of this technology will be supported by our molecular biology findings aimed to elucidate the etiopathogenesis of SPAT detected hypoxia and angiogenesis. SPAT will be useful for monitoring the development of hypoxia, which may have an important role in determining the timing and type of therapy. We want to explore if hypoxia and hypoxia-induced factors contribute to tumor invasion and metastasis. Previous studies showed that fibroblast growth factors 1 or

acidic (FGF-1) is one of the factors released in response severe hypoxia [45]. FGF-1 signaling also appears to play in important role in tumor growth and angiogenesis, and autocrine and paracrine FGF signaling may be particularly important in the progression of cancer. However, there are a number of unresolved issues regarding the mechanism(s) by which FGFs signaling contributes to cancer progression. We want to investigate the role of FGF-1 in matrix metalloproteinase 9 (MMP-9) expression in breast cancer cells which might contribute to cancer progression. Such an understanding will facilitate the development of cancer therapies to target this signaling pathway. Our hypothesis is that hypoxia and hypoxia-induced factors contributes to tumor invasion and metastasis.

The first objective is to study the role of hypoxia and hypoxia-induced factors in tumor detection and progression (*in vivo* and *in vitro* study). The first approach will be to detect tumor hypoxia in a rat by measuring the brain tumor oxygen saturation (SO2) through the intact skin and skull using a novel noninvasive spectroscopic photoacoustic tomography (SPAT) technology. To achieve this goal, Sprague-Dawley rats will be inoculated intracranially with ENU1564, a carcinogen-induced rat mammary adenocarcinoma cell line, and will be imaged with SPAT two-three weeks post inoculation. Sprague-Dawley rats inoculated intracranially with DMEM medium, will be used as controls. Our analysis will focus on histological examination of the neoplastic tumor foci inside the rat brain imaged by SPAT will be achieved.

The second approach is to study the role of hypoxia in driving tumor invasion and metastasis through upregulation of target genes important for these functions. Our *in vivo* studies will focus on characterization of HIF-1α, VEGF-A, VEGFR2, and MMP-9

expression in hypoxic brain foci compared with normal brain. We will evaluate and quantify HIF-1α, VEGF-A, and VEGFR2 protein expression by Western blot (WB) and immunohistochemistry (IHC) and will quantify MMP-expression by gelatin zymography. We will also quantify the expression of HIF-1α, VEGF-A, VEGFR2, MMP-9 mRNA by semi-quantitative RT-PCR. Our *in vitro* studies will determine if hypoxia influences the tumor invasion and the expression of HIF-1α, VEGF, VEGFR2, and MMP-9 proteins in ENU1564 cells. Our analysis will focus on the evaluation of *in vitro* invasiveness of ENU1564 cells grown under hypoxic conditions and compare with ENU1564 cells grown under normoxic conditions. We will also evaluate the expression of HIF-1α, VEGF-A, VEGFR2, and MMP-9 mRNA and proteins in breast cancer cells grown under hypoxic conditions and determine the mechanism of hypoxia-induced HIF-1α, VEGF-A, VEGFR2, and MMP-9 gene expression in ENU1564 cells.

The second objective is to study the role of fibroblast growth factor-1 (FGF-1) in the expression of MMP-9 in ENU1564 cells *(in vitro* study). To achieve this goal we will determine if FGF-1 upregulates MMP-9 mRNA (RT-PCR) and protein expression (WB and gelatin zymography) in FGF-1 treated ENU1564 cells grown in culture and compared with untreated ENU1564 cells. Next we will investigate the mechanisms of MMP-9 activation in FGF-1 treated ENU1564 cells. We will investigate both mitogen activated protein kinase (MAPK), and phosphoinositil-3-OH kinase (PI3K/Akt) pathways and determine if use of MAPK or Akt inhibitors will alter FGF-1 mediated MMP-9 upregulation. We will also investigate the transcription factor(s) with critical role in MMP-9 transcriptional regulation by FGF-1: activator protein-1 (AP-1), nuclear

factor-k beta (NF-kB) or both- WB analysis of the cytoplasmic and nuclear FGF-1 treated ENU1564 cells extracts (target the expression of c-jun, c-fos, IkBα. Our analysis will also involve cloning of the MMP-9 promoter and transient transfection experiments using a reporter plasmid (GFP or luciferase) bearing full length MMP-9 promoter (wild-type) or MMP-9 promoter with AP-1 or NF-kB mutation sites into the ENU1564 cells. We will perform electromobility shift assay (EMSA) to confirmed which transcription factor(s) is/are critical for FGF-1 mediated MMP-9 up-regulation (also super-shift assay to determine the exact factor or combination of factors responsible for transcriptional up-regulation of MMP-9 by FGF-1.

Summary

In summary, the objectives of this project are two fold. The first objective will provide an integrated approach to define the oxygen status (hypoxia) of tumors by using SPAT and to correlate hypoxia with tumor invasion and metastasis by using ENU1564 cell line. Such information can be used not only as a prognostic tool for tumor invasion but also as the basis for developing and evaluating patient-specific treatment modalities for many types of cancers. For the second objective, we will investigate the mechanism of MMP-9 regulation by FGF-1. A clear understanding of the mechanism by which FGF-1 signaling contributes to tumor progression and/or metastasis will facilitate the development of cancer therapies to target this signaling pathway. By upregulation of MMP-9 in the cancer cells, the FGF-1 may contribute to cancer progression (invasion)

not only by facilitating enzymatic cleavage of ECM by MMP-9 but also by increasing the availability of FGFs to cancer cells due to mobilization of FGF from the ECM, which in turn can act on cancer or stromal cells. If ENU1564 cells express and secret FGF-1 and also express FGFRs receptors, FGF-1 might play a role in the tumor progression of breast cancer cells not only by a paracrine but also by an autocrine mechanism.

CHAPTER II

ROLE OF HYPOXIA IN BRAIN TUMOR DETECTION USING SPECTROSCOPIC PHOTOACOUSTIC TOMOGRAPHY TECHNOLOGY (SPAT) *

Introduction

The oxygen status of tumors plays a central role in tumor pathophysiology and treatment. It is also a powerful prognostic factor of disease-free survival. In addition, it appears to be strongly associated with tumor growth, malignant progression, and resistance to various therapies including radiotherapy, photodynamic therapy, and chemotherapy [46]. Prior studies involving different techniques have measured one or more parameters to define tumor hypoxia status. These include magnetic resonance imaging to monitor vascular oxygenation and blood flow [47], phosphorescence lifetime (quench) imaging [48] to measure oxygen diffusion distances between microvessels [49] and evaluate longitudinal tissue gradients of oxygen [50], cryospectrophotometry to measure hemoglobin saturation [51] single-photon emission computed tomography and positron-emission tomography assays to measure perfusion and mark hypoxic areas [52,53] and hypoxia markers to identify hypoxic tumor regions [54].

---

*Reprinted with permission from "In vivo imaging and characterization of hypoxia induced neovasculatization and tumor invasion" by Lungu GF, Li LM, Xie X, Wang LV, Stoica G, 2007. International Journal of Oncology, 30:45-54, Copyright 2008 by International Journal of Oncology.

Unfortunately, none of these technologies have produced a reliable measurement of tumor oxygen status and tumor vascularity primarily because solid tumors are usually characterized by a high degree of vascular and oxygen tension heterogeneity. The technique used in this study, spectroscopic photoacoustic tomography (SPAT) is based on the measurement of laser-induced ultrasonic waves and has contrast similar to that of pure optical imaging with spatial resolution similar to that of pure ultrasonic imaging. Therefore SPAT combines the advantages of two imaging modalities in a single modality. The laser-induced ultrasonic signals from biological samples depend on optical absorption in the sample to reveal the structure of the tissue based on optical contrast [55]. The distribution of optical absorption in the object can be reconstructed using photoacoustic signals which are detected by highly sensitive piezoelectric devices. This technique used for detection of oxygen saturation (SO_2) is a noninvasive imaging modality, based on the spectroscopic differences between oxyhemoglobin (O_2Hb) and deoxyhemoblobin (HHb) [56]. Since HHb and O_2Hb are the dominant absorbers in the rat brain, with the reconstructed images at multiple optical wavelengths, the contributions to the photoacoustic signals from HHb and O_2Hb can be separated by SPAT; thus spatial distribution of total hemoglobin (HbT) and SO_2 based on the estimated concentration of HHb and O_2Hb can be reconstructed. SPAT has the ability to image HbT and SO_2 with satisfactory penetration depth in the rat brain.

Here we are defining the oxygen status (hypoxia) of tumors by using SPAT. In the next chapter we will correlate hypoxia with the invasion process of mammary adenocarcinoma cell line ENU1564 inoculated intracranially in a rat model. The

mechanism of tumor invasion may apply to tumor metastasis because metastasis mediators are involved in both of these processes. Here we were able to successfully obtain the brain oxygenation images, which clearly showed tumor hypoxia.

Materials and methods

Reagents

Chemicals, stains and solutions were obtained from Sigma Chemical Company (St. Louis, MO, USA) unless otherwise indicated.

Cell culture

The ENU1564 tumor cell line used in this study was originally developed in our laboratory and originated from an *N*-ethyl-*N*-nitrosourea-induced mammary adenocarcinoma in a female Berlin-Druckrey IV (BD-IV) rat. This cell line is highly metastatic to brain and bone tissues [13]. Prior to inoculation, the cell line was maintained in Dulbecco's modified Eagle's medium (Invitrogen, Carlsbad, CA, USA), (DMEM) supplemented with 10% fetal bovine serum (Invitrogen) and antibiotics (100 units/ml penicillin and 100 μg/ml streptomycin).

Rat inoculation

Three-week old Sprague–Dawley (SD) rats obtained from a colony maintained at Texas A& M University were used. All animal experiments were done in accordance

with protocol approved by our Institutional Animal Care and Use Committee (IACHC) and following National Institute of Health (NIH) guidelines for animal welfare. Stereotaxic implantation of tumor cells was performed under full anesthesia using a mixture of Ketamine (Ketant, Fact Dodge Animal Health) and xylazin (Ane Sed, Lloud Laboratories). A stereotaxic frame was used to stabilize the animal's head. The hair on the rat's head was gently removed with hair-removal lotion. The site of inoculation was marked at a point 2.5 mm lateral and 1 mm anterior to the bregma. This point was chosen because of its location directly above the caudate nucleus, which has been shown to be a highly reliable intracranial site for tumor engraftment. The cells were inoculated intracranially at 3 mm depth from the cranial surface. A 10µl Hamilton syringe was used to inoculate 3 µl tumor cell suspensions ($5x10^6$ cells) over 5 minutes period. Three weeks post inoculation the animals were subjected to SPAT evaluation. After the SPAT evaluation the animals were euthanatized with Pentobarbital (150 mg/kg, intraperitoneal injection) and the brains were used for imunohistochemistry analysis.

Immunohistochemistry

Five-micron (5µm) paraffin-embedded sections were used for immunohistochemical study. After deparafinization, the sections were subjected to an antigen retrieval protocol by heating them in 10 mM citrate buffer (pH 6.0) for 10 minutes. Potential non-specific binding sites were blocked with 5% normal goat or rabbit serum in PBS. After blocking, the sections were incubated for 1 hour to overnight with primary antibody. For activated microglial cells we used a mouse anti rat CD68: biotin

from Serotec Company (Hidlington, Oxford, UK). Mouse anti-glial fibrillary acidic protein (GFAP) was purchased from Chemicon International (Temecula, CA, USA). Following primary antibody reaction, sections were washed and incubated with either biotin-conjugated anti-rabbit or anti-goat IgG (Vector Laboratories, Burlingame, CA, USA). A Vector-ABC streptavidin-peroxidase kit with a benzidine substrate for color was used for color development. Counter-staining was done with diluted hematoxylin. Sections that were not incubated with primary antibody served as negative control. To visualize the tumor foci on paraffin-embedded sections, hematoxylin and eosin staining was performed.

Experimental setup of SPAT

Three weeks after intracranial inoculation, experimental rats had developed neurological signs such as ataxia and head tilt. At that time the experimental rats were imaged using SPAT. Four successful SPAT images showing tumor hypoxia in the SD rat brains were achieved as described in **(Figure 13).** Rats of similar age, inoculated intracranially with 3 µl of DMEM medium, were used as controls. Briefly, each animal was anesthetized using Ketamine (87mg/kg, intramuscular injection) and the hair from the top of the head was removed. A tunable Ti:Sa nanosecond pulse laser (LT-2211A, Lotis T II, Minsk, Belarus) pumped by an Nd:YAG laser was employed to provide laser pulses with a pulse repetition rate of 10 Hz. The laser beam was expanded by a concave lens and homogenized by a light diffuser and then delivered to the animals head (**Figure 13).** The incident energy density of the laser beam on the surface of the rat head was

controlled at ~ 20mJ/cm2 (within the ANSI standard). Each single laser pulse's energy was monitored using a photodiode (PD) and recorded. The photoacoustic signals were normalized by the recorded PD signals to reduce the effect of laser-energy fluctuation. A 2.25-MHz ultrasonic transducer (V323, Panametrics) was used to detect the laser-induced acoustic signals. The active area diameter was 6 mm and it had a nominal bandwidth of 66%. A computer controlled step motor drove the 2.25MHz transducer to circularly scan the head of the SD rat at a depth of ~3mm below the skin surface, at a radius of 4.5 cm, and with a step size of 3 degree. During the SPAT scan, the rat was fixed by a homemade restraint mount. A water tank was used that had a sealed opening in the bottom such that the rat's head could protrude along the bottom of the water surface and stay dry **(Figure 13).** The hole was sealed with a piece of polyethylene membrane. The rat head surface was covered with a thin layer of ultrasonic coupling gel. Health status, pulse rate and the global arterial blood oxygenation of the rat were monitored throughout the entire experiment using a pulse oximeter. The detected photoacoustic signals were amplified, digitized by an oscilloscope, and then transferred to a computer. Four wavelengths (764 nm, 784 nm, 804 nm, and 824 nm) were changed at each scanning step. After a single full-view scan, the images at different wavelengths were reconstructed based on a modified back projection algorithm [57]. Then the reconstructed images at the four different wavelengths were used to estimate the spatial distribution of the concentration of HHb and O2Hb using a standard linear least-squares method.

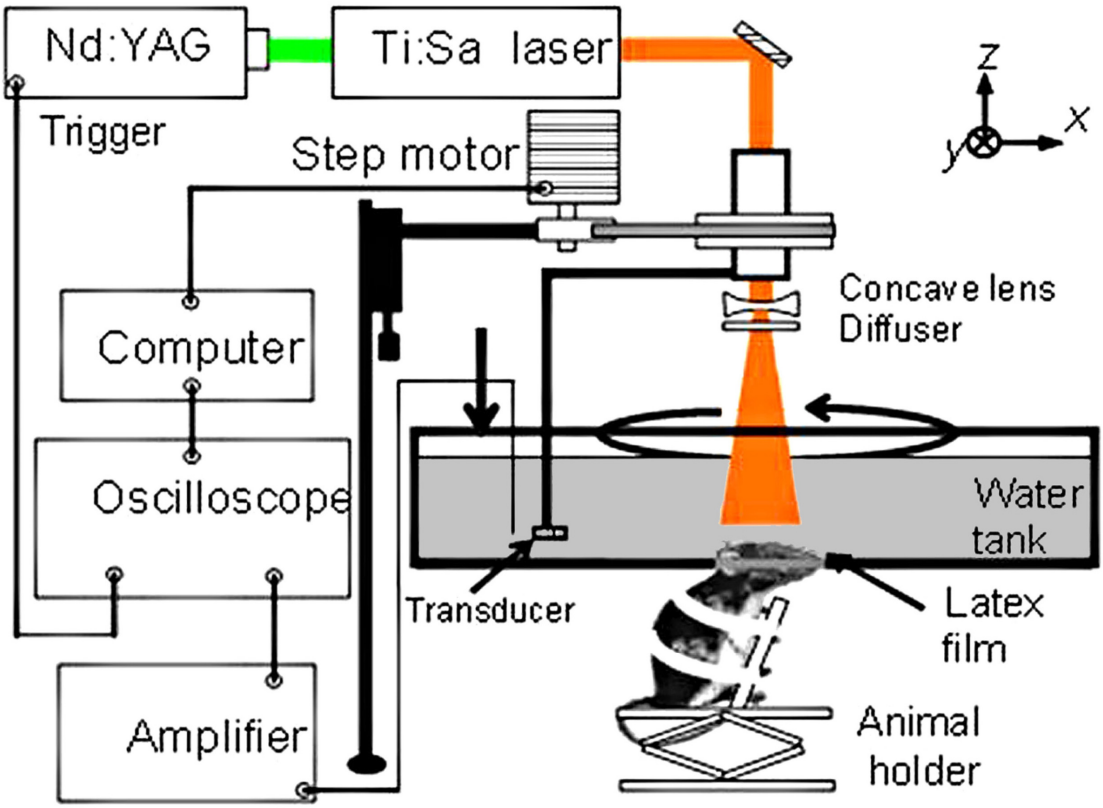

Figure 13. Experimental setup for the *in vivo* SPAT analysis.

Results

Spectroscopic photoacoustic tomography (SPAT) imaging of the SD rat brain tumor three weeks after inoculation with ENU1564 cell line

SPAT images from four tumor-bearing SD rat brains showed hypoxia. The most representative SPAT image of brain tumor hypoxia is showed in **Figure 14**. None of the SPAT images of tumor-free SD rat control brains showed hypoxia. Differences in brain vasculature between a tumor-free SD rat brain **(Figure 14a)** and a tumor-bearing SD rat brain **(Figure 14b)** are illustrated. Compared with the tumor-bearing rat brain, SPAT images of the tumor-free brain showed a well-defined symmetrical vascular architecture in both cerebral hemispheres. In **Figure 14c**, an open-skull photograph of the rat brain taken right after the SPAT experiment, showed a tumor in the right hemisphere. The position of the tumor corresponded with the location of the tortuous irregular distorted vessels shown in **Figure 14c**. The SO_2 image of the rat brain with intra-cranial inoculation of ENU1564 cells is represented in **Figure 14d**. The SO_2 value is lower in the brain tumor area compared to the rest of the brain.

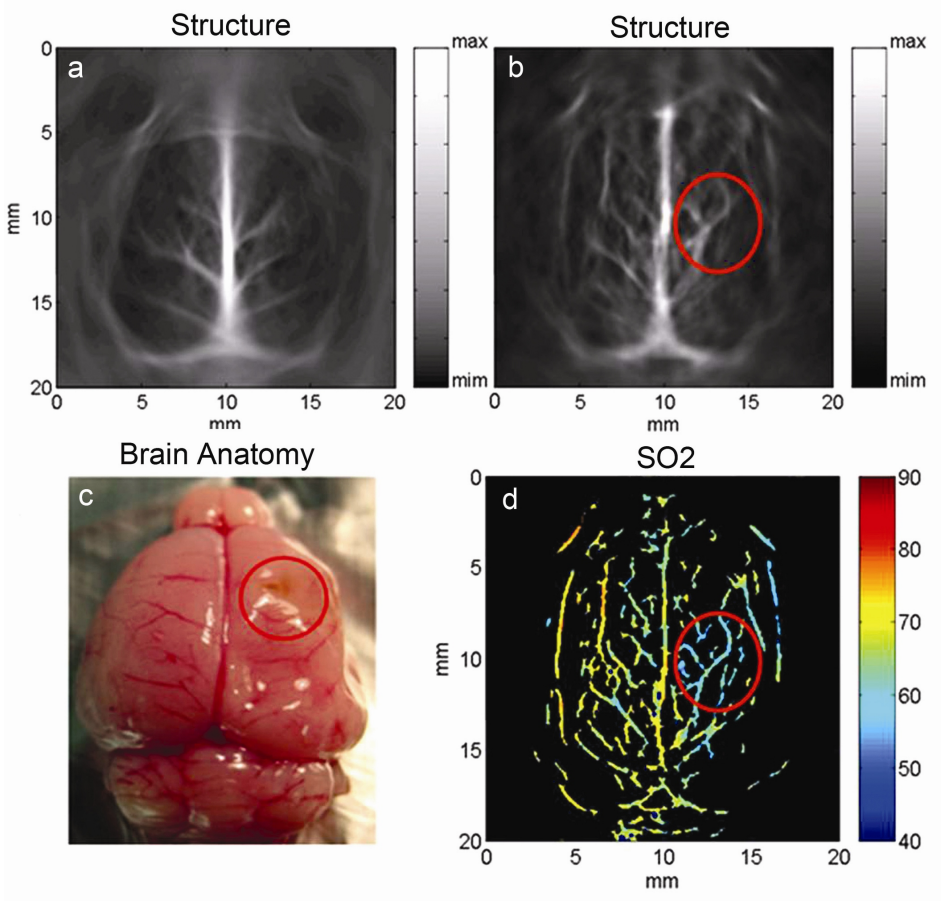

Figure 14. Estimated brain blood oxygen saturation image from noninvasive *in vivo* spectroscopic photoacoustic tomography. The circle indicates the position of the tumor. (**a**) SPAT image of a tumor-free rat brain, which shows well-defined symmetrical vascular architecture in both cerebral hemispheres. (**b**) SPAT image of the rat brain inoculated intracranially with ENU1564 cells and reveals the vascular architecture associated with the tumor, which is different from that of a normal brain SPAT image. (**c**) Open-skull photograph of the rat brain after SPAT experiment shows the tumor position in the cerebral hemisphere. (**d**) Estimated brain blood oxygen saturation (SO2) image.

H&E staining of the tumor foci inside the rat brain imaged by SPAT is represented in **Figure 15**. The diameter of the tumor area was approximately 2.5 mm. Histological examination of H&E-stained brain sections revealed an increased mitosis in the tumor cells which demonstrated that ENU1564 cell line was highly invasive.

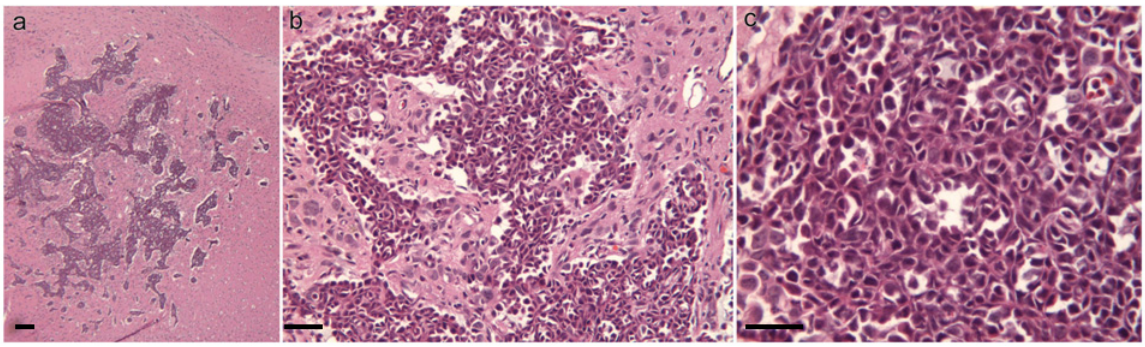

Figure 15. H&E staining of the tumor foci inside the SD rat brain at various microscopic magnifications. The tumor is observed as a basophilic, hypercellular area composed of neoplastic epithelial cells. Bars indicate 200 μm.

Histological evaluation of the neoplastic foci

Three weeks after intracranial inoculation with ENU1564 cells the rats were euthanatized. Histological evaluation of the brain revealed intra-cranial neoplasia affecting the caudate nuclei most frequently. Morphologically, clusters of epithelial neoplastic cells resembling the cultured cell line were observed. Marked gliosis consisting of astrocytes (**Figure 16a)** and microglial cells **(Figure 16b)** was observed around and inside the neoplastic foci.

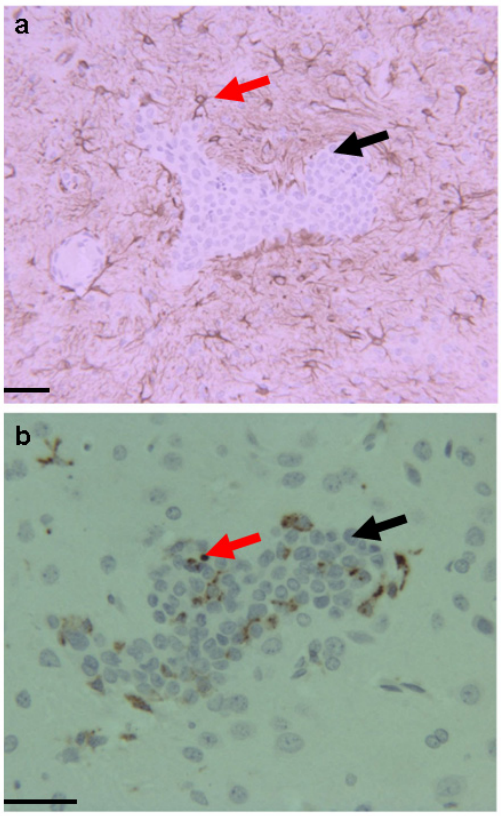

Figure 16. Activation of astrocytes and microglial cells around and inside the brain tumor foci. Panel (**a**) shows activation of astrocytes (brown color) around tumor foci (immunohistochemical staining for GFAP). No reactivity of astrocytes was observed inside the brain tumor foci. Panel **(b**) shows active microglial cells around and inside the tumor foci (brown color). Black arrows indicate the tumor foci and red arrows indicate activated glial cells. The data represent three separate experiments with similar results. Bars indicate 200 µm.

Discussion

In the present study we were able to detect tumor hypoxia in a rat intracranially implanted with a malignant mammary tumor cells by measuring the brain tumor SO2 through the intact skin and skull using a novel noninvasive spectroscopic photoacoustic tomography technology. Validation of this technology will be supported by our molecular biology findings. Detection and measurement of the level of brain blood oxygenation can be used to monitor tumor hypoxia, an important parameter of tumor pathogenesis.

Previously, Mendes et al., using an *in vivo* animal model, showed that MMP-2, -3, and -9 are involved in mammary adenocarcinoma metastasis to the brain [12]. The animal model used in those studies was developed in our laboratory [13]. The syngeneic animals inoculated with ENU1564 cells via the left ventricle consistently produced brain metastasis. For our study we chose to inoculate the tumor cells (ENU1564) intracranially into the rat forebrain since we were mainly interested in locating tumor implant and detecting tumor hypoxia inside the brain using SPAT, as an assessment of this new technology. The mechanism of tumor invasion resulting from the tumor implant may apply for tumor metastasis because metastasis mediators are involved in both of these processes. Our results showed the presence of tumor hypoxia in the rat brain three weeks post inoculation.

Because evidence suggested that astrocytes and /or glial cells may have a role in tumor invasion [12] we analyzed how these cell types reacted in a tumor –bearing brain. Prior studies showed that astrocytes are thought to play a role in MMP-9 activation and

expression [58]. Immunohistochemical staining using GFAP antibody (glial fibrillary acidic protein) demonstrated marked astrocytic proliferation around neoplastic foci **(Figure 16a).** Astrocytes, which populated brain parenchyma, synthesized a host of biological proteins including TGF-β, TNF-α, interferon-γ, IL-1, IL-3, IL-6, and other cytokines which may be very important for tumor invasion [58]. Studies showed that brain metastatic and parental cancer cell line co-cultured with astrocytes or cell culture supernatants of astrocytes, exhibited increased adherence to astrocytes and grew better in response to the conditioned media [59]. Microglial reactivity around and inside the tumor foci was also confirmed **(Figure 16b).** The presence of reactive glial cells around tumor cells in the brain suggests the possibility that these cell types could be interacting. Further studies are needed in order to characterize the role of those cells in tumor progression into the brain parenchyma.

Tumor oxygen status appears to be strongly associated with tumor growth, malignant progression, and resistance to various therapies [46]. Among the genes upregulated in hypoxia, those involved in angiogenesis and degradation of extracellular matrix appears to be very important in malignant progression [62]. Tumor oxygen status may also be important in the assessment of the efficacy of agents classified as antiangiogenic compounds, which target tumor vasculature [46]. Therapy with antiangiogenic compounds may be more important than those which cause direct cytotoxicity to malignant cells. Detection of tumor hypoxia can be used as a prognostic tool and for developing and evaluating patient specific treatment modalities for many types of cancer. In 2004, Evans et al., showed that the presence of more severe hypoxia

in glial tumors correlated with a more aggressive clinical behavior [61]. Also, the presence of hypoxia in locally cured high-grade sarcomas was associated with a greater likelihood of metastasis and death [62].

This study shows that SPAT can be an important tool for noninvasive detection of intracranial tumors. Moreover, SPAT would be useful for monitoring the development of hypoxia, which may have an important role in determining the timing and type of therapy. SPAT is also a promising imaging modality for the study of the functional and structural organization of the brain. In combination with reporter genes, SPAT offers promise for imaging pathological processes at molecular levels, and monitoring the delivery of vectors to specific cells by gene therapy.

CHAPTER III

ROLE OF HYPOXIA-INDUCED FACTORS IN TUMOR INVASION AND METASTASIS*

Introduction

Angiogenesis is an essential component for the growth of tumors. It is an invasive process that requires lyses of the extracellular matrix (ECM) plus proliferation and migration of the endothelial cells [60]. This complex process, regulated by angiogenic factors and cytokines, is important for tumor invasion [63]. Vascular endothelial growth factor (VEGF), an angiogenic mitogen secreted from various types of cells, is involved in various physiological and pathological conditions, including embryonic development, wound healing and solid tumor growth. VEGF is known to stimulate the production of various cytokines, growth factors, and proteinases, including MMP-1, -3, and -9 [64]. The expression of VEGF is regulated by various physiological and pathological stimuli. Hypoxia is a strong inducer of VEGF, and hypoxia-induced VEGF expression determines the course of various disease conditions, such as solid tumor growth [65].

---

*Part of this data reported in this chapter is reprinted with permission from "In vivo imaging and characterization of hypoxia induced neovasculatization and tumor invasion" by Lungu GF, Li LM, Xie X, Wang LV, Stoica G, 2007. International Journal of Oncology, 30:45-54, Copyright 2008 by International Journal of Oncology.

VEGF binds to a family of class III tyrosine kinase receptors, including fms-like tyrosine kinase 1 and 4 (flt-1 or VEGFR1 and flt-4 or VEGFR-3) and kinase insert domain-containing receptor (flk1/KDR or VEGFR2) [5].

Among these receptors, VEGFR-2 is responsible for the mitogenic signaling and proliferation, thus is has been thought to be the principal receptor for VEGF signaling [5]. The interaction between VEGF and VEGFR-2 in an autocrine manner may play a role in tumor cell growth. It has been shown that VEGFR-1 is transcriptionally upregulated by HIF-1α under hypoxic conditions [66], while VEGFR-2 receptor expression is mediated by posttranscriptional mechanisms such as enhanced protein stability [67]. Tang et al*.,* 2004 demonstrated that VEGFR-2 protein expression was upregulated by hypoxia in endothelial cells and that loss of HIF-1α results in a decreased VEGF expression and loss of autocrine response of VEGFR-2 [68].

Hypoxia has been shown to provide an important prognostic value in clinical trials involving radiation and chemotherapy. It is usually associated with adverse clinical outcomes and reduced patient survival [69]. Although tissue hypoxia usually occurs very early in tumor development due to inadequate blood supply, hypoxia remains a constant feature of these tumors even after neovascularization [8]. Several studies have shown that the regulation of gene expression by oxygen is an important feature of many biological processes, and hypoxia is a powerful modulator of gene expression [70,71]. The main regulator which orchestrates the cellular responses to hypoxia is hypoxia-inducible factor-1 (HIF-1), a heterodimeric transcription factor composed of α and β subunits critical for adaptive responses to reduced oxygen [72]. The HIF-1β is thought to

be expressed constitutively and ubiquitously. HIF-1α is also constitutively expressed, but is continuously degraded in the presence of oxygen, by von Hippel Lindau tumor suppressor protein leading to decreased HIF1α levels in normoxia and high levels in hypoxia. Elevated HIF-1α expression, which could be an indicator of the existence of hypoxia, has been reported in a variety of human tumors and pre-neoplastic lesions [73,74]. The critical role of HIF-1α in tumor metastasis arises from the fact that it is a potent activator of angiogenesis and invasion through its upregulation of target genes important for these functions. Hill and co-workers have found that exposure of tumor-bearing rodents to cyclical, but not chronic, hypoxia produces a significant increase in metastasis to the lungs [75]. Hypoxia was also found to be important in activation of extracellular matrix degrading proteases [76].

Matrix metalloproteinases (MMPs) are structurally related endopeptidases that play a role in proteolytic degradation of structural components of extracellular matrix [77]. They not only facilitate breakdown of extracellular matrix, but also affect early carcinogenesis, tumor development and growth. They also play an important role in angiogenesis and mammary gland involution [27]. Among these enzymes, matrix metalloproteinase-9 (MMP-9) or gelatinase B plays an important role in tumor invasion and metastasis because of its specificity for type IV collagen. Recent studies have demonstrated that the switch from vascular quiescence to angiogenesis involves MMP-9/ gelatinase B, which is upregulated in angiogenic islets and tumors, releasing VEGF from an extracellular reservoir [78]. Prior observations have suggested that acidity in the tumors can be caused by hypoxia-dependent and/or-independent pathways and MMP-9

was found to be induced by culturing cells at acidic pH [79]. Acidic pH was also found to increase the expression of vascular endothelial growth factor in glioma [80], and glioblastoma [81].

Here we evaluated the expression of HIF-1α, VEGF-A, VEGFR2 and MMP-9 protein and mRNA levels in the hypoxic brain tumor foci identified by SPAT and in ENU1564 cells exposed to hypoxia. We demonstrated by Western blot analysis and imunohistochemistry that the levels of HIF-1α, VEGF-A, VEGFR2 proteins were higher in brain tumor foci compared to those from normal brain tissues. Additionally, MMP-9 enzymatic activity was higher in brain tumor foci. The results were confirmed by semi-quantitative RT-PCR. Next we analyzed the expression of these proteins *in vitro* in ENU1564 cells grown in hypoxic conditions. We found that the levels of HIF-1α, VEGF-A, VEGFR2 and MMP-9 from ENU1564 cells grown in hypoxia are higher compared to those from normoxic ENU1564 cells. We demonstrated that hypoxia leads to activation of ERK1/2, Akt, but not p38 or SAPK/JNK in ENU1564 cells. We also demonstrated that MEK1/-ERK pathway is important in hypoxic regulation of VEGF-A, VEGFR2 and MMP-9 while PI3K-Akt is important in hypoxic regulation of MMP-9 and VEGF-A but not VEFGR2, by using specific MEK1/2 and PI3k inhibitors. The regulation of proteins targeted in our *in vivo* study may be directly correlated with hypoxia detected in the brain tumor foci by SPAT. Such informations can be used not only as a prognostic tool for tumor invasion but also as the basis for developing and evaluating patient-specific treatment modalities for many types of cancers. It should be

possible to target hypoxic cells by developing a gene therapy strategy that uses plasmids containing suicide genes that are selectively expressed under hypoxic conditions.

Materials and methods

Reagents

Chemicals and solutions were obtained from Sigma Chemical Company (St. Louis, MO, USA) unless otherwise indicated. PD98059 was purchased from EMD Biosciences (EMD Biosciences, Inc. San Diego, CA). LY294002 was purchased from Cell Signaling Technology (Cell Signaling Technology, Inc. Danvers, MA).

Cell culture

The ENU1564 tumor cell line used in this study was originally developed in our laboratory and originated from an *N*-ethyl-*N* nitrosourea-induced mammary adenocarcinoma in a female Berlin-Druckrey IV (BD-IV) rat. This cell line is highly metastatic to brain and bone tissues [13]. Prior to inoculation, for the *in vivo* experiments, the cell line was maintained in Dulbecco's modified Eagle's medium (Invitrogen, Carlsbad, CA, USA), (DMEM) supplemented with 10% fetal bovine serum (Invitrogen) and antibiotics (100 units/ml penicillin and 100 µg/ml streptomycin). For the *in vitro* experiments ENU1564 cells were incubated at 37°C in a humidified atmosphere of 5% CO_2 in air or in hypoxic conditions of 5% CO_2, and 95% N2 for 24 hours.

Treatment of ENU1564 cells with LY294002 and PD98059.

For these experiments, ENU1564 cells were preincubated with either PI3K inhibitor LY294002 (10 μM), or MEK1/2 inhibitor PD98059 (25μM) (EMD Bioscience, Inc., San Diego, CA) for an hour. Cells were then incubated at 37°C in hypoxic conditions of 5% CO_2, and 95% N2 for 24 hours. Control cells were incubated at 37°C in a humidified atmosphere of 5% CO_2 in air for 24 hours.

Invasion assay

In vitro invasiveness was evaluated using the method previously described [82] which used Boyden invasion chambers. Briefly, each Boyden chamber (Becton Dickinson Biosciences, NJ, USA) consists of a BD Falcon TC Companion Plate with Falcon Cell Culture inserts containing an 8-μm pore PET membrane with a thin layer of Matrigel basement membrane matrix. First, the interior of the inserts was rehydrated for 2 h with warm (37°C) bicarbonate based culture medium. The upper chambers were filled with 0.5 ml of cell suspension ($1.25x10^5$cells/ml) of ENU1564 in serum free DMEM medium. Ten percent fetal bovine serum in Dulbecco's Modified Eagle Medium (Invitrogen) was placed in the lower chambers as a chemoattractant. The chambers were incubated at 37°C in a humidified atmosphere of 5% CO_2 in air or in hypoxic conditions of 5% CO_2, and 95% N2 for 24 hours. Non-migrating cancer cells on the upper surface of the inserts was removed by wiping with a cotton swab; migrating cells on the lower surface were fixed and stained with Insta Stain 3 Step (S&K Reagent, Denver, CO, USA). The invasive potential was quantified by counting the total number of cells on the

lower surface of the inserts under a light microscope. Three random visual fields were counted for each assay. Each invasion experiment was carried out in triplicate.

Rat inoculation

Three-week old Sprague–Dawley (SD) rats obtained from a colony maintained at Texas A& M University were used. All animal experiments were done in accordance with protocol approved by our Institutional Animal Care and Use Committee (IACHC) and following National Institute of Health (NIH) guidelines for animal welfare. Stereotaxic implantation of tumor cells was performed under full anesthesia using a mixture of Ketamine (Ketant, Fact Dodge Animal Health) and xylazin (Ane Sed, Lloud Laboratories). A stereotaxic frame was used to stabilize the animal's head. The hair on the rat's head was gently removed with hair-removal lotion. The site of inoculation was marked at a point 2.5 mm lateral and 1 mm anterior to the bregma. This point was chosen because of its location directly above the caudate nucleus, which has been shown to be a highly reliable intracranial site for tumor engraftment. The cells were inoculated intracranially at 3 mm depth from the cranial surface. A 10µl Hamilton syringe was used to inoculate 3 µl tumor cell suspensions ($5x10^6$ cells) over 5 minutes period. Three weeks post inoculation the animals were sacrificed and the brain tumors used for Western blot, immunohistochemistry, gelatin zymography, and RT-PCR experiments.

Tissue processing and tumor collection

For Western blot, gelatin zymography, and RT-PCR, brains were immediately removed after death and placed on powdered dry ice. Brains from rats inoculated intracranially with tumor cells (n=3) and from age-matched-non-inoculated control rats (n=3) were used. Samples were kept at -80^{o}C. Brain tumors were collected from frozen brain sections. The half of the brain that was frozen in powdered dry ice was sectioned using a cryostat (Bright Instrument Company, LTD, Huntington Cambs, England) in 12 μm sections and placed on slides. Every fifth slide was stained with 0.1% thionine solution. Thionine solution stained the cell nuclei and displayed the tumor foci under light microscopy. The information was used to dissect the tumor foci, on frozen brain tissue sections. For immunohistochemistry, brain tumor-bearing (n=3) and tumor-free (n=3) SD rats were perfused with 4% paraformaldehyde (PFA) solution (Electron Microscopy Science, PA, USA) in PBS (phosphate buffer saline) using a peristaltic pump. Brains were then removed and post fixed in 4% PFA in PBS for 24 hours, after which the brains were further processed.

Immunohistochemistry

Five-micron (5μm) paraffin-embedded sections were used for immunohistochemical study. After deparafinization the sections were subjected to an antigen retrieval protocol by heating them in 10 mM citrate buffer (pH 6.0) for 10 minutes. Potential non-specific binding sites were blocked with 5% normal goat or rabbit serum in PBS. After blocking, the sections were incubated for 1 h at room temperature to

overnight at 4°C with primary antibody. The primary antibodies, MMP-9, VEGF-A, VEGFR2, and HIF-1α were purchased from Santa Cruz Bitotech (Santa Cruz, CA) and a 1:50 dilution was used. Following primary antibody reaction, sections were washed and incubated with either biotin-conjugated anti-rabbit or anti-goat IgG (Vector Laboratories, Burlingame, CA, USA). A Vector-ABC streptavidin-peroxidase kit with a benzidine substrate for color and Streptavidin-Phosphatase Kit (KPL, Maryland, USA) with a HistoMark Red substrate (KPL, Maryland, USA) were used for color development. Counter-staining was done with diluted hematoxylin. Sections that were not incubated with primary antibody served as negative control. To visualize the tumor foci on paraffin-embedded sections, hematoxylin and eosin staining was performed.

Western blot analysis

After microscopic dissection of frozen brain specimens, the tissues was homogenized in lysis buffer containing 50 mM Tris-HCl (pH 7.4), 150 mM NaCl, 1 mM CaCl2, 1 mM MgCl2, 0.1% Triton X-100. For the *in vitro* experiments, the cells were washed twice with cold Hank's balanced salt solution and lysed in the same buffer solution as for the tissue. The lysates were cleared by centrifugation at 13,000 x g at 4°C for 30 min., and the supernatant kept frozen at 80°C. The protein content of the lysates was determined using Bradford Assay (Bio-Rad), with bovine serum albumin as the standard. Proteins (15 to 30 μg) were separated by 9-12% SDS polyacrylamide gel electrophoresis (SDS-PAGE) and transferred to nitrocellulose membranes (Schleicher and Schuell, Keene, NH, USA). Membranes were incubated one hour in blocking buffer

(20 mM Tris-HCl buffered saline containing 5% nonfat milk powder and 0.1% Tween 20) at room temperature and then probed with appropriate antibodies in blocking buffer or blocking buffer including 5% bovine serum albumin instead of 5% nonfat milk overnight at 4^{o}C. Blots were incubated at 4^{o}C overnight with anti-MMP9 (1:200); anti-HIF-1α (1:200), anti-VEGF-A (1:200), anti-VEGFR2 (Fkl-1) (1:100), (all antibodies from Santa Cruz Bitotech, Santa Cruz, CA) The blots were also incubated with anti-phospho-Akt (1:1000), anti-phospho p-44/42 MAPK (1:1000), anti-phospho p38 (1:1000), and anti-phospho SAPK/JNK(1:1000) (all antibodies were purchased from Cell Signaling Technology, Inc.). The blots were washed extensively and then incubated for one hour with a 1:5000 dilution of secondary antibody. Peroxidase labeled anti-rabbit and anti-mouse secondary antibody were purchased from Kirkegaard and Perry Laboratories (Maryland, USA). Monoclonal mouse IgG antibody against beta-actin was purchased from Sigma Chemical Company. After additional washes, the blots were incubated with chemiluminescent substrate, according to directions in the kit (Super Signal West Pico, Pierce, Rockford, IL).

Gelatin zymography

Gelatinolytic activities were analyzed by gelatin zymography as previously described [83]. After microscopic dissection of frozen brain specimens, the tissues was homogenized in lyses buffer containing 50 mM Tris-HCl (pH 7.4), 150 mM NaCl, 1 mM CaCl2, 1 mM MgCl2, 0.1% Triton X-100. For the *in vitro* experiments, the conditioned media were collected after the cells were cultured in hypoxic and normoxic conditions,

concentrated 30-fold using an Amicon Ultra-15 Centrifugal Filter Device (Millipore, Bedford, MA). Protein lysates (*in vivo* experimnets) and concentrated conditioned media *(in vitro* experiments) (15 μg of protein) were incubated at 37°C for 30 minutes in SDS sample buffer without reducing agent and then subjected to SDS-PAGE in 10% (wt/vol) polyacrylamide gels containing 0.1% (wt/vol) gelatin. The gels were washed twice for 30 minutes in 2.5% (vol/vol) Triton X-100 at room temperature and then incubated for 24 h in substrate reaction buffer (50 mM Tris-HCl (pH 7.5), 100 mM NaCl, 10 mM CaCl2, 0.002% NaN3) at 37^{o}C. The gels were then stained with Coomasie Brilliant Blue R250 in 10% (vol/vol) acetic acid and 30% (vol/vol) methanol for 1 h and destained briefly in the same solution without dye. Proteolytic activities were detected as clear bands indicating the lysis of the substrate.

Total RNA extraction and semi-quantitative RT-PCR

Total RNA was extracted from frozen specimens or ENU1564 cells using a SV RNA extraction kit (Promega) using manufacturer's directions. RNA was quantified by absorbance at 260 nm. Using a Super Script III First Strand Synthesis System (Invitrogen), 100ng of total RNA was amplified by reverse transcription polymerase chain reaction (RT-PCR) and the cDNAs were amplified in a 25 μl reaction. PCR primers were as follows:

- HIF-1α primers: (forward5'-GTCGGACAGCCTCACCAAACAGAGC-3'; reverse, 5'-GTTAACTTGATCCAAAGCTCTGAG-3') [84];

- MMP 9 primers: (forward, 5'- CCCCACTTACTTTGGAAACGC-3'; reverse, 5'-ACCCACGACGATACAGATGCTG-3') [12];
- VEGF primers: (forward: 5'-GACCCTGGTGGACATCTTCCAGGA-3'; reverse, 5'-GGTGAGAGGTCTAGTTCCCGA-3') [64];
- VEGFR2 primers: (forward: 5'-GCCAATGAAGGGGAACTGAAGA-3'; reverse, 5'-CTCTGACTGCTGGTGATGCTGTC-3') [85];
- β-actin primers (forward, 5'- ATGTACGTAAGCCAGGC-3'; reverse, 5'-AAGGAACTGGAAAAGAGC -3') [12].

Expected size for MMP-9 PCR product was 686 base pairs (bp). PCR condition for MMP-9 was carried out with an initial denaturation of 94^{o}C for 2 minutes, followed by 30 cycles at a denaturation of 94^{o}C for 1 minute, annealing at 59.1^{o}C for 30 seconds and extension at 72^{o}C for 1 minute. A final extension of 5 minutes at 72^{o}C was carried out. For HIF-1α, 25 cycles were carried out with 30 seconds at 95^{o}C, 1 minute at 55^{o}C and 2.5 minutes at 72^{o}C. A final extension of 7 minutes at 72^{o}C was carried out. The PCR product size for HIF-1α was 487 bp. For VEGF, one set of rat primers, which amplified 3 splicing variants of a rat VEGF mRNA (VEGF $_{120}$, VEGF $_{164}$ and VEGF $_{188}$) was used. The PCR profile consisted of initial denaturation at 94^{o}C for 7 minutes, followed by 35 cycles of denaturation at 94^{o}C for 30 seconds, annealing at 58^{o}C for 30 seconds, extension at 72^{o}C for 90 seconds, and extension at 72^{o}C for 7 minutes. The expected length of the PCR products was 330 bp for VEGF $_{120}$, 462 bp for VEGF $_{164}$, and 514 bp for VEGF $_{188}$. Expected size for VEGFR2 PCR product was 537 base pairs. PCR condition for VRGFR2 was carried out with an initial denaturation of 94^{o}C for 3

minutes, followed by 30 cycles at a denaturation of 94^{o}C for 30 seconds, annealing at 60^{o}C for 30 seconds and extension at 72^{o}C for 30 seconds. A final extension of 5 minutes at 72^{o}C was carried out. To demonstrate the integrity of the RNA samples used in the RT-PCR reactions, parallel amplifications with oligonucleotide primers for mouse β-actin were performed. The expected size for β-actin PCR product was 403 bp. PCR fragments were analyzed on 1.5% agarose gels stained with ethidium bromide.

Statistical analysis

Quantification of the Western blot, gelatin zymography, and semi-quantitative RT-PCR bands density was performed on a Macintosh computer using the public domain NIH Image program (developed at the U.S. National Institutes of Health and available on the Internet at http://rsb.info.nih.gov/nih-image. Data were presented as mean ± S.D., and statistical comparisons were made using Student *t*-test. A *P*-value of < 0.05 was considered statistically significant.

Results: *In vivo* studies

Immunolocalization of HIF-1α protein in the tumor foci

Tumor cells respond to low-oxygen conditions via the stabilization and activation of hypoxia-inducible factor 1α (HIF-1α), a transcription factor critical for adaptive responses to reduced oxygen. Immunohistochemistry for HIF-1α was performed in order to demonstrate that hypoxia was localized within the tumor foci. IHC results

showed the cytoplasmic and nuclear immunolabeling with moderate intensity of the neoplastic cells within the brain tumor foci **(Figure 17a, and 17b).** Positive control, represented in **Figure 17c and 17d**, showed that some neurons also had moderate staining in the cytoplasm but not in the nucleus. A negative control is represented in the **Figure 17e**.

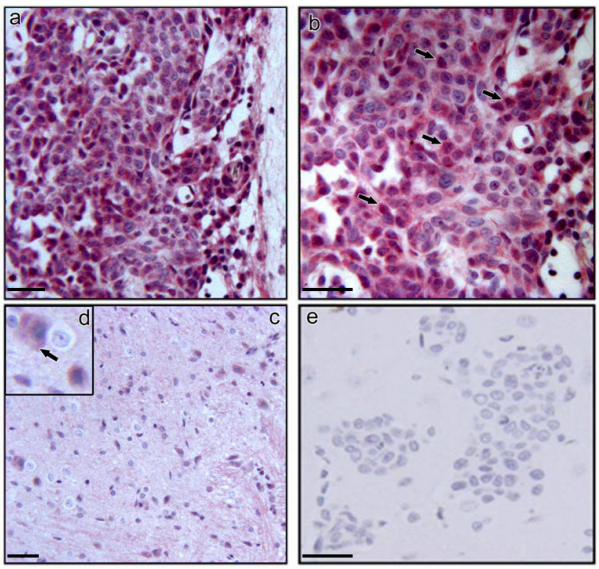

Figure 17. Localization of HIF-1α in hypoxic tumor foci. Immunohistochemical staining (red) of HIF-1α protein in the tumor foci revealed positivity within neoplastic cell cytoplasm and nucleus (**a, b**). Arrows indicate the neoplastic cells within tumor foci which stain positive for HIF-1α in both cytoplasm and nucleus. Positive control is represented in panel (**c**) and revealed cytoplasmic HIF-1α staining. (**d**) Higher magnification view of the neurons in panel (**c**). Note the absence of nuclear HIF-1α staining in neurons. Arrow indicates cytoplasmic HIF-1α staining of the neurons. Sections exposed to a negative control antibody showed no staining reactions (**e**). Bars indicate 200 μm.

Immunohistochemistry for vascular endothelial growth factor (VEGF-A) and vascular endothelial growth factor receptor VEGFR2 (Flk-1)

Further analysis was focused on the VEGF-A and VEGF receptor, VEGFR2 (Flk-1). Immunohistochemical staining for VEGF and VEGFR2 (Flk-1) was performed in order to characterize the expression of these proteins within tumor foci. Previous studies showed that HIF-1α is the major transcription factor responsible for induction of VEGF production and secretion. IHC staining for VEGFR2 (Flk-1) showed immunolabeling of the neoplastic cells **(Figure 18a, 18b and 18c).** Endothelial cells lining blood vessels also show positivity for VEGFR2 **(Figure 18d)**. No staining was observed in the negative controls (data not shown).

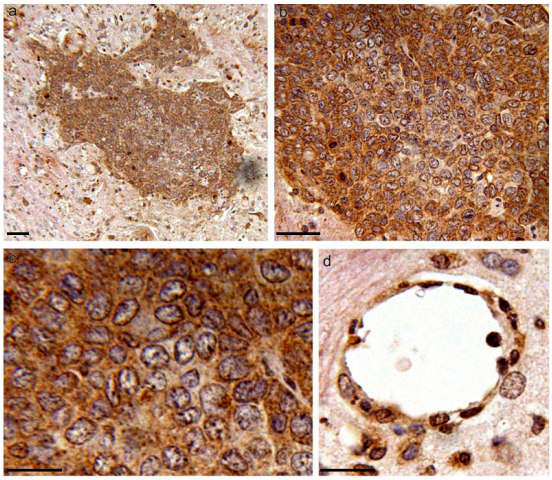

Figure 18. Localization of VEGFR2 (Flk-1) in the brain tumor foci. (**a**) VEGFR2 labeling of the tumor foci. (**b, c**) Higher magnification views of tumor cells showing cytoplasmic and membrane VEFGR2 staining. (**d**) Endothelial cells lining a blood vessel adjacent to the tumor foci also stain positive for VEGFR2. Bars indicate 200 μm.

VEGF staining was observed in the cytoplasm of the neoplastic cells **(Figure 19a and 19b).** Positive control revealed that some glial cells are also labeled for VEGF-A (**Figure 19c).** Endothelial cells lining blood vessels also show positivity for VEGF-A (**Figure 19d).** No staining was observed in the negative controls (data nor shown).

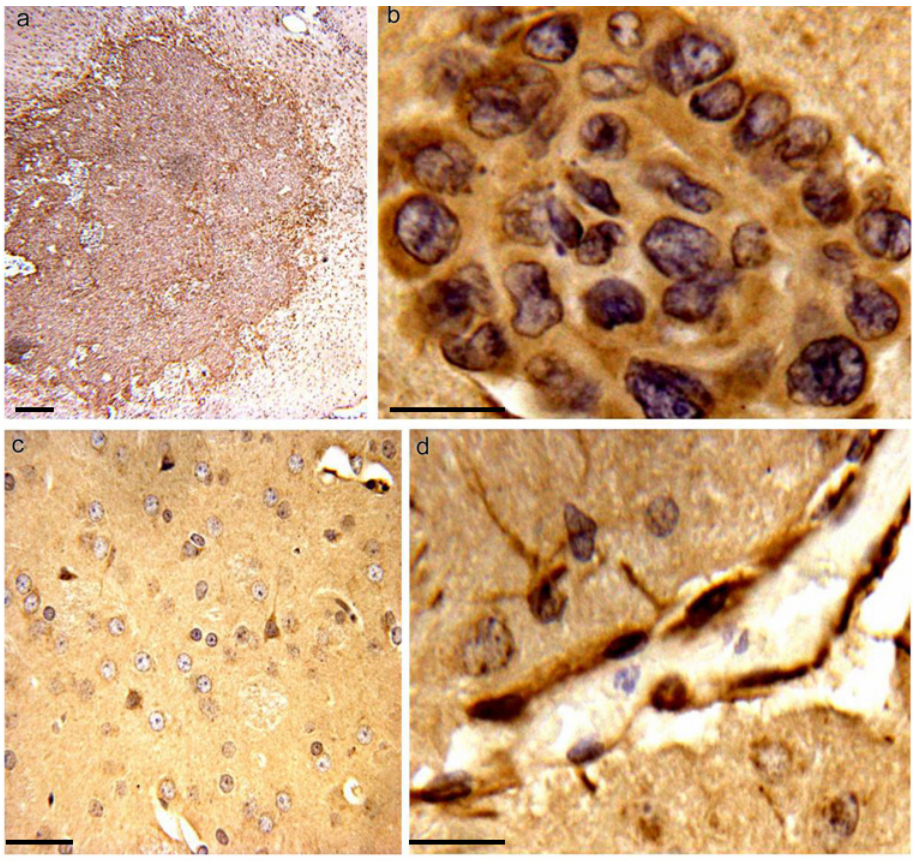

Figure 19**.** Immunolocalization of VEGF-A in brain tumor foci and surrounding glial cells. (**a**) low-power view of VEGF-A-positive tumor foci. (**b**) Higher magnification view of tumor cells showing cytoplasmic VEGF-A staining. (**c**) positive control showing VEGF-A labeling of some glial cells. (**d**) Endothelial cells lining a blood vessel adjacent to the tumor foci also stain positive for VEGF-A. Bars indicate 200 µm.

Immunohistochemistry for MMP-9 in brain tumor foci

Given the fact that in addition to the upregulation of VEGF, hypoxia may be a factor in activation of extracellular matrix degrading proteases, we evaluated IHC for MMP-9. Immunohistochemical staining for MMP-9 showed immunolabeling with moderate intensity in the neoplastic cell cytoplasm and faint staining of the glial cells **(Figure 20a and 20b).** Negative control slide is represented in **Figure 20c.**

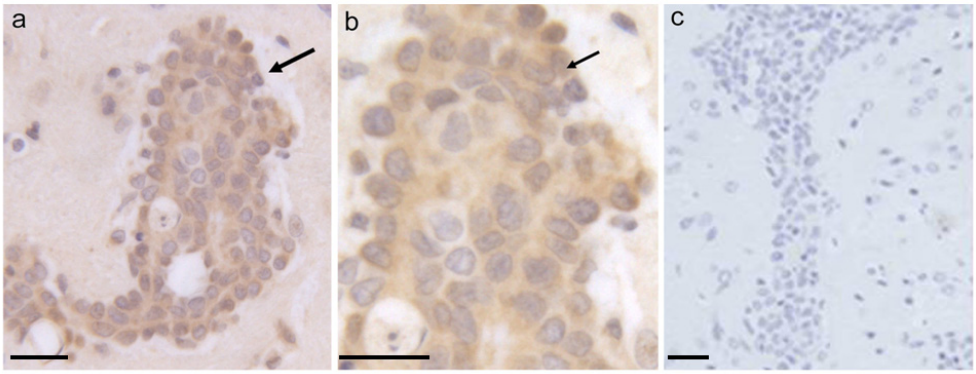

Figure 20**.** Localization of MMP-9 in the brain tumor foci. (**a**) Immunohistochemical staining (brown) of MMP-9 protein in the tumor foci. Note moderate staining in the neurons. (**b**) Higher magnification view of the tumor cells showing cytoplasmic MMP-9 staining. Arrows indicate the tumor foci. Negative control for MMP-9 is shown in panel (**c**). Bars indicate 200 μm.

Increased expression of HIF-1α, VEGF-A and VEGFR2 (Flk-1) proteins in brain tumor foci

To confirm the IHC results on HIF-1α, VEGF-A and VEGFR2 (Flk-1) we extracted proteins from brain tumor foci and control brain. Evaluation of protein expression by Western blotting revealed that all three proteins were significantly higher

in tumor foci compared with control tissue from brains of age-matched-non-inoculated rats **(Figure 21a).**

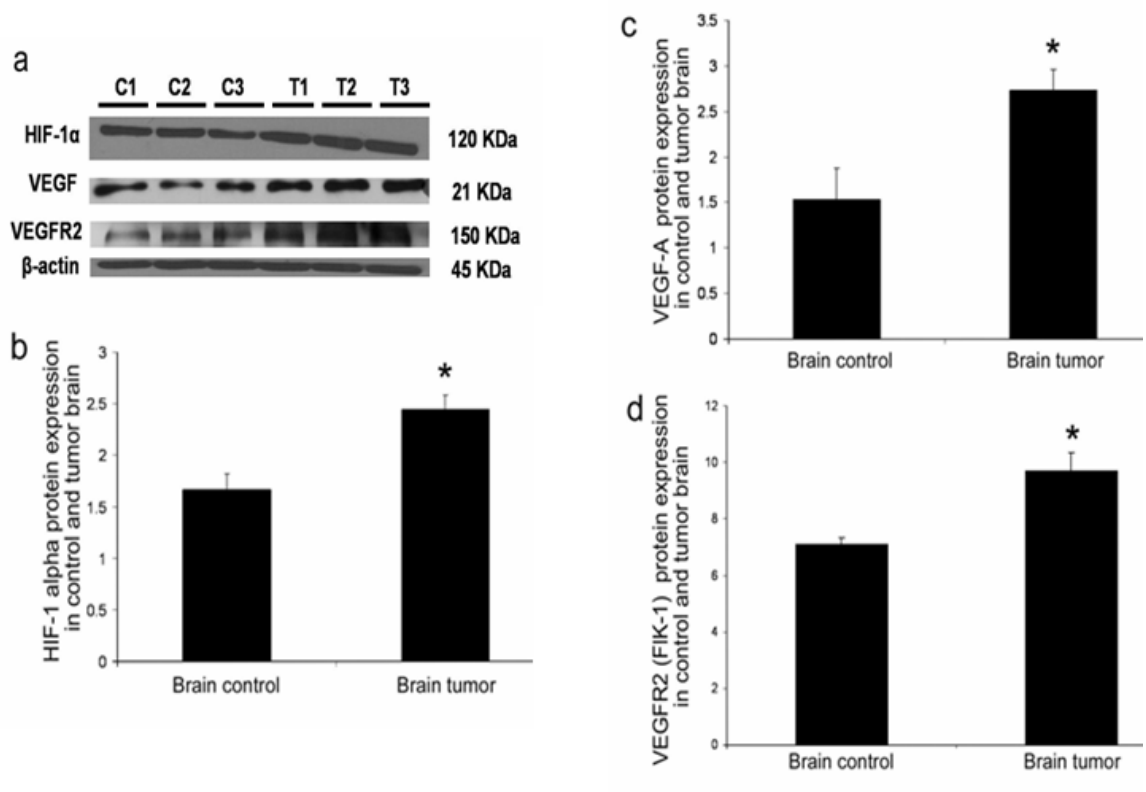

Figure 21**.** Increased expression of HIF -1α, VEGF-A, and VEGFR2 (Flk-1) proteins in neoplastic cells. (**a**) Evaluation of protein expression by Western blotting. The membranes were stripped and re-probed with β-actin antibody to confirm equal loading. (**b, c, d**) Densitometric analysis of HIF -1α, VEGF-A, and VEGFR2 (Flk-1) protein expression in tumor cells showed significant increases compared with control brain. The results represent the mean ± standard deviation for three control and three tumor samples. C-control, T-tumor; Asterisks indicate statistically significant differences (*, $P < 0.05$).

Given that HIF-1α is the major transcription factor responsible for induction of VEGF production and secretion it was important to determine if VEGF was also upregulate in neoplastic cells. VEGFR2 (Flk-1) protein, which is a VEGF receptor was also found to be significantly upregulate in tumor foci. Quantitative analysis **(Figure 21b, 21c, and 21d)** was determined by densitometry.

Increased MMP-9 activity in brain tumor foci

To confirm the IHC results on MMP-9 protein expression and to evaluate the enzymatic activity of MMP-9 in the brain tumor foci gelatin zymography was performed. The results revealed an increase in enzymatic activity of MMP-9 in brain tumor foci compared with control brain **(Figure 22A)**. Quantitative analysis determined by densitometry revealed an increase in pro and active forms of MMP-9. **Figure 22B** represents the quantitative analysis of MMP-9 determined by densitometry of the active band (b).

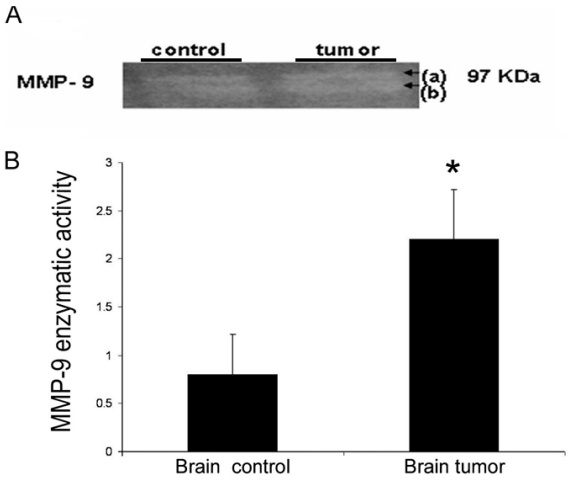

Figure 22. MMP-9 enzymatic activity in brain tumor foci compared with brain control. (**A**) Increased MMP-9 enzymatic activity in the tumor foci. The double band at 97 KDa corresponded to the latent form (a) (proenzyme) and active form (b) of MMP-9. (**B**) Quantitative analysis of MMP-9 was determined by densitometry of the active band (b). Data are represented as mean ± standard deviation, for three independent experiments and asterisks indicate statistically significant differences (*, $P < 0.05$).

Increased expression of HIF-1α, VEGF-A, and MMP-9 mRNA in the SD rat brain tumor cells

To confirm the IHC and Western blot results on HIF-1α, VEGF-A, and MMP-9 protein expression, we prepared cDNA from dissected tumor sample and performed semi-quantitative RT-PCR analysis. Although this technique is semi-quantitative, our results indicate that there were higher levels of HIF-1α, VEGF-A, and MMP-9 mRNA in brain tumor foci than in normal brain tissues from age-matched-non-inoculated rats (**Figure 23a).**

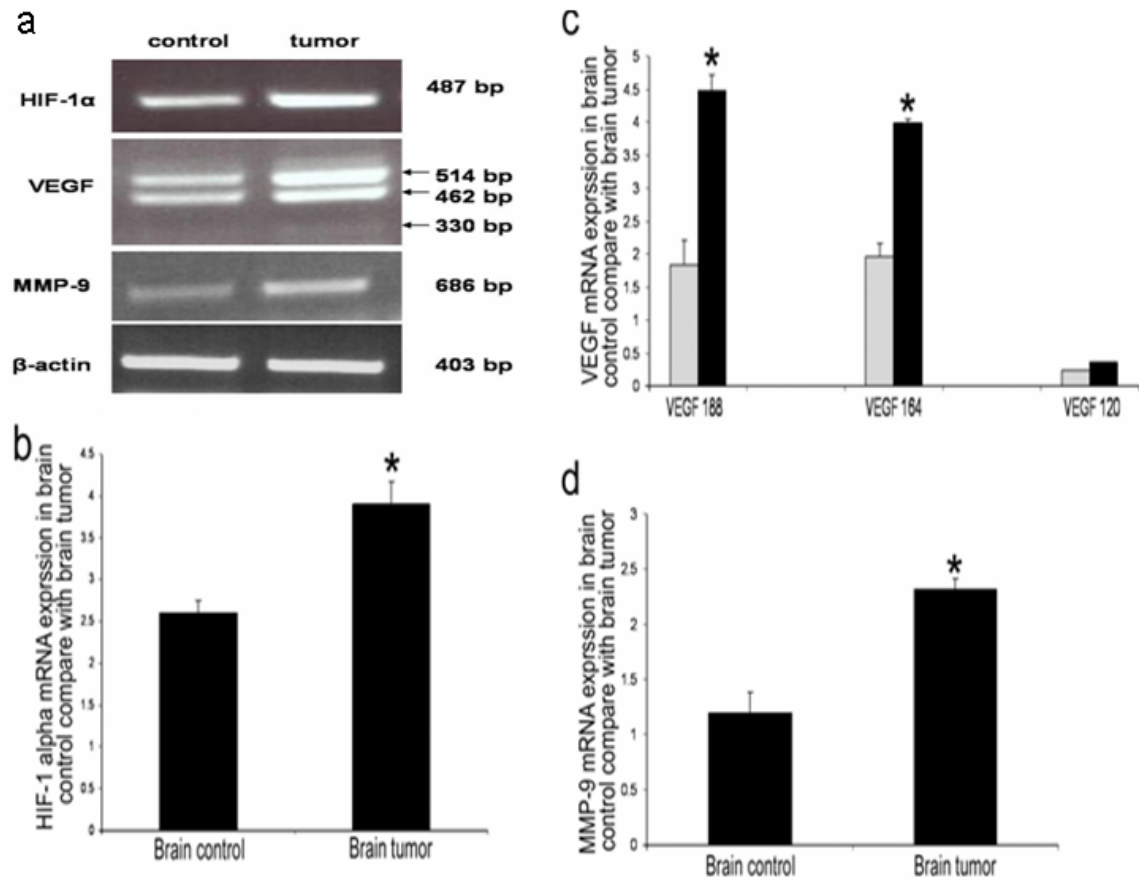

Figure 23**.** Increased expression of HIF-1α, VEGF, and MMP-9 mRNA in the rat neoplastic brain foci. (**a**) Semi-quantitative RT-PCR was used to detect HIF-1α, VEGF, and MMP-9 and β-actin in total RNAs from normal brain and neoplastic brain foci. β-actin was used as an internal control. For VEGF three alternative splicing variants were identified. A 330 bp product, which is identical to that of the alternative splicing VEGF 120 isoform. A second 462 bp product, corresponding to the VEGF164 isoform, and a third 514 bp product, corresponding to the VEGF188 isoform were also detected. VEGF188 isoform expression was greater than those of $VEGF_{164}$ and $VEGF_{120}$. (**b, c, d**) .Quantitative analysis of VEGF, MMP-9, and HIF-1 was determined by densitometry. The results are mean ± standard deviation from three controls and three tumor samples. * P <0.05.

Results: *In vitro* studies

In vitro invasive potential of cancer cells

To determine whether hypoxia influences the *in vitro* ENU1564 cells invasive potential we used a Matrigel-based invasion assay. The *in vitro* invasive potential of ENU1564 cells grown under hypoxic conditions were compare with ENU 1564 cells grown under normoxic conditions. Boyden chamber chemoinvasion analysis showed that a significant smaller number of hypoxic ENU1564 cells ($P< 0.05$) invaded the Matrigel compared with ENU1564 cells grown in normoxic conditions **(Figure 24).**

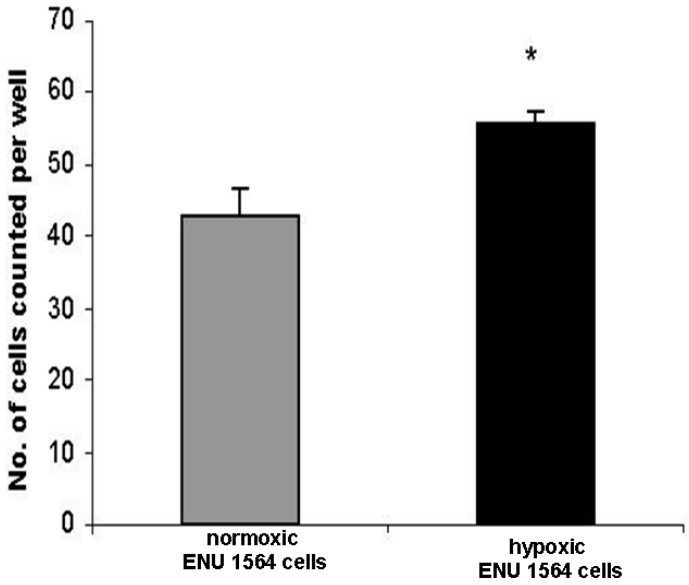

Figure 24. Metastatic potential of hypoxic ENU1564 cells. *In vitro* invasive chamber assay was performed as described in material and methods. The results showed in the histogram are the mean of ± standard deviation of two independent experiments run triplicate; (*) statistically significant ($P< 0.05$).

Increase HIF-1α protein expression in hypoxic ENU1564 cells

Next we investigated whether exposure of ENU1564 cells to hypoxia for 24 hours would increase HIF-1α protein levels. As expected, HIF-1α protein levels were increased in response to hypoxia after 24 hours (**Figure 25**) compared with ENU1564 cells grown in normoxic conditions, where the levels of HIF-1α protein was very low.

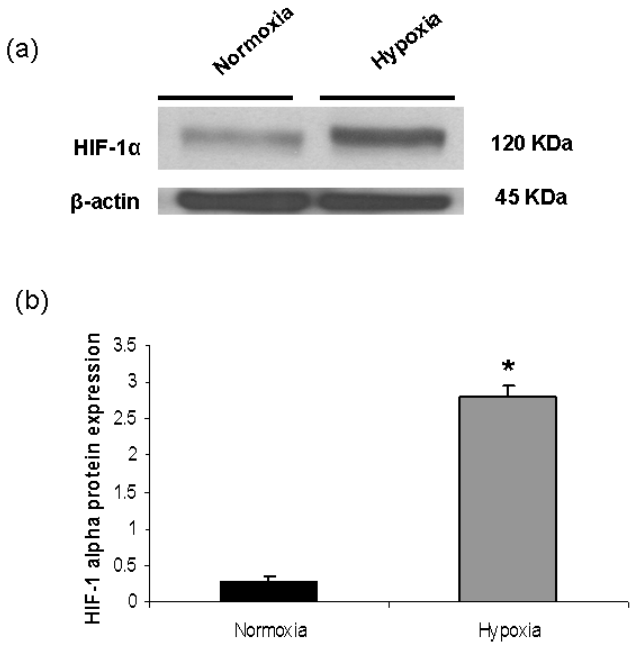

Figure 25. Increased HIF-1α protein expression in hypoxic ENU1564 cells. (a) Western blot analysis showing increase HIF-1α protein expression in hypoxic ENU1564 cells. (b) Quantitative analysis of HIF-1 was determined by densitometry. The results are mean ± standard deviation from three independent experiments. * P <0.05.

Increased MMP-9 mRNA expression in hypoxic ENU1564 cells

MMP-9 plays an important role in tumor invasion and metastasis. Prior observations have suggested that acidity in the tumors can be caused by hypoxia-dependent and/or-independent pathways and MMP-9 was found to be induced by culturing cells at an acidic pH [79]. We investigated the MMP-9 mRNA expression in ENU1564 cells grown in normoxic and hypoxic environment to asses the role of MMP-9 in tumor invasion and metastasis. We found a significant increase in MMP-9 mRNA expression in hypoxic ENU1564 cells compared with normoxic ENU1564 cells **(Figure 26).** MMP-9 is one of the proteins responsible for degradation of extracellular matrix and increased invasion potential of ENU1564 cells. We can conclude that hypoxia through upregulation MMP-9 expression is a powerful stimulus for cancer cell invasion and metastasis.

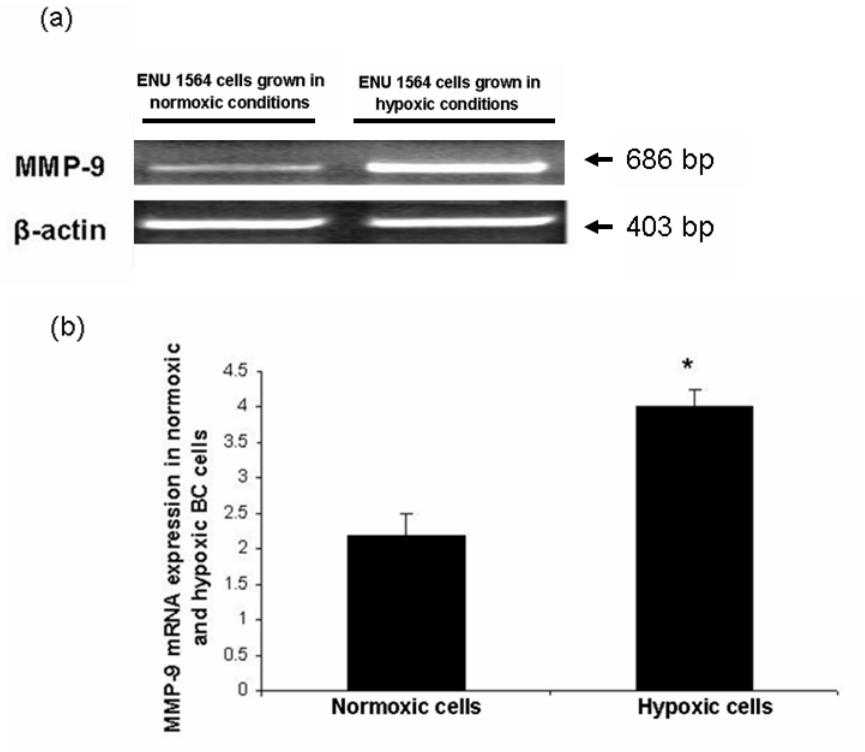

Figure 26. Increased expression of MMP-9 mRNA in hypoxic ENU1654 cells. (**a**) Semi-quantitative RT-PCR was used to MMP-9 and β-actin in total RNAs from ENU1564 cells grown in hypoxic and normoxic conditions as described in materials and methods. β-actin was used as an internal control. (**b**) Quantitative analysis of MMP-9 mRNA was determined by densitometry. The results are mean ± standard deviation from three controls (cells grown in normoxia) and three hypoxic samples. * P <0.05.

Increased MMP-9 activity in hypoxic ENU1564 cells

To confirm the RT-PCR results on MMP-9 mRNA expression we evaluated the enzymatic activity of MMP-9 in the conditioned media collected from ENU1564 cells grown in hypoxic and normoxic condition by gelatin zymography. The results revealed that hypoxia increases MMP-9 secretion from ENU1564 cells when compared with the levels of MMP-9 from normoxic ENU1564 cells **(Figure 27)**. Quantitative analysis

determined by densitometry revealed an increase in pro and active forms of MMP-9. **Figure 27** represents the quantitative analysis of MMP-9 determined by densitometry of the active band (b).

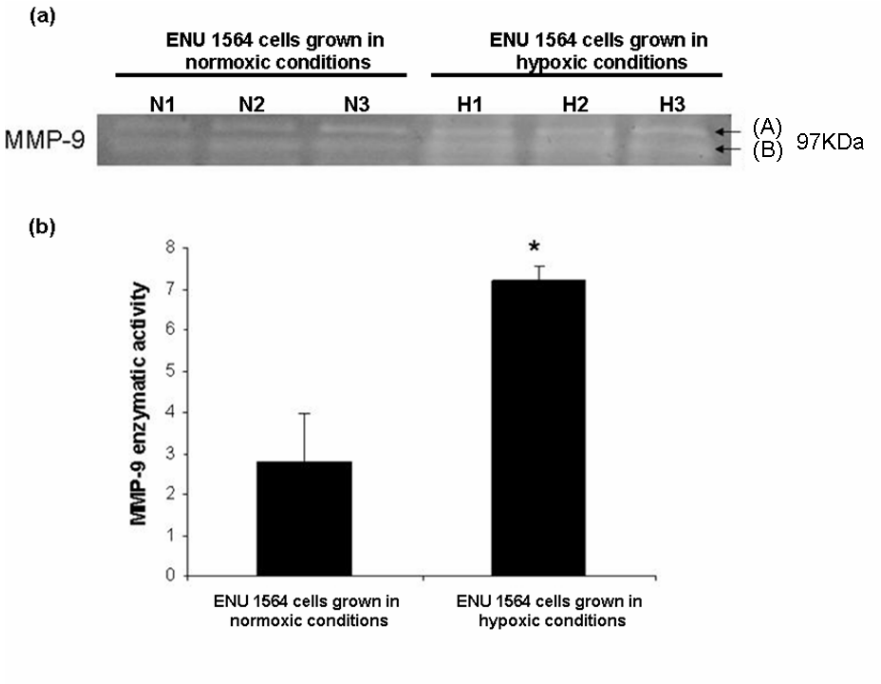

Figure 27**.** Increased MMP-9 enzymatic activity in hypoxic ENU1564 cells. (**a**) Gelatin zymography of ENU1564 conditioned media was performed as described in Materials and Methods. Conditioned media was collected from ENU1564 cells grown in normoxic and hypoxic condition. The double band at 97 KDa corresponded to the latent form (A) (proenzyme) and active form (B) of MMP-9. (**b**) Quantitative analysis of MMP-9 was determined by densitometry of the active band **(B).** Data are represented as mean ± standard deviation, for three independent experiments and asterisks indicate statistically significant differences (*, $P < 0.05$); N1-N2, normoxic cells; H1-H3, hypoxic cells.

Increased expression of VEGF-A and VEGFR2 in hypoxic ENU1564 cells

Hypoxia was found to be is a strong inducer of VEGF, and hypoxia-induced VEGF expression determines the course of various disease conditions, such as solid tumor growth [65]. We found that both VEGF-A and VEGFR2 mRNA expression are significantly elevated in hypoxic ENU1564 cells compared to normoxic ENU1564 cells **(Figure 28).**

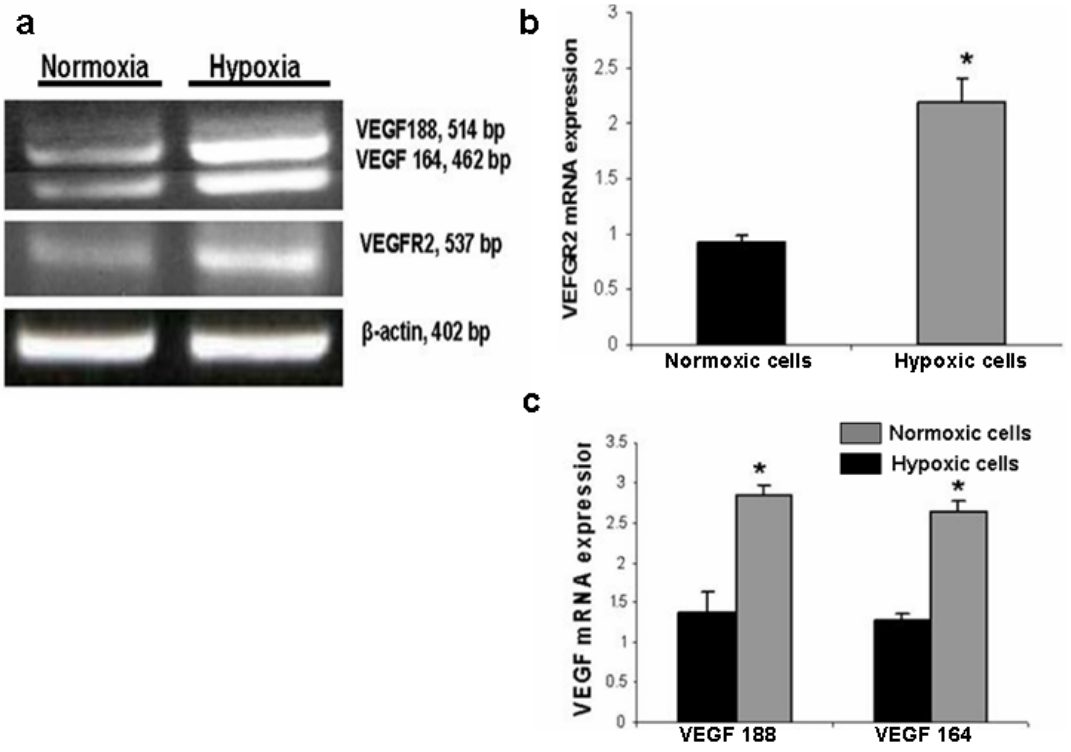

Figure 28. Increased VEGF-A and VEGFR2 mRNA expression in hypoxic ENU1564 cells. (**a**) VEGF-A and VEGFR2 mRNA expression in hypoxic ENU1564 cells compared with normoxic cells. β-actin was used as an internal control. **(b)** Quantitative analysis of VEGF-A and VEGFR2 mRNA expression was determined by densitometry. The results are mean ± standard deviation from three controls and three tumor samples. * P <0.05.

Increased Akt phosphorylation in hypoxic ENU1564 cells

Several kinase pathways, including PI3K-Akt and ERK1/2 have been described to be activated by hypoxia [86]. Here we provide evidence that hypoxia induce a significant increase in phosphorylation of Akt in ENU1564 cell line compared with normoxic ENU1564 cells (**Figure 29**).

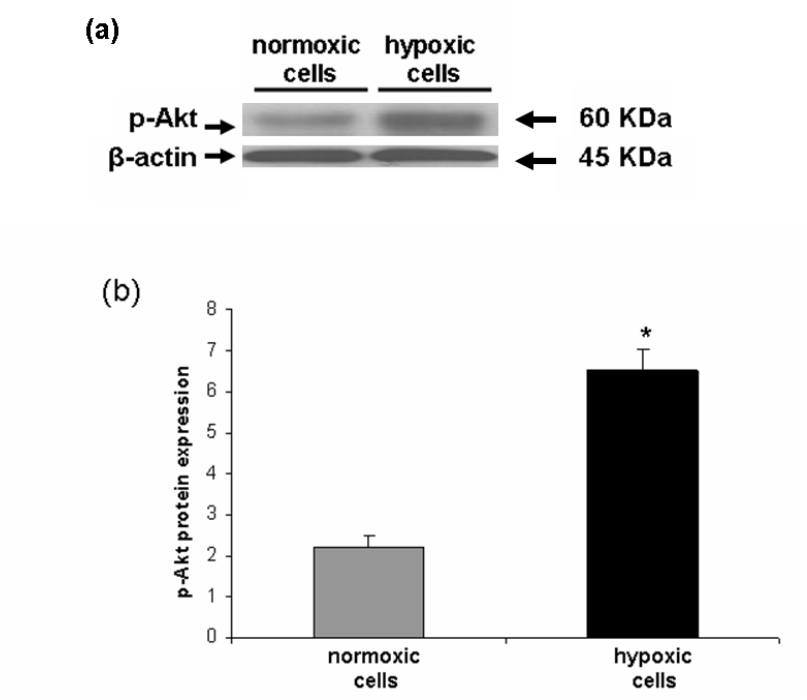

Figure 29. Increased Akt phosphorylation in hypoxic ENU1564 cells. (**a**) Western blot analysis of phospho–Akt expression in ENU1564 cells grown in hypoxic and normoxic conditions for 24 hour as described in Materials and Methods. β-actin was used as an internal control. (**b**) Quantitative analysis of phospho-Akt was determined by densitometry. The results are mean ± standard deviation from three controls (cells grown in normoxia) and three hypoxic samples. * P <0.05.

Hypoxia-induced expression of MMP-9, VEGF-A but not VEGFR2 involves PI3K-Akt pathway

We next investigated the role of PI3K-Akt pathway in hypoxia-induced expression of MMP-9, VEGF-A, and VEGFR2 by using a specific PI3K inhibitor, LY294002. The ENU1564 cells were pretreated with or without (DMSO only) the inhibitor for 1 hour and then cultured in hypoxic conditions for 24 hours as described in materials and methods. ENU1564 cells grown in normoxic conditions were used as controls. We investigated the expression of the proteins of interest by Western blot analysis. We showed that hypoxia induced increased expression of MMP-9, VEGF-A and VEGFR2, and the pretreatment of ENU1564 cells with PI3K inhibitor significantly decreased the levels of MMP-9 and VEGF-A but there was no change in the levels of VEGFR2 compared with untreated cells **(Figure 30)**. From this experiment we conclude that hypoxia regulation of VEGFR2 levels in ENU1564 cells may involve a different signaling pathway other than PI3K-Akt.

Increased ERK1/2 phosphorylation in hypoxic ENU1564 cells

The mitogen activated protein kinase (MAPK) pathway is one of most important transduction signaling pathways that is related with numerous pathogenic processes, including neoplasia. ERK1/2 has been described to be activated by hypoxia [86].

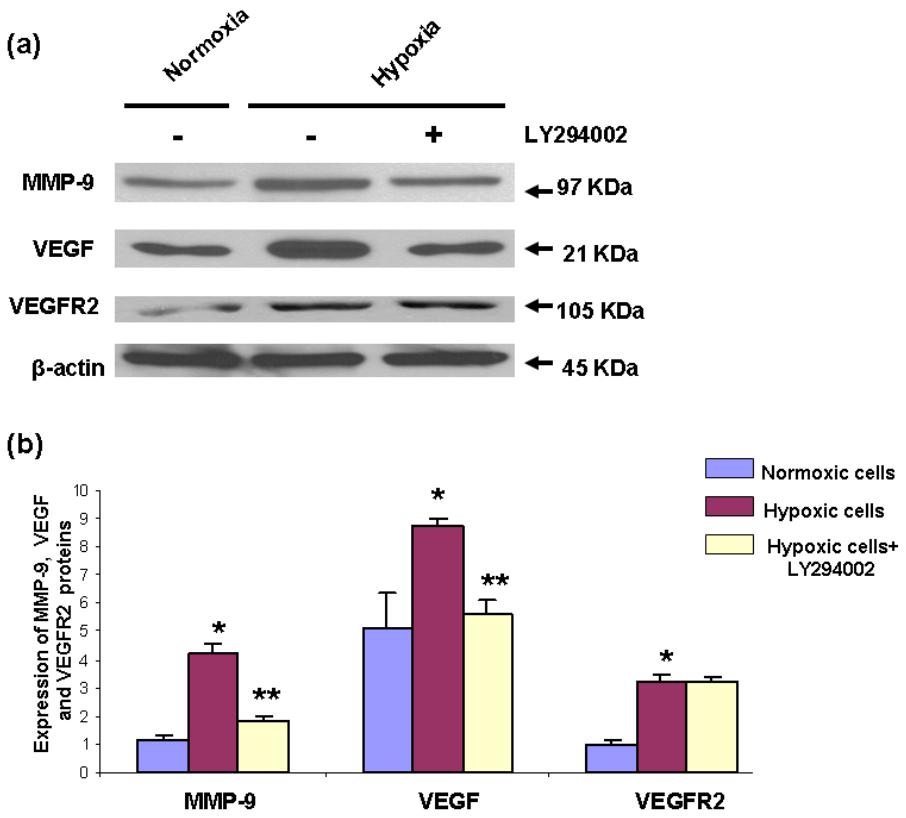

Figure 30. Involvement of PI3K-Akt signaling pathway in hypoxia-induced expression of MMP-9, VEGF-A, but not VEGFR2 expression. (a) Western Blot analysis using anti-MMP-9, anti-VEGF-A, anti-VEGFR2 and β-actin antibodies (loading controls) were performed and show increased levels of MMP-9, VEGF, and VEGFR2 in hypoxic ENU1564 cells compared with normoxic ENU1564 cells. The levels of MMP-9 and VEGF-A proteins significantly decreased when the cells were pretreated with PI3K inhibitor for 1 hour prior to exposure to hypoxic conditions but there was no change in VEGFR2 levels; (b) Quantitative analysis of MMP-9, VEGF, and VEGFR2 was determined by densitometry, The results represent the mean of ± standard deviation from three independent experiment; (*significant different from normoxic cells, $P< 0.05$, (**,significant different from hypoxic untreated cells, $P< 0.05$).

These points prompted us to investigate if ERK1/2 is activated in hypoxic ENU1564 cells. Our results showed that there is a significant increase of phospho-ERK1/2 in hypoxic ENU1564 cells **(Figure 31).**

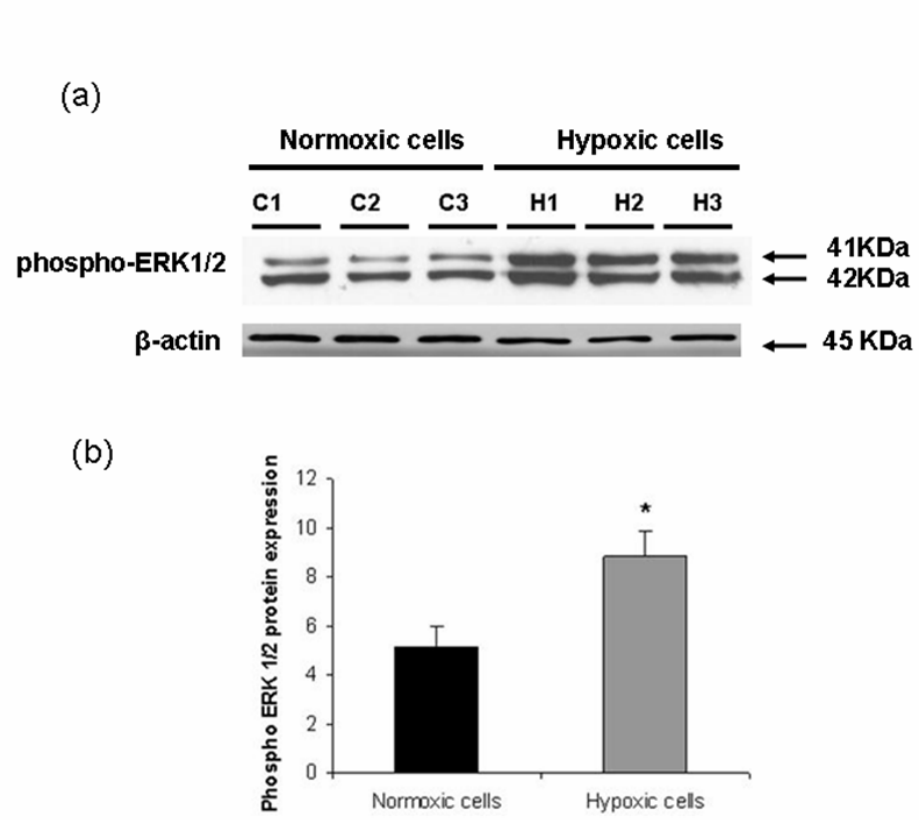

Figure 31. Increased ERK1/2 phosphorylation in hypoxic ENU1654 cells. (**a**) Western blot analysis of phospho–ERK1/2 expression in ENU1564 cells grown in hypoxic and normoxic conditions as described in materials and methods. β-actin was used as an internal control. (**b**) Quantitative analysis of phospho-ERK 1/2 was determined by densitometry. The results are mean ± standard deviation from three controls (cells grown in normoxia) and three hypoxic samples. * P <0.05; C1-C3, normoxic cells (control), H1-H3, hypoxic cells.

Activation of the MAPK pathway in tumor cells is well correlated with cancer cell invasive and metastatic phenotype [87]. MAPK pathway has been related to MMP activation and expression [81, 87].

Hypoxia-induced expression of MMP-9, VEGF and VEGFR2 involves ERK1/2

Next we wanted to investigate the role ERK1/2 pathways in hypoxia-induced expression of MMP-9, VEGF-A and VEGFR2 protein expression. The ENU1564 cells were pretreated with or without (DMSO only) the inhibitor for 1 hour and then cultured in hypoxic conditions for 24 hours. Cells grown in normoxic conditions were used as controls. Total lysates were collected for WB analysis. **Figure 32** shows that there is a significant increase in phospho-ERK1/2 in hypoxia which was prevented by MEK1/2 inhibitor, PD98059. Also, it shows that there is a significant increase in MMP-9, VEGF-A and VEGFR2 in hypoxic ENU1564 cells compared with normoxic cells, which was decreased by MEK1/2 inhibitor, PD98059. These results confirm the involvement of MEK1/2-ERK1/2 in hypoxic stimulation of MMP-9, VEGF and VEGFR2 proteins.

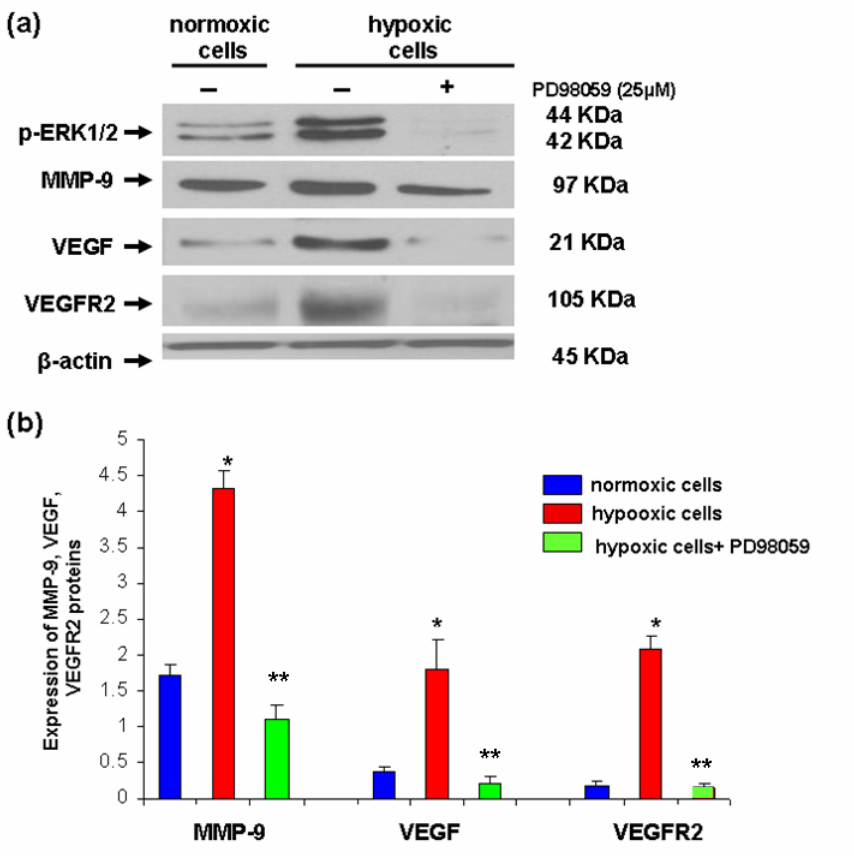

Figure 32. Involvement of MEK1/2-ERK1/2 signaling in hypoxia-induced expression of MMP-9, VEGF-A, and VEGFR2 expression. (a) Western blot analysis using anti-phospho ERK1/2, anti-MMP-9, anti-VEGF-A, anti-VEGFR2 and β-actin antibodies (loading controls) were performed and show increased levels of phospho-ERK1/2, MMP-9, VEGF-A and VEGFR2 in hypoxic ENU 1564 cells compared with normoxic ENU 1564 cells. The levels of these proteins significantly decreases when the cells were pretreated with MEK1/2 inhibitor for 1 hour prior to exposure to hypoxic conditions; (b) Quantitative analysis of MMP-9 proteins, VEGF-A, and VEGFR2 was determined by densitometry, The results represent the mean of ± standard deviation from three independent experiment; (*,significant different from normoxic cells, $P<0.05$, (**,significant different from hypoxic untreated cells, $P< 0.05$).

Hypoxia did not activate p38 nor SAPK/JNK in ENU15464 cells

We demonstrated that hypoxia activates both Akt and ERK1/2 signaling pathways in ENU1564 cells. Since hypoxia is a typical stress factor for rapidly growing tumors cells, it was interesting to analyze whether hypoxia might infuce p38 or SAPK/JNK activation in cancer cells. Surprisenly, Western blot analysis showed no difference in the phosphorylation levels of these proteins in normoxic and hypoxic cells (F**igure 33**). Activation of there proteins might be a cell specific phenomenon.

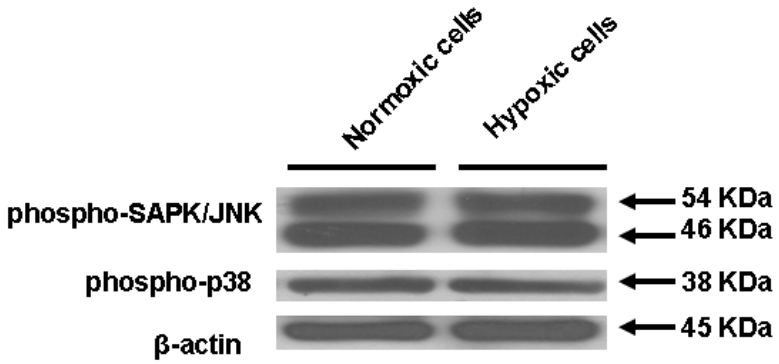

Figure 33. Hypoxia did not activate p38 nor SAPK/JNK in ENU1564 cells. (a) Western Blot analysis using anti-phospho p38, anti-SAPK/JNK, and anti-β-actin antibodies (loading controls) were performed and show no change in the levels of phospho-p38 and phospho-SAPK/JNK in hypoxic ENU1564 cells compared with normoxic ENU 1564 cells. The experiment was run in triplicate with the same result.

Discussion

We found increased expression of HIF-1α, VEGF-A, VEGFR2, and MMP-9 mRNA and proteins in the brain tumor foci suggesting that these molecules may be induced by tumor hypoxia and may be directly involved in the invasion of the tumor cells into the brain parenchyma.

We used non-inoculated brains of age-matched rats as controls, assuming that differences in HIF-α, VEGF, VEGFR2, and MMP-9 would be attributable to the presence of tumors. Our results showed the increased expression of HIF-1α at both protein and mRNA levels, which is an indicator of the existence of hypoxia in the brain tumor foci. These results were in accordance with previous studies, which showed elevated HIF-1α expression in a variety of human tumors and pre-neoplastic lesions [73, 74]. Immunohistochemistry revealed the localization of HIF-1α protein in the cytoplasm and nucleus of neoplastic cells. Localization of the HIF-1α in the nucleus is an indication of protein stability in hypoxic conditions which is the major transcription factor responsible for induction of VEGF production but can also activate different genes by binding to their promoter sequences. Hypoxia-induced expression of VEGF has been well established in various types of non-neoplastic and neoplastic cells [88, 89].

Considering that previous studies showed that matrix metalloproteinases are important in tumor invasion and metastasis [27, 78, 12], we focused on MMP-9 expression in brain tumor foci. Evidence suggested that MMP-9 was associated with intra-tumoral angiogenesis and with the metastatic process of breast cancer. Our results showed an increase expression of protein and mRNA level of MMP-9 in the brain tumor

foci compared with non-inoculated control brain. Gelatin zymography confirmed an increase in gelatinase activity of MMP-9 in tumor brain foci. These results are in accordance with the previous reports correlating MMP-9 activity with invasive and metastatic behavior [90]. The upregulation of MMP-9 in brain tumor foci might be directly related to the presence of hypoxia in the brain tumor foci. Interestingly, previous studies showed that besides the upregulation of HIF-1α in hypoxia other transcription factors such as c-jun/AP-1 (activator protein) are also upregulated [69]. Elevation of AP-1 level in hypoxic cells can be one possible mechanism of the MMP-9 upregulation since the promoter of MMP-9 has a site for binding of AP-1 complex.

We analyzed the expression level of VEGFR2 and VEGF-A in brain tumor foci since the mechanism involved in tumor invasion may include hypoxic regulation of cytokine release, and growth factor receptor. In this study, comparison of tumor xenograft and control brains demonstrated that the brain tumor up-regulated the expression of VEGF mRNA and protein, which arose as three alternative splicing variants VEGF120, VEGF164 and VEGF188. The genetic studies showed that the VEGF120 isoform alone is able to initiate, but not complete, the angiogenic programme [63]. Although the target of VEGF was thought to be restricted to endothelial cells, more and more evidence has indicated that nonendothelial cells can be VEGF targets by expressing VEGF receptors [63]. The production and upregulation of VEGF in brain tumor foci is important for tumor vascularization and may confer proteolytic activity to the neoplastic cells by induction of MMP-9. Our results showed that VEGFR2 protein was upregulated in brain tumor foci compared with brain control (Fig. 9a). VEGFR2 is

considered to be the main mitogenic signaling receptor for VEGF [91]. Skobe *et al,* demonstrated the role of VEGFR2 for the invasive growth of skin squamous cell carcinoma cells [91]. Recently, Noda *et al*., 2005 demonstrated the hypoxic upregulation of VEGF and VEGFR2 and their involvement in hypoxia-induced MT1-MMP expression in retinal glial cells. This upregulation was abrogated in the presence of SU1498, a selective inhibitor of VEGFR2 or by using a neutralizing anti-VEGF antibody [92]. The upregulation of VEGF, VEGFR2 and MMP-9 might be a consequence of decreased tissue oxygen concentration which leads to upregulation of HIF-1α. Direct or indirect interaction of both transcription factors c-jun/AP-1 and HIF-1α is a suggested mechanism for regulation of at least some of the known hypoxia-inducible genes. Upregulation of all these factors under hypoxic conditions enables the cells to survive reduced tissue oxygen concentration by promoting angiogenesis and tumor metastasis.

In order to confirm the *in vivo* results regarding the expression of HIF-1α, MMP-9, VEGF-A and VEGFR2 proteins we cultured our cells line ENU1564 in hypoxic and normoxic conditions and analyzed the expression of these proteins. We found an increased expression of HIF-1α proteins, MMP-9, VEGF-A and VEGFR2 mRNA and proteins in hypoxic ENU1564 cells compared with normoxic cells. We also demonstrated the involvement of PI3K-Akt pathway in hypoxic regulation of MMP-9 and VEGF but not VEGFR2 by using specific PI3K inhibitor. Also we showed that hypoxic regulation of MMP-9, VEGF and VEGFR2 also involve MEK1/2-ERK pathway by using MEK1/ inhibitor. We conclude that hypoxia-induced expression of MMP-9 and VEGF involved a dual signaling pathway, PI3K-Akt and MEK1/2-ERK, and a single

signaling pathway for VEGFR2, MEK1/2-ERK. The difference in the regulation of these proteins in hypoxic ENU1564 cells may reside in the different promoter regions of these proteins. W also analyzed the activation of p38 and SAKP/JNK in hypoxic ENU1564 cells and found no difference in the phosphorylation levels of these proteins in normoxic and hypoxic cells.

These results demonstrated that hypoxia frequently observed within solid tumors, can stimulate multiple signaling pathways that regulate important factors in tumor angiogenesis and invasion.

CHAPTER IV

ROLE OF FIBROBLAST GROWTH FACTOR-1 (FGF-1) IN THE EXPRESSION OF MMP-9 IN ENU 1564 CELLS*

Introduction

Matrix metalloproteinases (MMPs) are structurally related zinc- and calcium-dependent endopeptidases that play a role in proteolytic degradation of structural components of the extracellular matrix [93]. They not only facilitate breakdown of the extracellular matrix, but also affect early carcinogenesis, tumor development and growth, and play an important role in angiogenesis and mammary gland involution [27]. Among these enzymes, matrix metalloproteinase-9 (MMP-9) or gelatinase B plays an important role in tumor invasion and metastasis because of its specificity for type IV collagen. Previous studies demonstrated that MMP-9 plays an important role in an array of patho-physiological processes including wound healing, inflammation, tumor invasion and metastasis [94, 95]. Signal transduction responsible for MMP-9 regulation was investigated by several laboratories.

---

*Reprinted with permission from "FGF-1-induced matrix metalloproteinase-9 expression in breast cancer cells is mediated by increased activities of NF-κB and activating protein-1" by Lungu G, Covaleda L, Mendes O, Stoica HM, Stoica G, 2007, Molecular Carcinogeneis In press. Copyright 2008 by Wiley-Liss Inc. a subsidiary of John Wiley & Sons Inc.

Their results indicated that depending on stimulus and cell types, induction of MMP-9 synthesis involves several signaling cascades, including extracellular signal-regulated kinase (ERK), jun-N-terminal kinase (JNK), protein kinase C (PKC), serine/threonine protein kinase (Akt/PKB) and phospholipase D signaling pathway [96,97].

Fibroblast growth factors (FGFs) and FGF signaling pathways appear to play significant roles not only in normal development and wound healing, but also in resistance to cell death, increased motility and invasiveness, increased angiogenesis, enhanced metastasis, and resistance to chemotherapy and radiation, all of which can enhance tumor progression and clinical aggressiveness [36]. FGF-1, also known as acidic FGF, is a pleiotropic growth factor whose biological activities are mediated by high-affinity cell surface receptors that possess tyrosine kinase activity [38]. FGF-1 binds at the cell surface to any of four closely related high affinity receptors (FGFR1-4). FGF-1 also binds with a relatively high affinity to heparan sulphates, which in general are present as covalently linked side chains on cell-surface proteoglycans [98]. Unlike other members of FGF family, which currently includes 23 members, FGF-1 and FGF-2 lack a classical signal sequence for secretion [99]. Previous studies showed that FGF-1 is released in response to severe cellular injuries such as hypoxia [45] and serum starvation [100].

FGF-1 and its receptors were found to play a role in autocrine and paracrine growth control of malignant tumors; their overproduction is often associated with cancer [38,101]. Also, FGF-1 was found to play a key role in early stages of angiogenesis by

mediating MMP-1 proteolytic activity in endothelial cells [102]. Recent reports indicate that FGF-2 (bFGF), the other primary member of the FGF family, can regulate MMP-9 secretion from MCF-2 cancer cells through PKC activation of the Ras/ERK pathway [103].

Activator protein-1 (AP-1) and nuclear factor kappa B (NF-κB) are transcription factors important in the regulation of MMP-9, as the promoter of MMP-9 gene contains binding sites for both AP-1 and NF-κB [104]. AP-1 is a ubiquitous protein complex that can be induced by multiple stimuli, and its activation can lead to various pathological outcomes, such as carcinogenesis [105,106]. Stimulation of AP-1 occurs through a combination of signaling events, leading to an increased activity of proteins that directly potentiate Jun and Fos family members or activates transcription factors that regulate expression of *jun* and *fos* [107,108,109]. NF-κB comprises a family of inducible transcription factors which regulate host inflammatory and immune responses [110]. Stimulation of NF-κB pathway is mediated by diverse signal transduction cascades [110]. In unstimulated cells, NF-κB proteins are localized in the cytoplasm, and associated with a family of inhibitor proteins known as IκB. NF-κB was found to be activated following the interaction of FGF-1 with FGFR-1 [111]. Regarding the activation of the transcription factors AP-1 and NF-κB, previous studies showed that MEK1/2-ERK signaling pathway is important for activation of c-jun/AP-1, whereas activation of NF-κB requires PI3K-Akt, or p38 depending on cell type [97,112,113]. Extracellular signal-regulated kinase belongs to the mitogen-activated protein (MAP)

kinase family and is predominantly stimulated by mitogens and hormones, inducing proliferation, cell growth or differentiation [114,115].

In our previous study [116], we detected tumor hypoxia in a rat intracranially implanted with ENU1564 mammary adenocarcinoma cells by measuring the brain tumor oxygen saturation (SO_2) through the intact skin and skull using a novel noninvasive spectroscopic photoacoustic tomography (SPAT) technology. We also found and increased expression of MMP-9 in the brain tumor foci suggesting that increased expression of MMP-9 may be induced by tumor hypoxia and may be directly involved in the invasion of the tumor cells into the brain parenchyma. We also found an increase in MMP-9 expression in hypoxic ENU1564 cells **(Figure 34).** We demonstrated that hypoxic regulation of MMP-9 involves a dual signaling pathway, PI3K-Akt and MEK1/2-ERK. The mechanism by which FGF-1 regulates MMP-9 expression in cancer cells was not elucidated.

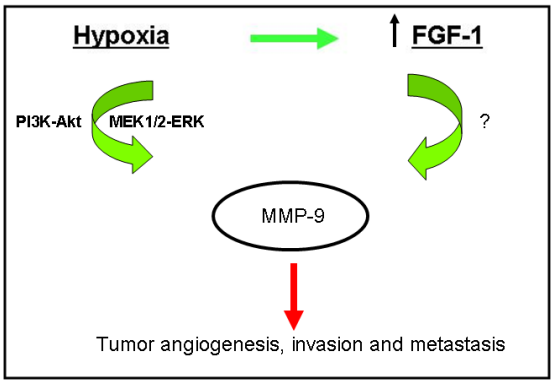

Figure 34. Hypoxia and FGF-1 induce MMP-9 expression in ENU1564 cell. We found that hypoxia-induced MMP-9 expression involves a dual signaling pathway, PI3K-Akt and MEK1/2-ERK. The mechanism by which FGF-1 regulates MMP-9 expression in ENU1564 cells was not elucidated.

Here we investigate the mechanisms involved in FGF-1-mediated regulation of MMP-9 expression in ENU1564 mammary adenocarcinoma cells. We showed for the first time that FGF-1-upregulates MMP-9 expression in ENU1564 cell lines by increasing the activities of NF-κB and AP-1 and involve activation of a dual signaling pathway, PI3K-Akt and MEK1/2-ERK.

Materials and methods

Reagents

Recombinant human FGF acidic was purchased from R&D Systems (R&D System, Inc. Minneapolis, MN). PD98059 was purchased from EMD Biosciences (EMD Biosciences, Inc. San Diego, CA). LY294002 was purchased from Cell Signaling Technology (Cell Signaling Technology, Inc. Danvers, MA). Heparin and all other chemicals were purchased from Sigma Chemical Company (St. Louis, MO) unless otherwise indicated.

Cell culture

The ENU1564 breast cancer cell line used in this study was originally developed in our laboratory and originated from an N-ethyl-N nitrosourea-induced mammary adenocarcinoma in a female Berlin-Druckrey IV (BD-IV) rat. This cell line is highly metastatic to brain and bone tissues [12]. The cell line was maintained in Dulbecco's modified Eagle's medium (Invitrogen, Carlsbad, CA), (DMEM) supplemented with 10%

fetal bovine serum (Invitrogen) and antibiotics (100 units/ml penicillin and 100 µg/ml streptomycin).

Treatment with FGF-1, LY 294002 and PD98059

Stock solution of recombinant FGF-1 (10 µg/ml) was prepared in 5,000 USP units/mL heparin in PBS [100]. For all experiments ENU1564 cells were maintained in serum-free medium for 24 hours before inhibition assays and FGF-1 treatment. After 24 hours of starvation, cells were washed twice with Hank's balanced salt solution (Invitrogen, Carlsbad, CA) and stimulated with FGF-1 at the indicated concentrations for 24 hours before preparation of cell lysates. For time-course experiments, cells were treated with 10 ng/ml FGF-1 for different time points (0- 24 hours). Control cells were incubated with 5U/ml heparin in PBS. PI3K inhibitor LY294002 (10 µM) or the MEK1/2 inhibitor PD98059 (25 µM) was added at least 1 hour before FGF-1 treatment. For inhibition experiments, cells were incubated with either the inhibitor or dimethyl sulfoxide (DMSO) (control cells).

Western blot analysis

The cells were washed twice with cold Hank's solution and lysed in buffer containing 50 mM Tris-HCl (pH 7.4), 150 mM NaCl, 1 mM CaCl2, 1 mM $MgCl_2$, 0.1% Triton X-100. The lysates were cleared by centrifugation at 13,000 x g at 4^oC for 30 minutes and the supernatant kept frozen at 80^oC. Nuclear and cytoplasmic extracts for Western blot analysis were prepared as described previously [117]. The protein content

of the lysates was determined using Bradford Assay (Bio-Rad Laboratories, Hercules, CA), with bovine serum albumin as the standard. Proteins (15 to 30 μg) were separated by 9-12% SDS polyacrylamide gel electrophoresis (SDS-PAGE) and transferred to nitrocellulose membranes (Schleicher and Schuell, Keene, NH). Membranes were incubated one hour in blocking buffer (20 mM Tris-HCl buffered saline containing 5% nonfat milk powder and 0.1% Tween 20) at room temperature, then probed with appropriate antibodies in blocking buffer or blocking buffer including 5% bovine serum albumin instead of 5% nonfat milk overnight at 4^{o}C. Blots were incubated at 4^{o}C overnight with anti-MMP-9 (1:200), anti-c-jun (1:200), anti-NF-κBp65 (1:200), IκBα (1:200) antibodies (all antibodies were obtained from Santa Cruz Biotechnology, Inc., Santa Cruz, CA). Monoclonal mouse IgG antibody against beta-actin was purchased from Sigma Chemical Company (St. Louis, MO). The blots were also incubated with anti-phospho-Akt (1:1000), and anti-phospho p-44/42 MAPK (1:1000) (all antibodies from Cell Signaling Technology, Inc. Danvers, MA). The blots were washed extensively, and then incubated for one hour with a 1:5000 dilution of secondary antibody. Peroxidase labeled anti-rabbit (1:10000) and anti-mouse secondary antibody (1:5000) were purchased from Kirkegaard and Perry Laboratories (Gaithersburg, MD). After additional washes, the blots were incubated with chemiluminescent substrate, according to directions in the kit (Super Signal West Pico, Pierce, Rockford, IL).

Gelatin zymography

Gelatinolytic activities were analyzed by gelatin zymography as previously described [83]. For the preparation of conditioned medium, cells were washed with Hank's balanced salt solution and maintained for 24 hours in serum-free medium. After the starvation period, cells were stimulated with the indicated concentrations with FGF-1 and cultured for 24 hours. The conditioned media were collected, concentrated 30-fold using an Amicon Ultra-15 Centrifugal Filter Device (Millipore, Bedford, MA). Concentrated conditioned media (15 μg of protein) were incubated at 37°C for 30 minutes in SDS sample buffer without reducing agent, then subjected to SDS-PAGE in 10% (wt/vol) polyacrylamide gels containing 0.1% (wt/vol) gelatin. The gels were washed twice for 30 minutes in 2.5% (vol/vol) Triton X-100 at room temperature and then incubated for 24 hours in substrate reaction buffer (50 mM Tris-HCl (pH 7.5), 100 mM NaCl, 10 mM $CaCl_2$, 0.002% NaN_3) at 37^{o}C. The gels were then stained with Coomasie Brilliant Blue R250 in 10% (vol/vol) acetic acid and 30% (vol/vol) methanol for 1 hour and destained briefly in the same solution without dye. Proteolytic activities were detected as clear bands indicating the cleavage of the substrate.

Total RNA extraction and semi-quantitative RT-PCR

Total RNA was extracted from ENU1564 cells using an SV RNA extraction kit (Promega Corporation, Madison WI) using the manufacturer's directions. RNA was quantified by absorbance at 260 nm. Using a Super Script III First Strand Synthesis System (Invitrogen), 100 ng of total RNA was amplified by reverse transcription

polymerase chain reaction (RT-PCR) and the cDNAs were amplified. We used primers for MMP-9 (forward, 5'-CCCCACTTACTTTGGAAACGC-3'; reverse, 5'-ACCCACGACGATACAGATGCTG-3') [12], β-actin (forward, 5'-ATGTACGTAAGCCAGGC-3'; reverse, 5'-AAGGAACTGGAAAAGAGC-3') [12], c-jun (forward, 5'-ATGACTGCAAAGATGGAAACG-3'; reverse, 5'-TGCCGCGGAGGTGACACTGGG-3') [118], and c-fos (forward 5'-ATGATGTTCTCGGGTTTCAAC-3'; reverse, 5'-AGGAGATAGCTGCTCTACTTT-3') [118]. The expected size for the MMP-9 PCR product was 686 base pairs (bp). PCR conditions for MMP-9 were an initial denaturation of 94^{o}C for 2 minutes, followed by 30 cycles of denaturation at 94^{o}C for 1 minute, annealing at 59.1^{o}C for 30 seconds and extension at 72^{o}C for 1 minute. A final extension of 5 minutes at 72^{o}C was carried out. The expected size for c-jun and c-fos products was 402 bp. PCR conditions for c-jun and c-fos were an initial denaturation at 94^{o}C for 2 minutes, followed by 32 cycles of denaturation at 94^{o}C for 60 seconds, annealing at 58^{o}C for 75 seconds and extension at 72^{o}C for 1 minute.

DNA extraction

DNA was extracted from ENU1564 cells using the Wizard Genomic DNA Purification kit (Promega Corporation, Madison WI) following manufacturer's directions. DNA was quantified by absorbance at 260 nm.

Cloning of rat MMP-9 promoter and transient transfection

A 630-bp fragment of the 5'-flanking region of the MMP-9 gene (-595 to +17), containing one AP-1 and one NF-κB binding sites [104], was obtained by PCR amplification using stringent conditions on genomic DNA isolated from ENU1654 cells, using the following primers: 5'-CGGCTAGCGGAGTCAGCCTGCTGGGGTTAG-3' (forward); 5'-CGCTCGAGTGAGAACCGAAGCTTCTGGGT-3' (reverse). The fragment obtained by PCR was gel analyzed and cloned into p-Glow-TOPO vector encoding for green fluorescence protein (GFP) (Invitrogen Corporation, Carlsbad, CA) using the manufacturer's directions to generate p-Glow-TOPO-MMP-9 wild type (MMP-9 wt). Introduction of a double-point mutation into the NF-κB-site (GGAATTCCCCC to GGAATTGGCCC) to generate pGlow-MMP-9-Δ NF-κB was performed using the following (forward) primer: 5'-GGGTTGCCCCGTGGAATTGGCCCAAATCCTGC-3' (corresponding to a region from -572 to -541). Creation of a double transition within the AP-1 binding site (CTGAGTCA to CTGAGTTG) to generate pGlow-MMP-9 ΔAP-1 was performed using the following (forward) primer: 5'-CACACACCCTGAGTTGGCGTAAGCCTGGAGGG-3' (corresponding to a region from -98 to -65). The mutants were generated using the Quik Change Site-Directed Mutagenesis Kit (Stratagene, La Jolla, CA). Transient transfections of ENU1564 cells were performed using Lipofectamine (Invitrogen Carlsbad, CA) according to the manufacturer's instructions. Transfections were performed in triplicate and were repeated at least twice to ensure reproducibility of the results. After transfections,

ENU1564 cells were incubated for 24 hours with 10 ng/ml of FGF-1 or 5U/ml heparin in PBS (control). Transfection efficiency was monitored by co-transfection with 0.2 μg of the pSV/β-gal plasmid encoding for β-galactosidase (Promega Corporation, Madison, WI). Twenty-four hours post-transfection GFP activity was measured using a Spectra Max GeminiEM dual detector (Sunnyvale, CA). The β-galactosidase activity was detected using the Beta-Glow Assay System (Promega Corporation, Madison, WI) according with manufacturer's instructions. The luminescence signal generated by the Beta-Glow Reagent was measured with the same detector used for GFP expression. The ratio of fluorescence activity to β-galactosidase activity in each sample served as a measure of normalized fluorescence activity.

Electrophoretic mobility shift assay (EMSA)

For EMSA we used FGF-1 treated and untreated ENU1564 cell nuclear extract. EMSA analysis was performed using consensus oligonucleotides for NF-κB and AP-1. The crude nuclear extracts from FGF-1 (10 ng/ml) treated ENU1564 cells were obtained as previously described [117]. Both NF-κB (AY1030P) and AP-1(AY1055P) EMSA kits were obtained from Panomics (Panomics, Inc. Redwood, CA) and used according to manufacturer's instructions. Competition experiments were performed by adding excess unlabeled double-stranded oligonucleotide (cold probe) in the DNA-protein binding reaction. For supershift assays, polyclonal antibodies to NF-κBp65, NF-κBp50, c-jun and c-fos (Santa Cruz Biotechnology, Inc.) were preincubated for 30 minutes with the nuclear extracts before the probe was added.

Statistical analysis

Quantification of the Western blot, gelatin zymography, and semi-quantitative RT-PCR bands density was performed on a Macintosh computer using the public domain NIH Image program (developed at the U.S. National Institutes of Health and available on the Internet at http://rsb.info.nih.gov/nih-image. Data were presented as mean ± S.D., and statistical comparisons were made using Student *t*-test. A *P*-value of < 0.05 was considered statistically significant. Data are representative of three independent experiments.

Results

FGF-1 stimulates expression and secretion of MMP-9

We first examine the effect of FGF-1 on the MMP-9 expression in ENU1564 cells. The cells were cultured for 24 hours in a serum-free medium and then treated with incremental concentrations of FGF-1 (0-10 ng/ml) for an additional 24 hours. We measured the mRNA levels of MMP-9 after FGF-1 treatment by semi-quantitative RT-PCR, **(Figure 35A and B),** MMP-9 protein expression by Western blot analysis, and gelatinolytic activity in the conditioned medium by gelatin zymography.

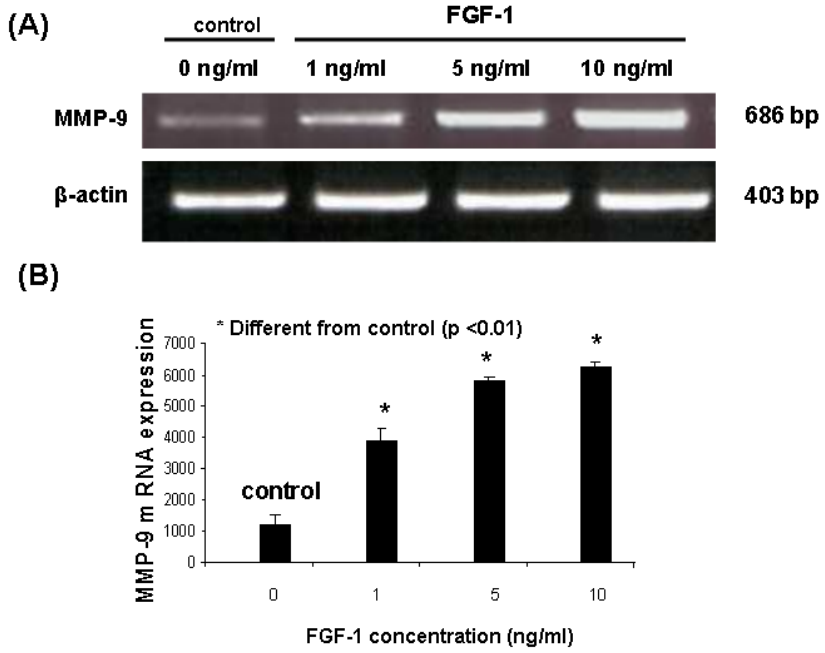

Figure 35. Increased expression of MMP-9 mRNA in FGF-1 treated ENU1564 cells. ENU1564 cells were incubated with FGF1 (0- 10 ng/ml) for 24 hours. (A) RT-PCR analyses of MMP-9 mRNA in ENU1564 cells treated with FGF-1. Total RNA was extracted, and mRNAs encoding for MMP-9 and β-actin were identified and measured. (B) Densitometric analysis of MMP-9 mRNA in ENU1564 cells The results represent the mean ± standard deviation for three independent experiments. Asterisks indicate statistically significant differences ($P < 0.01$).

As shown in **Figure 35A**, FGF-1 stimulation of ENU1564 cells increases MMP-9 mRNA expression in a concentration-dependent manner. Densitometry analysis of MMP-9 mRNA in FGF-1-treated ENU1564 cells shows an increased of 3-, (1 ng/ml FGF-1) 4.8- (5 ng/ml FGF-1) and 5- (10 ng/ml FGF-1) fold, respectively, compared to untreated cells **(Figure 35B).**

To confirm the RT-PCR results, we evaluated the MMP-9 protein expression in FGF-1 treated ENU1564 cells by Western blot analysis. As shown in **Figure 36A**, FGF-1 stimulated MMP-9 protein expression in a concentration- dependent manner. Densitometry analysis shows increased levels of MMP-9 protein (*Different from controls, $P<0.01$) in FGF-1 treated ENU1564 cells compared to untreated cells, which is consistent with the increases in MMP-9 mRNAs **(Figure 36B).** Treatment of ENU1564 cells with FGF-1 also activated MMP-9 secretion in a concentration-dependent manner (**Figure 36C).** The densitometry results revealed a significant increase in enzymatic activity of MMP-9 (*Different from control $P<0.01$) in FGF-1 treated cells compared with control cells **(Figure 36D).**

Activation of Akt is required for FGF-1-dependent MMP-9 expression

Next, we wanted to investigate the signaling pathway(s) involved in FGF-1 stimulation of MMP-9 expression in our cell line. Previous reports provided evidence that PI3K-Akt can be stimulated by growth factors and it was demonstrated that PI3K-Akt is an important signaling pathway in FGF-1 cell-mediated angiogenesis response [119]. First, we examined if stimulation of ENU1564 cells with FGF-1 activates Akt in a time-dependent manner by measuring its phosphorylation level.

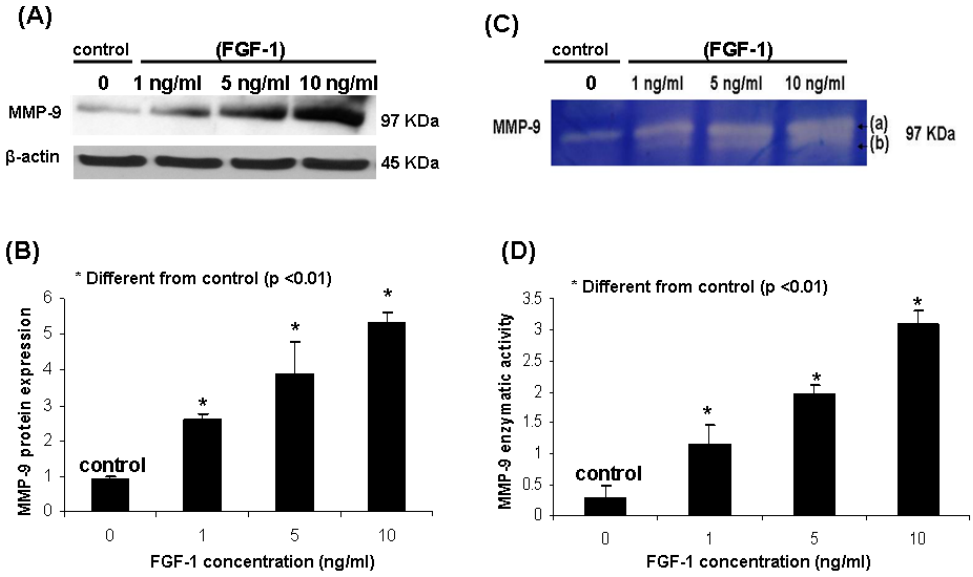

Figure 36. Increased MMP-9 protein expression and gelatinolytic activities in FGF-1 treated ENU1564 cells. (A) Western blot analysis showing increased MMP-9 protein expression in FGF-1 treated ENU1564 cells. β-actin used as loading control**.** (B) Densitometric analysis of MMP-9 protein expression in ENU1564 cells shows a significant increase when compared to untreated cells. The results represent the mean ± standard deviation for three independent experiments. Asterisks indicate statistically significant differences (p<0.01). (C) Gelatin zymography of ENU1564 cells conditioned medium was performed as described in Material and Methods. ENU1564 cells were stimulated with FGF-1 at 1, 5 and 10 ng/ml or left untreated as controls. Conditioned media was collected after 24 hours. (D) Quantitative analysis of MMP-9 enzymatic activity was determined by densitometry and was found to be increased in FGF-1 treated ENU1564 cells compared with control. The double band at 97 KDa corresponded to the latent form (proenzyme) (a) and active form (b) of MMP-9. Figure 2D represents the quantitative analysis of MMP-9 determined by densitometry of the active band (b). The results represent the mean ± standard deviation for three independent experiments. Asterisks indicate statistically significant differences (P < 0.01).

As shown in Figure 3A, treatment of ENU1564 cells with 10 ng/ml FGF-1 led to increased phosphorylation of Akt in a time- dependent manner (0-24 hours), starting at 2 hours and continuing to 24 hours after the treatment. To confirm whether the effect of FGF-1 on MMP-9 expression involves the PI3K-Akt pathway, we used the specific PI3K inhibitor, LY294002. ENU1564 cells were pretreated with LY294002 or DMSO (control) for 1 hour and subsequently stimulated with FGF-1 (10 ng/ml) for 24 hours. Total lysates were collected and subjected to the Western blot analysis for Akt activation and MMP-9 protein expression. The expression of MMP-9 protein significantly increases in FGF-1 treated cells compared with untreated cells **(Figure 37B and 37C**, *significantly different from control $P<0.01$). Pretreatment of ENU1564 cells with the inhibitor completely blocked the FGF-1 dependent activation of Akt and decreased MMP-9 protein levels (Figure 3B and 3C) compared with untreated cells (** significantly different from untreated cells $P<0.05$). The level of MMP-9 protein expression in ENU1564 cells treated with only the inhibitor was similar to that in control cells **(Figure 37B and 37C).**

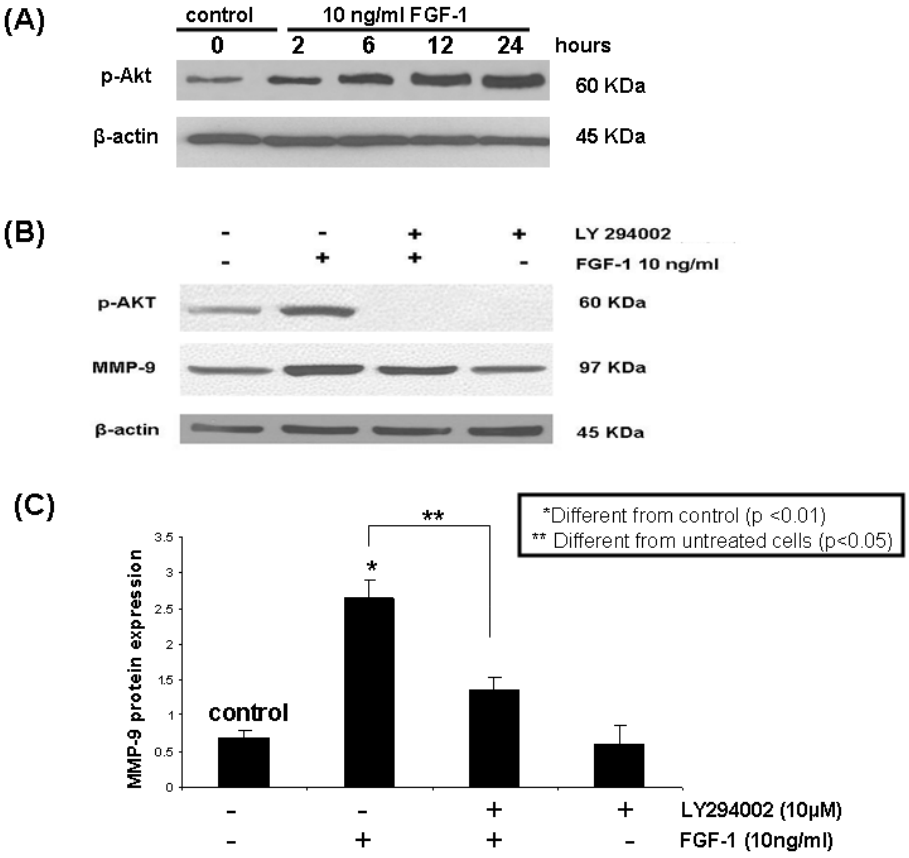

Figure 37. Requirement of PI3K-Akt signaling for FGF-1-dependent MMP-9 expression. (A). Western blot analyses show increased levels of phospho-Akt in FGF-1(10 ng/ml) treated ENU1564 cells in a time-dependent manner compared with untreated cells. Similar results were obtained from two independent experiments run in duplicates. (B) Cells were pretreated with LY294002 or DMSO for 1 hour and then stimulated with 10 ng/ml FGF-1 for 24 hour. Total lysates were probed with anti-phospho Akt, anti-MMP-9 and anti-β actin (loading control). (C) Quantitative analysis of MMP-9 protein expression was determined by densitometry. The amount of MMP-9 protein in ENU1564 cells treated with FGF-1(10 ng/ml) was significantly increased when compared with untreated cells (*significantly different from control $P<0.01$). Pretreatment of ENU1564 cells with the inhibitor completely blocked the FGF-1 dependent activation of Akt and decreases MMP-9 protein levels compared with untreated cells (**significantly different from untreated cells $P<0.05$). The results represent the mean ± standard deviation for three independent experiments.

FGF-1 stimulation of ENU1564 cells induces nuclear translocation of NF-κB and cytoplasmic degradation of IκB-α protein

In our effort to elucidate the mechanisms of FGF-1-induced MMP-9 expression in our system, we investigated the activation of two transcription factors, NF-κB and AP-1, both binding to the corresponding regulatory elements within the promoter region of MMP-9 gene. Previous studies show that cytokine-mediated regulation of MMP-9 expression critically depends on the activation of NF-κB and AP-1 [95, 104]. We demonstrated that PI3K-Akt pathway is involved in FGF-1-induced MMP-9 expression in ENU1564 cells and previous studies showed that this pathway is important for activation of NF-κB transcription factor [120, 121]. Using Western blot analysis, we examined whether FGF-1 stimulation of ENU1564 cells will result in nuclear translocation of NF-κBp65 proteins. As shown in **Figure 38A**, treatment of ENU1564 cells with FGF-1 (10 ng/ml) results in nuclear translocation of NF-κBp65 in a time-dependent manner (0-24 hours) when compared with untreated cells. Previous studies show that NF-κB proteins are retained in the cytoplasm by their inhibitors (IκB) in an inactivated state, and that activation of NF-κB and nuclear translocation requires a rapid degradation of their inhibitors [117]. We demonstrated that FGF-1 (10 ng/ml) treatment of ENU1564 cells displayed a marked decrease in IκBα protein expression in a time-dependent manner **(Figure 38B).**

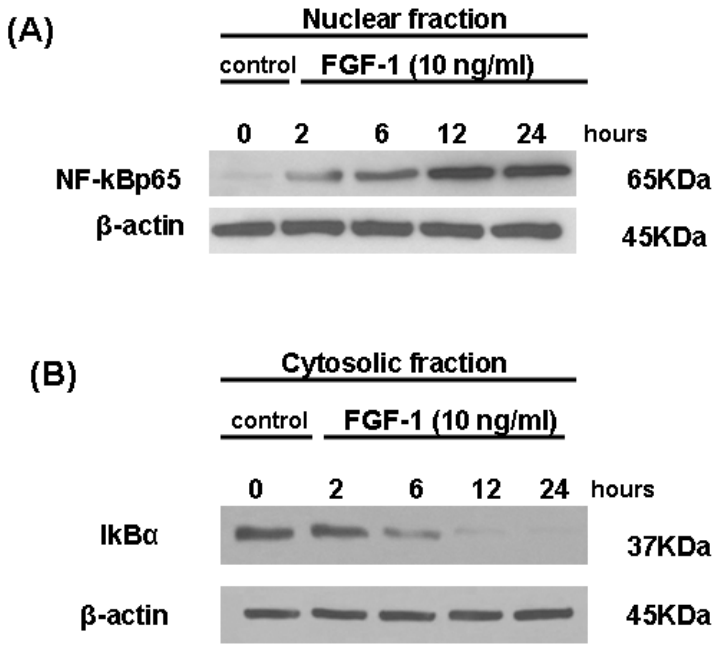

Figure 38. Nuclear accumulation of NF-κBp65 and IκBα protein degradation in FGF-1 treatment of ENU1564 cells. (A) Western blot analysis showing increased levels of NF-κBp65 in nuclear extracts from in FGF-1 (10 ng/ml) treated ENU1564 cells in a time-dependent manner (0-24 hours) compared with untreated cells; β actin was used as loading control. Nuclear extracts were prepared from stimulated and unstimulated cells (control) as described in Materials and Methods. Similar results were obtained from two independent experiments run in duplicates. (B) ENU1564 cells were treated for different time points (0-24 hours) with 10 ng/ml FGF-1. Cytosolic extracts were prepared from stimulated and unstimulated cells (control) as described in Materials and Methods and subjected to Western blot analysis using anti-IκBα antibodies and anti-β actin as loading control. Western blot analysis is showing a decrease in the levels of cytoplasmic IκBα in treated compared with untreated ENU1564 cells. Similar results were obtained from two independent experiments run in duplicates.

Activation of ERK1/2 is required for FGF-1-dependent MMP-9 expression

MEK1/2-ERK pathway has been reported to be activated by growth factors [96].This pathway was found to be involved in FGF-1 stimulation of MMP-14 expression in prostate carcinoma cells [122]. First, we examined if stimulation of ENU1564 cells with FGF-1 activates ERK in a time-dependent manner by measuring its phosphorylation level. As shown in Figure 5A, treatment of ENU1564 cells with 10 ng/ml FGF-1 led to increased phosphorylation of ERK in a time-dependent manner (0-24 hours). Increase started at 2 hours after the treatment, continued at 6 hours, then decreased at 12 hours after the treatment and increase again at 24 hours. To determine the role of MEK1/2-ERK pathway in FGF-1-dependent expression of MMP-9, we used the specific MEK1/2 inhibitor, PD98059. ENU1564 cells were pre-treated with PD98059 or DMSO (control) for 1 hour and then stimulated with FGF-1 (10 ng/ml) for 24 hours. Cell lysates were collected and assayed for phosphorylated ERK1/2, β-actin, and MMP-9 protein expression. Treatment of ENU1564 cells for 24 hours with FGF-1 increased phosphorylation of ERK1/2, (Figure 5B). MMP-9 protein expression is upregulated in FGF-1 treated cells when compared to untreated cells (*significantly different from control, $P < 0.01$) **(Figure 39B and 39C).** Pre-treatment of cells with the MEK1/2 inhibitor completely inhibited FGF-1 dependent activation of ERK1/2 and suppressed MMP-9 protein expression compared with untreated cells (** significantly different from untreated cells $P<0.05$).

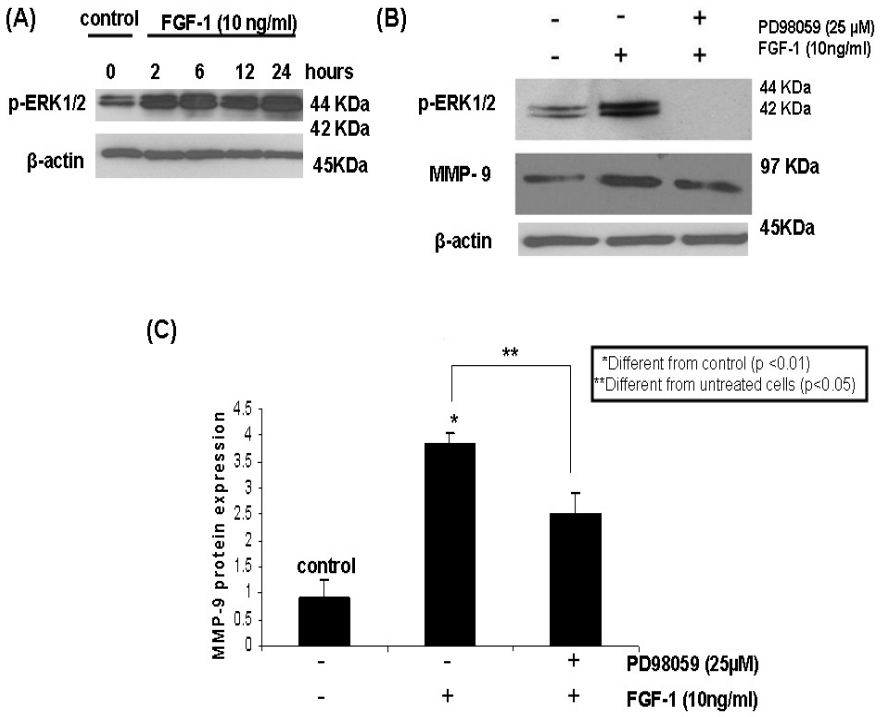

Figure 39. Requirement of MEK1/2-ERK signaling for FGF-1-dependent MMP-9 expression. (A). Western blot analyses using anti-phospho ERK and anti-β-actin (loading control) were performed and show increased levels of phospho-ERK in FGF-1(10 ng/ml) treated ENU1564 cells in a time-dependent manner (0-24 hours). Similar results were obtained from two independent experiments run in duplicates. (B) Cells were pretreated with PD98059 or DMSO for 1 hour and then stimulated with 10 ng/ml FGF-1 for 24 hours. Western blot analysis using anti-phospho ERK1/2, anti-MMP-9, and anti-β-actin antibodies was performed. Phospho-ERK1/2 was increased in FGF-1 stimulated ENU1564 cells compared with β-actin and was completely abrogated in ENU1564 cells treated with the MEK1/2 inhibitor. (C) Quantitative analysis of MMP-9 protein expression was determined by densitometry. The amount of MMP-9 protein in ENU1564 cells treated with FGF-1(10 ng/ml) was increased when compared with untreated cells (*significantly different from control $p<0.01$). Pretreatment of cells with MEK1/2 inhibitor decreased MMP-9 protein levels compared with untreated cells (**significantly different from untreated cells $P<0.05$). The results represent the mean ± standard deviation for three independent experiments.

FGF-1 induces early gene expression of c-fos and c-jun in ENU1564 cells

Previous studies have shown that MEK1/2 –ERK signaling pathway is important for activation of AP-1 transcription factor [97]. Since both c-jun and c-fos are members of the AP-1 transcription factor complex, it is important to determine if treatments of ENU1564 cells with FGF-1 will upregulate their expression. RT-PCR analysis demonstrated that mRNA levels of early gene expression c-jun and c-fos are upregulated in FGF-1 treated ENU1564 cells as early as 15 minutes after FGF-1 stimulation, compared with control ENU1564 cells **(Figure 40A).** Quantitative analysis of c-jun and c-fos mRNA determined by densitometry is represented in **Figure 40B** and shows the transient activation of both c-jun and c-fos genes by FGF-1. Next, we determined if FGF-1 will affect the nuclear translocation of one of the active subunits of the AP-1 transcription factor, c-jun. For this purpose we used nuclear extracts from ENU1564 cells treated with FGF-1 (10 ng/ml) for different time points (0-24 hours).

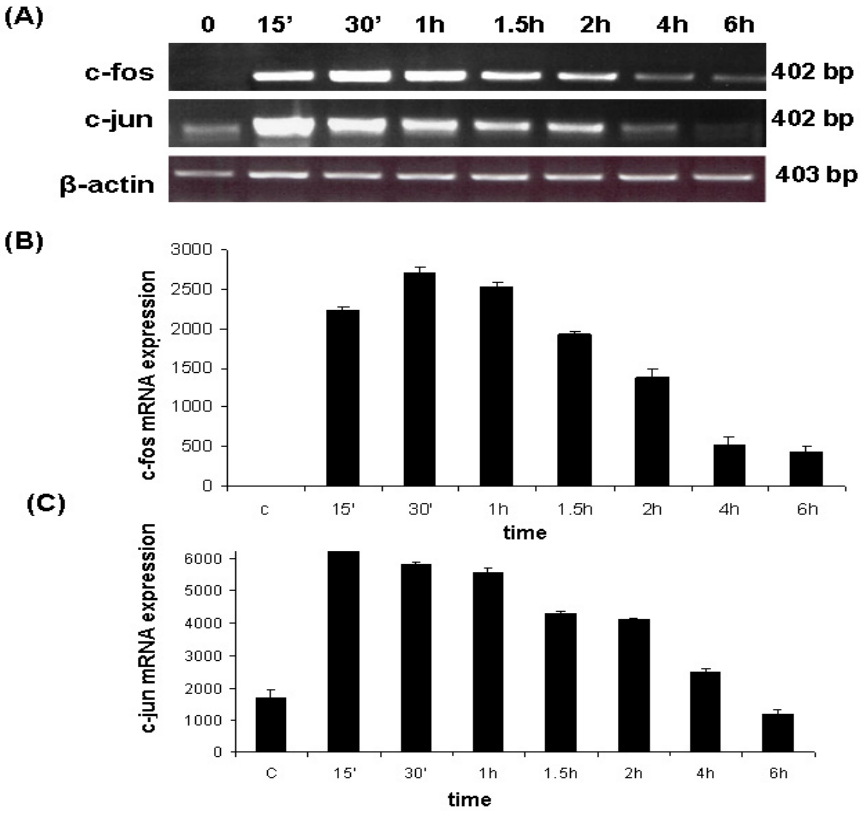

Figure 40. Regulations of early gene expression c-jun and c-fos in FGF-1 treated ENU1564 cells. (A) ENU1564 cells were serum starved for 24 hours and treated with 10ng/ml FGF-1. Total RNA was extracted at indicated time points and mRNAs encoding for c-jun, c-fos and β-actin were identified and measured using semi-quantitative RT-PCR. (B, C) Quantitative analysis of c-jun and c-fos was determined by densitometry. Data are represented as mean ± standard deviation for three independent experiments.

Figure 41 shows that FGF-1 induces nuclear translocation of c-jun in a time-dependent manner compared with untreated cells.

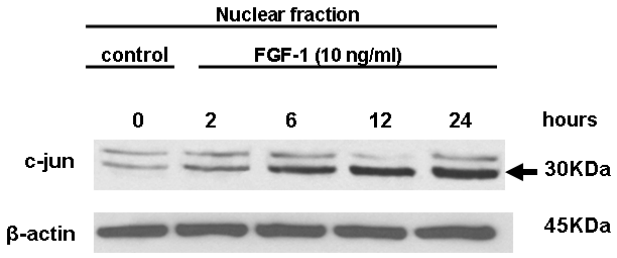

Figure 41. Nuclear accumulation of c-jun in ENU1564 cells is modulated by FGF-1. ENU1564 cells were treated for different time points (0-24 hours) with 10 ng/ml FGF-1. Nuclear extracts were prepared from stimulated and unstimulated cells (control) as described in Materials and Methods and subjected to Western blot analysis using anti-c-jun antibodies and anti-β actin as loading control. Similar results were obtained from two independent experiments run in duplicates.

FGF-1 treatment of ENU1564 cells increases DNA binding activity of NF-κB and AP-1

Further, we wanted to demonstrate that FGF-1 treatment of ENU1564 cells would lead to an increase in DNA binding capacity of NF-κB and AP-1, in addition to their nuclear translocation. To accomplish this, we performed EMSA analysis using consensus oligonucleotides for NF-κB, AP-1 and 24 hours FGF-1 (10 ng/ml) treated and control ENU1564 cells nuclear extract. As shown in **Figure 42A**, stimulation of ENU1564 cells with 10 ng/ml FGF-1 confirmed increased DNA binding activity of NF-

κB-bound complexes compared with control cells (untreated). Competition experiments with unlabeled competitor probe confirmed the specificity of binding. To detect the presence of specific NF-κB protein in the DNA-protein complexes, we performed gel supershift assays using anti-antibodies against NF-κBp65 and NF-κBp50. As shown in **Figure 42A**, antibodies against these proteins completely supershifted the DNA complexes formed with these proteins. Using the same extract, we performed EMSA analysis using AP-1 specific oligonucleotides. As shown in **Figure 42B**, treatment of ENU1564 cells with 10 ng/ml FGF-1 confirmed binding of AP-1 to DNA compared with control ENU1564 cells nuclear extract (untreated). Competition experiments using an unlabeled competitor probe confirmed specificity of binding. We performed gel supershift assay with antibodies against c-jun and c-fos to detect their presence in the DNA protein complexes. Antibodies against either c-jun or c-fos completely supershifted the DNA complexes formed with these proteins **(Figure 42B)**. Taken together, the data indicate that an increased translocation of c-jun and NF-κB proteins demonstrated in FGF-1 treated ENU1564 cells is functionally linked to a rise in DNA binding affinity of transcription factors AP-1 and NF-κB.

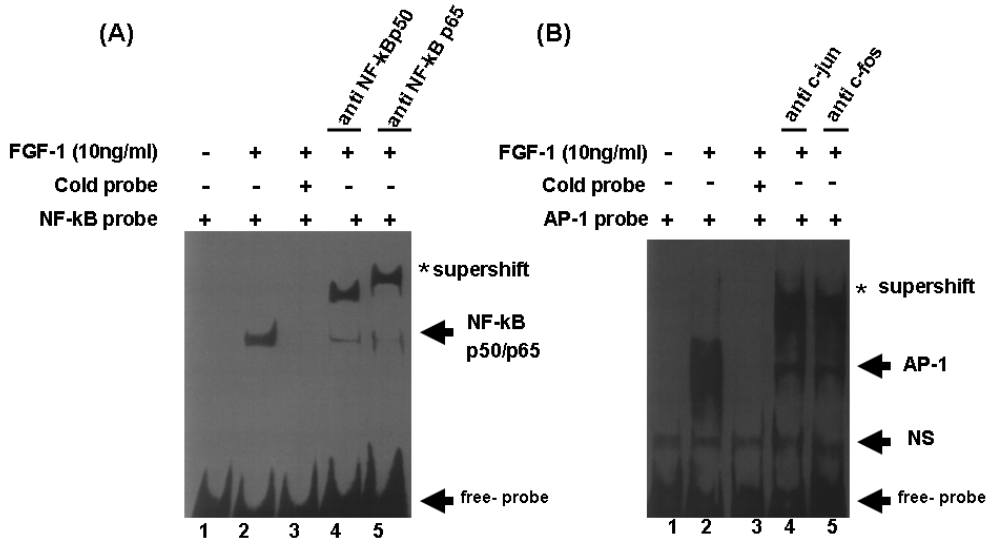

Figure 42. FGF-1 induced NF-κB and AP-1 DNA binding activity. EMSA analysis was carried out to determine the NF-κB and AP-1 DNA binding activity as described in Materials and Methods. (A) Treatment of ENU1564 cells with FGF-1(10 ng/ml) for 24 hours induces DNA binding activity of NF-κB (2) compared with untreated cells (1). The band representing the specific binding of NF-κB to the DNA, was completely abolished by competition assay using an excess of unlabeled oligonucleotide (3). For supershift analysis antibodies against NF-κBp65 (4), and NF-κBp50 (5) were included to the binding reaction. (B) Treatment of ENU1564 cells with FGF-1(10 ng/ml) for 24 hours induces DNA binding activity of AP-1 (2) compared with untreated cells (1). The band representing the specific binding of AP-1 to the DNA, was completely abolished by competition assay using an excess of unlabeled oligonucleotide (3). The specificity of DNA-bound complexes was determined by supershift analysis. For supershift analysis, antibodies for c-jun (4) and c-fos (5) were included in the binding reaction. NF-κB (arrow) and AP-1 (arrow) indicates specific NF-κB and AP-1 binding complexes. NS, Nonspecific binding, * supershift bands.

NF-κB and AP-1 binding sites are important in FGF-1 activation of MMP-9

Next, we investigated if FGF-1-mediated MMP-9 expression critically depends on NF-κB or/and AP-1 binding sites within MMP-9 promoter. We used reporter gene constructs containing the MMP-9 promoter harboring a double-point mutation in NF-κB binding site and a double transition in AP-1 binding sites as described in Materials and Methods **(Figure 43A).** We transiently transfected ENU1564 cells with plasmids containing MMP-9 wild type (MMP-9wt) and mutated promoters, and treated the cells with FGF-1 (10 ng/ml) or heparin (control) for 24 hours. As shown in **Figure 43B,** transient transfection of ENU1564 cells with p-Glow-MMP-9wt showed a 1.7-fold increase in fluorescence activity 24 hours after FGF-1 (10 ng/ml) treatment compared with control cells. This induction was lost in both promoter mutants. The results indicated that FGF-1-mediated MMP-9 expression critically depends on both KF-κB and AP-1 binding sites.

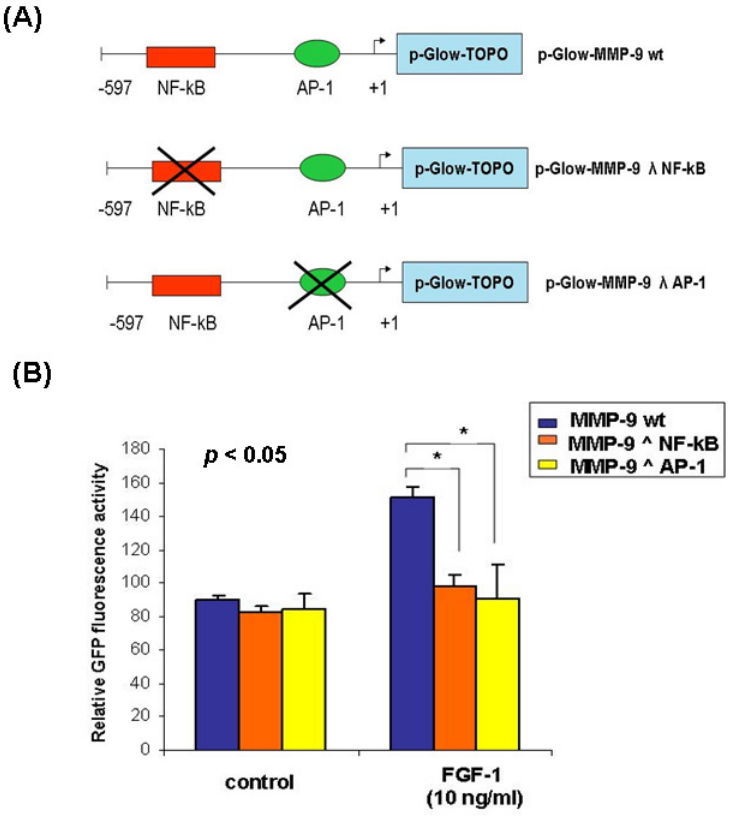

Figure 43. Increase of MMP-9 promoter activity by FGF-1 is inhibited by mutation in either NF-κB or AP-1 binding sites. (A) MMP-9 promoter was obtained as described in Materials and Methods**.** Reporter gene constructs containing MMP-9 promoter harboring a double point mutation in NF-κB binding site and a double transition in AP-1 binding sites were used**.** (B) ENU1564 cells were cultured in 96 well plates and co-transfected with 0.2 μg of pGlow-TOPO-MMP-9wt, pGlow-TOPO-MMP-9-^ NF-κB, or pGlow-TOPO-MMP-9-^AP-1 and 0.2 μg of pSV/β-gal. Six hours after transfection cells were treated with 10 ng/ml FGF-1 for 24 hours or with 5U/ml heparin in PBS (control). Values of GFP fluorescence activities were corrected for transfection efficiency by assaying for β-galactosidase activity as described in Materials and methods. Data are the mean of ± SD. Statistical analysis was carried out using Student's *t*-test. $P < 0.05$.

Discussion

MMP-9 expression can be upregulated by a number of factors, including growth factors and cytokines [123,124]. Previous reports indicate that inflammatory cytokines, interleukin-1 (IL-1) and tumor necrosis factor-α (TNF-α) were able to induce MMP-9 expression in rat C6 glioma cells [97,125]. MMP-9 was also found to be induced in MCF-7 cells by a member of FGFs family, called basic fibroblast growth factor along with 12-O-tetradecanoylphorbol 13-acetate (TPA) [103].

In this report, we provide evidence of the mechanism involved in regulation of MMP-9 expression in ENU1564 mammary adenocarcinoma cell line by another member of FGFs family called acidic fibroblast growth factor (FGF-1). Previous studies demonstrate that FGF-1 is released in response to severe cellular injuries, hypoxia [45] and in breast cancer [126,127]. FGF-1 also regulates several matrix metalloproteinases. It induces promarilysin (MMP-7) expression through activation of ERK pathway [122], and transcriptionally induces MT1-MMP expression in LNCaP prostate carcinoma cells in a mechanism that involves FGFRs and STAT [38]. FGF-1 also plays a key role in the early stages of angiogenesis by mediating MMP-1 proteolytic activity [102].

We previously reported that MMP-9 mRNA and protein expression was upregulated in brain tumor foci originating from ENU1564 cells [116]. Here, we demonstrate that FGF-1 transcriptionally induces MMP-9 expression in ENU1564 cells. Consistent with current literature [36,127], we observed that ENU1564 breast cancer cells produce FGF-1 and express FGFR-1, as confirmed by RT-PCR and IHC analysis (data not shown).

In this report, we show that FGF-1 stimulation of ENU1564 cells increases MMP-9 mRNA expression in a dose-dependent manner, increases MMP-9 protein expression and increases enzymatic activity of MMP9. Additionally, we show that FGF-1 regulation of MMP-9 expression in ENU1564 cells is associated with MEK1/2-ERK and PI3K-Akt signaling pathways.

MMP-9 regulation and FGF-1 signaling have been associated with the PI3K-Akt pathway. IL-1β stimulation of Balb 3T3 cells activates MMP-9 secretion by activation of the PI3K-Akt pathway [97]. PI3K activity has been previously implicated as a requirement for translocation of exogenous FGF-1 into cytosol and nucleus [128]. Very recently, FGF-1 was shown to stimulate angiogenesis through stimulation of PI3K-Akt pathway [104]. FGF-1 was also found to target the degradation of IκBα [111]. We observed that treatment of ENU1564 cells with FGF-1 led to increased phosphorylation of Akt in a time-dependent manner and pretreatment of ENU1564 cells with LY294002 (PI3K inhibitor) decreased MMP-9 protein levels. Additionally, treatment of ENU1564 cells with FGF-1 resulted in nuclear translocation of NF-κBp65, and targets the degradation of IκBα in a time-dependent manner.

MMP-9 expression and FGF-1 regulation have been associated with the MEK1/2-ERK pathway. Previous studies showed that MMP-9 secretion by FGF-2 requires activation of MEK1/2-ERK signaling in breast cancer line, MCF-7 [129]. Other studies reported that regulation of MMP-9 by heregulin-beta1 in cancer cells was ERK, p38, and PKC- dependent [96]. IL-1β stimulation of Balb 3T3 cells activates MMP-9 secretion by activation of the MEK1/2-ERK pathway [97]. The report by Udayakumar et

al. showed that FGF-1 was able to induce promarilysin (MMP7) expression in LNCaP through activation of ERK pathway [115]. Previous studies showed that FGF-2 induces the expression of c-jun and c-fos members of AP-1 complex [130]. We observed that treatment of ENU1564 cells with FGF-1 lead to increased phosphorylation of ERK1/2 in a time-dependent and treatment of ENU1564 cells with PD98059 (MEK1/2) inhibitor decreased FGF-1 dependent-MMP-9 expression. Also, we showed that FGF-1 induces nuclear translocation of c-jun, and increased early gene expression *c-jun* and *c-fos*.

Previous reports demonstrated that the induction of MMP-9 transcriptional promoter activity in response to FGF-2 is dependent on AP-1, but not NF-κB, response elements in rabbit corneal fibroblasts [131]. Other studies reported that regulation of MMP-9 by heregulin-beta1 in cancer cells was ERK, p38, PKC- dependent but Akt-independent [96]. Previous reports showed that MEK1/2-ERK signaling pathway is important for AP-1 binding activity, while NF-κB require Akt or p38 depending on the cell type [97,112,113]. We observed that stimulation of ENU1564 cells with FGF-1 increased DNA binding activity of NF-κB-bound and AP-1-bound complexes. Transient transfection of ENU1564 cells with p-Glow-MMP-9wt showed a 1.7-fold increase in MMP-9 promoter activity 24 hours after FGF-1 treatment which, was completely abolished by mutation in either NF-κB or AP-1 response elements.

In conclusion, this report shows for the first time that FGF-1-induced MMP-9 expression involves a dual signaling pathway PI3K-Akt **(Figure 44)** and MEK1/2-ERK **(Figure 45)** and depends on increased activities of two transcription factors NF-κB and AP-1.

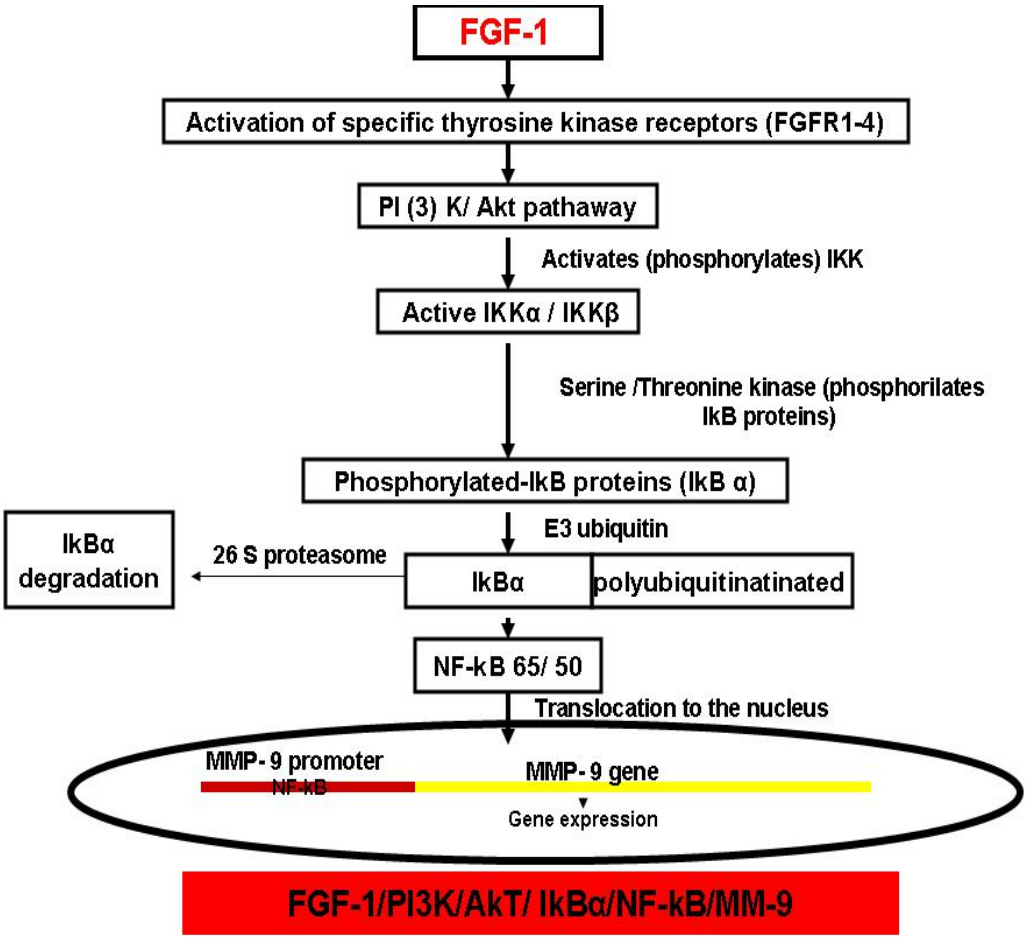

Figure 44. Involvement of PI3K-Akt signaling in FGF-1-induced expression of MMP-9 in ENU1564 cells.

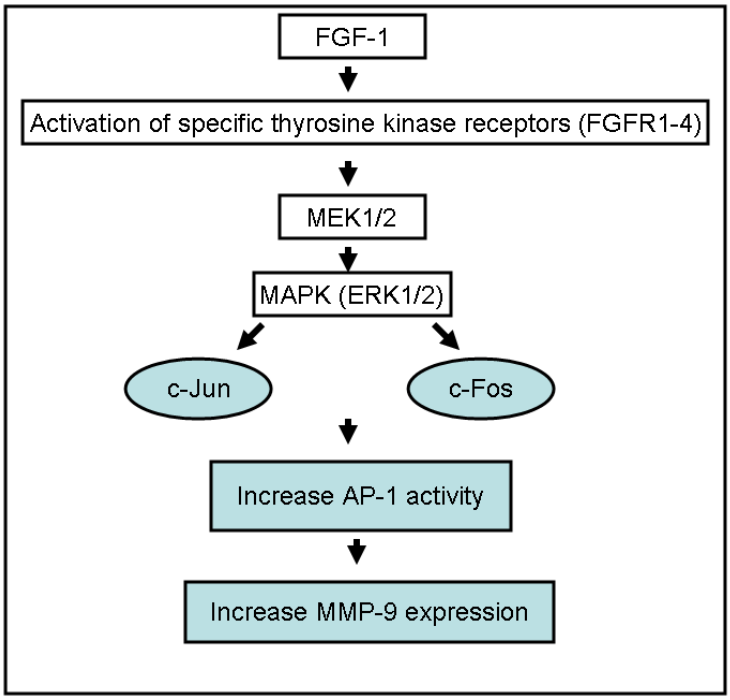

Figure 45. Involvement of MEK1/2-ERK signaling in FGF-1-induced expression of MMP-9 in ENU1564 cells.

These findings support the idea that FGF-1 can act as a paracrine and autocrine factor and plays an important role in the regulation of MMP-9 expression in mammary adenocarcinoma cells. We reason that secreted FGF-1 could rapidly bind to cancer cells due to its paracrine/autocrine function and promote metastasis. This study complements other studies regarding the mechanisms underlying dysregulated MMP-9 expression in breast cancer cells. A clearer understanding of the mechanism by which FGF-1-signaling contributes to tumor progression and/or metastasis will facilitate the development of cancer therapies to target this signaling pathway.

CHAPTER V

SUMMARY AND CONCLUSIONS

This dissertation provides a comprehensive analysis of the role of hypoxia and hypoxia-induced factors in the development of breast cancer invasion and metastasis by using a highly malignant tumor cell line ENU1564, originally developed in our laboratory.

Chapter I provides a comprehensive review of hypoxia and hypoxia-induced factors, FGF-1 and MMP biology and their role in cancer development and invasion. Also in this chapter we present the specific objectives of our study and the hypothesis.

Chapters II and III *(in vivo* studies only) contain the first manuscript generated from this work which was published in the *International Journal of Oncology* in January 2007. Chapter II describes a novel spectroscopic photoacoustic tomography technology (SPAT) for the detection of tumor hypoxia, an important parameter of tumor pathogenesis, by measuring the level of brain blood oxygenation. We showed that SPAT would be an important tool for noninvasive detection of intracranial tumors. Moreover, SPAT would be useful for monitoring the development of hypoxia, which may have an important role in determining the timing and type of therapy. Validation of this technology was supported by our molecular biology findings aimed to elucidate the etiopathogenesis of SPAT detected hypoxia and angiogenesis. In Chapter III (*in vivo* studies) we evaluated the expression of HIF-1 α, VEGF-A, VEGFR2 and MMP-9

protein and mRNA levels in the hypoxic brain tumor foci identify by SPAT. Chapters II and III provide an integrated approach to define the oxygen status (hypoxia) of tumors by using SPAT and to correlate hypoxia with the invasion process of a breast cancer cell line, ENU1564, inoculated intracranially in a rat model.

Chapter III (*in vitro* studies) describes the expression of HIF-1 α, VEGF-A, VEGFR2 and MMP-9 protein and mRNA in ENU1564 cells grown under normoxic and hypoxic conditions and is aimed to validate the role of hypoxia in the regulation of these proteins and their role in cancer invasion and metastasis. Additionally we explored the pathways involved in the regulation of these proteins in hypoxic ENU1564 cells by using specific inhibitors for each pathway.

Chapter IV contains the second manuscript generated from this work which was published in the *Molecular Carcinogenesis* journal in November 2007. This chapter describes the mechanism by which FGF-1, a factor found to be up-regulated in hypoxia, regulates MMP-9 expression in ENU1564 cancer cells. We showed for the first time that FGF-1-upregulated MMP-9 expression in ENU1564 cell lines by increasing the activities of NF-kB and AP-1 and involve activation of a dual signaling pathway PI3K/Akt and MEK1/2-ERK [132].

In conclusion, this work provides a comprehensive analysis of the role of hypoxia and hypoxia-induced factors in breast cancer brain metastatic disease. We also described a novel spectroscopic photoacoustic tomography technology (SPAT) for the detection of tumor hypoxia. Such information can be used not only as a prognostic tool for tumor invasion but also as the basis for developing and evaluating patient-specific

treatment modalities for many types of cancer including breast cancer. A clear understanding of the mechanism by which these factors contributes to tumor progression and /or metastasis will facilitate the development of cancer therapies to target these signaling pathways.

REFERENCES

1. Nabeshima K, Inoue T, Shimao Y, Sameshima T. Matrix metalloproteinases in tumor invassion: Role for cell migration. Pathol Int 2002; 52: 255-264.

2. Lafleur MA, Tester AM, Thompson EW. Selective involvement of TIMP-2 in the second activational cleavage of pro-MMP-2: refinement of the pro-MMP-2 activation mechanism. FEBS Lett 2003; 553(3): 457-63.

3. Vaupel P, Kallinowski F, Okunieff P. Blood flow, oxygen and nutrient supply, and metabolic microenvironment of human tumors: a review. Cancer Res 1989; 49: 644-6465.

4. Tong Q, Zheng L, Lin L et al. VEGF is upregulated by hypoxia-induced mitogenic factor via the PI3K-Akt-NF-kB signaling pathway. Respiratory Res 2006; 2:07-37.

5. Vaupel P. The role of hypoxia-induced factors in tumor progression. The Oncologist 2004; 9:10-17.

6. Kunz M, Saleh MI. Molecular response to hypoxia in tumor cells. Mol Cancer 2003; 2:23.

7. Hockel M, Vaupel P. Tumor hypoxia: definition and current clinical, biologic, and molecular ascpects. J Natl Cancer Inst 2001; 93: 266-276.

8. Helmlinger G, Yuan F, Dellian M, Jain RK. Interstitial pH and pO2 gradients in solid tumors *in vivo*: high resolution measurements reveal a lack of correlation. Nat Med 1997; 3:177-182.

9. Tester AM, Waltham M, Oh SJ et al. Pro-matrix metalloproteinase-2 transfection increases orthotopic primary growth and experimental metastasis of MDA-MB-231 human breast cancer cells in nude mice. Cancer Res 2004 Jan 15; 64(2):652-8.

10. Yoneda T. Cellular and molecular basis of preferential metastasis of breast cancer to bone. J Orthop Sci. 2000; 5(1):75-81.

11. Ohshiba T, Miyaura C, Inada M, Ito A. Role of RANKL-induced osteoclast formation and MMP-dependent matrix degradation in bone destruction by breast cancer metastasis. Br J Cancer. 2003;88(8):1318-26.

12. Mendes O, Kim HT, Stoica G. Expression of MMP-2, MMP-9 and MMP-3 in breast cancer brain metastasis in a rat model. Clin Exp Metastasis 2005; 22:237-246.

13. Hall DG, Stoica G. Characterization of brain and bone-metastazing clones selected from an ethylnitrosourea-induced rat mammary carcinoma. Clin Exp Metastasis 1994; 12:283-95.

14. Stoica G, Koestner A, Capen CC. Characterization of N-ethyl-N-nitrosourea-induced mammary tumors in the rat. Am J Pathol. 1983;110(2):161-9.

15. Singer B. Sites in nucleic acids reacting with alkylating agents of differing carcinogenicity of mutagenicity. J Toxicol Environ Health. 1977; 2(6):1279-95.

16. Singer B, Kusmierek JT. Alkylation of ribose in RNA reacted with ethylnitrosourea at neutrality. Biochemistry 1976; 15(23):5052-7.

17. Singer B. All oxygens in nucleic acids react with carcinogenic ethylating agents. Nature. 1976; 264(5584):333-9.

18. Druckrey H, Ivankovic S, Preussmann R. Teratogenic and carcinogenic effects in the offspring after single injection of ethylnitrosourea to pregnant rats. Nature 1966; 210(43):1378-9.

19. Kleihues P, Margison GP. Carcinogenicity of N-methyl-N-nitrosourea: possible role of excision repair of O6-methylguanine from DNA. J Natl Cancer Inst. 1974; 53(6):1839-41.

20. Singer B. The chemical effects of nucleic acid alkylation and their relation to mutagenesis and carcinogenesis. Prog Nucleic Acid Res Mol Biol. 1975; 15(1):219-84.

21. Flokman J. What is the evidence that tunors are angiogenesis dependent? J Natl Cnacer Inst 1990; 82:4-6.

22. Harris AL. Hypoxia a key regulator factor in tumor growth. Nature Rev Cancer. 2002; 2: 38-47.

23. Collisson EA, Suzuki H, Gambhir SS, Kolodney MS. Treatment of metastatic melanoma with an orally available inhibitor of Ras-Raf-MAPK cascade. Cancer Res 2003; 63: 5669-73.

24. Kunz F, Ibrahim SM. Molecular response to hypoxia in tumor cells. Mol Cancer. 2003.

25. Laderoute KR, Calaoagan JM, Brown CG et al. The response of c-Jun/AP-1 to chronic hypoxia is hypoxia-inducible factor 1 alpha dependent. Mol Cell Biol 2002; 2515- 2523.

26. Somerville RP, Oblander SA, Apte SS. Matrix metalloproteinases: old dogs with new tricks. Genome Biol 2003; 4(6):216.

27. Nabeshima K, Inoue T, Shimao Y, Sameshima T. Matrix metalloproteinases in tumor invasion: role for cell migration. Pathol Int. 2002;52(4):255-64.

28. Rudolph-Owen LA, Matrisian LM. Matrix metalloproteinases in remodeling of the normal and neoplastic mammary gland. J Mammary Gland Biol Neoplasia 1998; 3(2):177-89.

29. Scott KA, Holdsworth H, Balkwill FR, Dias S. Exploiting changes in the tumour microenvironment with sequential cytokine and matrix metalloprotease inhibitor treatment in a murine breast cancer model. Br J Cancer 2000; 83(11):1538-43.

30. Lee PP, Hwang JJ, Murphy G, Ip MM. Functional significance of MMP-9 in tumor necrosis factor-induced proliferation and branching morphogenesis of mammary epithelial cells. Endocrinology 2000;141(10):3764-73.

31. Dono R. Fibroblast growth factors as regulators of central nervous system development and function. Am J Physiol Regul Integr Comp Physiol. 2003; 284: 867-881.

32. Johnson DE, Willams LT. Structural and functional diversity in the FGF receptor multigene family. Adv Cancer Res 1993; 60: 1-41.

33. Klagsbrun M, Baird A. A dual receptor system is required for basic fibroblast growth factor activity. Cell 2000; 67:229-231.

34. Plontnikov A, Schlessinger J, Hubbard S, Mohammadi M. Structural basis of FGF receptor dimerization and activation. Cell 1999; 98: 641-650.

35. Dickson C, Spencer-Dene B, Dilon C, Fantl V. Tyrosine kinase signalling in breast cancer fibroblast growth factors and its receptors. Breast Cancer Res 2000; 2:191-196.

36. Powers CJ, Mc.Leskey SW, Wellstein A. Fibroblast growth factors, their receptors and signaling. Endocr. Relat. Cancer 2000; 7: 165-197.

37. Hashimoto M, Sagara Y, Langford D, et al. Fibroblast growth factor 1 regulated signaling via the glycogen synthase kinase-3 beta pathway. Biol Chem 2000; 277: 32985-32991.

38. Chandler LA, Sosnowski BA, Greenless L, et al. Prevalent expression of fibroblast growth factor (FGF) receptors and FGF2 in human tumor cell lines. Int. J. Cancer 1999; 81: 451-458.

39. Alessandrini A. The roles of map kinases in controlling cancer metastasis. In Cancer Metastasis-Related Genes. Volume 3. Edited by Welch D.R Boston: Kluwer Academic Publishers 2000; 35-51.

40. Aigner A, Renneberg H, Bojunga J, et al. Rybozyme-targeting of a secreted FGF-binding protein (FGF-BP) inhibits proliferation of prostate cancer cells *in vitro* and *in vivo*. Oncogene 2002; 21: 5733-5742.

41. Ahmed NU, Ueda M, Ito A, et al. Expression of fibroblast growth factor receptors in neuvus-cell naevus and mailgnant melanoma. Melanoma Res 1997;7: 299-305.

42. Ornitz DM, Itoh N. Fibroblast growth factors. Genome Biol 2001;12:3005-3009.

43. Mouta-Carreira C. The comparative release of FGF1 by hypoxia and temperature stress. Growth Factors 2001; 18: 277-285.

44. Shin JT. Serum starvation induces the extracellular appearance of FGF-1. Biochim. Biophys. Acta 1996; 1312: 27-38.

45. Mouta-Carreira C, Landriscina M, Bellum S, Prudovsky I, Maciag T. The comparative release of FGF1 by hypoxia and temperature stress. Growth Factors 2001; 18: 277-285.

46. Dewhirst MW, Klitzman B, Braun RD, et al. Review of methods used to study oxygen transport at the microcirculatory level. Int J Cancer 2000; 90: 237- 255.

47. Howe FA, Robinson SP, Griffiths JR. Modification of tumor perfusion and oxygenation monitored by gradient recalled echo MRI and 31P MRS. NMR Biomed 1999; 208-216.

48. Wilson D, Cerniglia G. Oxygenation of tumors as evaluated by phosphorescence imaging. Adv Exp Med Biol 1994; 345:539-547.

49. Helmlinger G, Yuan F, Dellian M, Jain RK. Interstitial pH and pO2 gradients in solid tumors in vivo: high-resolution measurements reveal a lack of correlation. Nat Med 1997 ;3: 177-182.

50. Dewhirst MW, Ong ET, Braun RD. Quantification of longitudinal tissue pO2 gradients in window chamber tumors: impact on tumor hypoxia. Br J Cancer 1999; 79: 1717-1722.

51. Mueller KW, Vaupel P, Manz R, Schmidseder R. Intracapillary oxyhemoglobin saturation of malignant tumors in humans. Int J Radiat Oncol 1991; 7:1397-1404.

52. Rasey JS, Koh WJ, Evans ML. Quantifying regional hypoxia in human tumors with positron emission tomography of [18F] fluoromisonidazole: a pretherapy study of 37 patients. Int J Radiat Oncol 1996; 36: 417-428.

53.Chapman JD, Engelhardt EL, Stobbe CC, Schneider RF, Hanks GE. Measuring hypoxia and predicting tumor radioresistance with nuclear medicine assays. Radiother Oncol 1998; 46: 229-237.

54**.** Evans S, Jenkins W, Joiner B, Lord E, Koch C. 2-Nitroimidazole (EF5) binding predicts radiation resistance in individual 9L s.c. tumors. Cancer Res 1996; 56: 405-411.

55. Ku G, Wang X, Xie X, Stoica G, Wang LV. Imaging of tumor angiogenesis in rat brains in vivo by photoacoustic tomography. Applied Optics 2005; 44:5.

56.Wang X, Pang Y, Ku G, Xie X, Stoica G, Wang LV. Non-invasive laser-induced photoacustic tomography for structural and functional imaging of the brain in vivo. Nature Biotech 2003; 21: 803-806.

57. Xu M, Xu Y, Wang LH. Time-domain reconstruction algorithms and numerical simulations for thermoacoustic tomography in various geometries IEEE Transactions on Biomedical Engineering 2003; 50:1086-1099.

58. Arai K, Lee S, Loo EH. Essential role for ERK mitogen-activated protein kinase in matrix metalloproteinase-9 regulation in rat cortical astrocytes. Glia 2003; 43:254-64.

59. Sierra A, Price J, Garcia RM et al. Astrocyte derived cytokines contribute to the metastatic brain specificity of breast cancer cells. Lab Invest 1997; 77:357-368.

60. Risau W. Mechanisms of angiogenesis. Nature 1997; 386: 671-674.

61. Evans SM, Judy KD, Dunphy I. Hypoxia is important in the biology and aggression of human glial brain tumors. Clin Cancer Res 2004; 10:8177- 8184.

62. Brizel DM, Scully SP, Harrelson JM. Tumor oxygenation predicts for the likelihood of distant metastases in human soft tissue sarcoma. Cancer Res 1996; 56:941-3.

63. Carmeliet P, Jain RK: Angiogenesis in cancer and other diseases. Nature 2000; 407(6801):249-57.

64. Wang H, Keiser JA. Vascular endothelial growth factor upregulates the expression of matrix metalloproteinases in vascular smooth muscle cells: role of flt-1. Circ Res 1998; 83: 832-840.

65. Vaupel P, Hockel M. Tumor oxygenation and its relevance to tumor physiology and treatment. Adv Exp Med Boil 2003; 510:45-49.

66. Gerber HP, Condorelli F, Park J, Ferrara N. Differential transcriptional regulation of two vascular endothelial growth factor receptor genes. Flt-1, but not Flk-1/KDR, is up-regulated by hypoxia. J. Biol. Chem 2002; 272: 23659-23667.

67. Waltenberger J, Mayr U, Pentz S, Hombach V. Functional upregulation of the vascular endothelial growth factor receptor KDR by hypoxia. Circulation 1996; 94: 1647-1654.

68. Tang N, Wang L, Esko J et al. Loss of HIF-1α in endothelial cells disrupts a hypoxia-driven VEGF autocrine loop necessary for tumorigenesis. Cancer Cell 2004;6.

69. Kunz M, Saleh MI. Molecular response to hypoxia in tumor cells. Mol Cancer 2003; 2:23.

70. Semenza GL. HIF-1 and tumor progression: pathophysiology and therapeutics. Trends Mol Med 2002; 8:S62-S67.

71. Semenza GL, Jiang BH, Leung SW. Hypoxia response elements in the aldolase A, enolase 1, and lactate dehydrogenase A gene promoters contain essential binding sites for hypoxia- inducible factor 1. J Biol Chem 1996; 271:32529-32537.

72. Kaur B, Khwaja FW, Severson EA et al. Hypoxia and hypoxia-inducible-factor pathway in glioma growth and angiogenesis. Neuro-Oncology 2005; 7:134-153.

73. Zhong H, De Marzo AM, Laughner E. Overexpression of hypoxia-inducible factor 1alpha in common human cancers and their metastases. Cancer Res 1999; 59:5830–5.

74. Talks KL, Turley H, Gatter KC, Maxwell C. The expression and distribution of the hypoxia-inducible factors HIF-1alpha and HIF- 2alpha in normal human tissues, cancers, and tumor-associated macrophages. Am J Pathol 2000; 157:411–20.

75. Cairns RA, Kalliomaki T, Hill RP. Acute (cyclic) hypoxia enhances spontaneous metastasis of KHT murine tumors. Cancer Res 2001; 61: 8903.

76. Rofstad EK. Microenvironment-induced cancer metastasis. Int J Radiat Biol 2000; 76:589–605.

77. Leppa S, Saarto T, Vehmanen L, Blomqvist C, Elomaa I. A high serum matrix metalloproteinase-2 level is associated with an adverse prognosis in node-positive breast carcinoma. Clin Cancer Research 2004; 10: 1057-63.

78. Chang C, Werb Z. The many faces of metalloproteases: cell growth, invasion, angiogenesis and metastasis. Trends Cell Biol 2000; 3: 11-18.

79. Kato Y**,** Lambert AC, Colige AC. Acidic extracellular pH induces matrix metalloproteinase-9 expression in mouse metastatic melanoma cells through the phospholipase D-mitogen-activated protein kinase signaling. J Biol Chem 2005; 12: 109-123.

80. Ikeda E, Achen MG, Breier G, Risau W. Hypoxia-induced transcriptional activation and increased mRNA stability of vascular endothelial growth factor in C6 glioma cells. J Biol Chem 1995; 270: 19761-19766.

81. Xu L, Fukumura D, Jain RK: Acidic extracellular pH induces vascular endothelial Growth factor (VEGF) in human glioblastoma cells via ERK 1/2 MAPK signaling pathway. J Biol Chem 2001; 13:11368-11374.

82. Brizel DM, Scully SP, Harrelson JM. Tumor oxygenation predicts for the likelihood of distant metastases in human soft tissue sarcoma. Cancer Res 1996; 56:941-3.

83. Lee P, Hwang J, Murphy G, Margot M. Functional significance of MMP-9 in tumor necrosis factor-induced proliferation and branching morphogenesis of mammary epithelial cells. Endocrinology 2000; 141:3764-73.

84. Turcotte S, Desrosiers RR, Beliveau R. HIF-1α mRNA and protein upregulation involves Rho GTPase expression during hypoxia in renal cell carcinoma. J Cell Sci 2003; 15:2247-2260.

85. Heffelfinger SC, Yan M, Gear RB et al. Inhibition of VEGFR2 prevents DMBA-induced mammary tumor formation. Lab Invest 2004; 84:989-998.

86. Kietzmann T, Jungermann K, Golach A. Regulation of the hypoxia-dependent plasminogen activator inhibitor 1 expression by MAP kinases. Thromb Haemost 2003; 89: 666-673.

87. Arai K, Lee SR, Lo EH. Essential role of ERK mitogen-activated protein kinase in matrix metalloproteinase-9 regulation in rat cortical actrocytes. Glia 2004; 43 (3): 254-64.

88. Kondo S, Kubota S, Shimo T. Connective tissue growth factor increased by hypoxia may initiate angiogenesis in collaboration with matrix metalloproteinases. Carcinogenesis 2002; 23:769-776.

89. Semeza GL. Angiogenesis in ischemic and neoplastic disorder. Annu Rev Med 2003; 54: 17-28.

90. Yu AQ, Stamenkovic I. Localization of matrix metalloproteinase-9 to the cell surface provides a mechanism for CD44-mediated invasion. Gene Dev 1998; 13: 35-48.

91. Skobe M, Rockwell P, Goldstein N, Vosseler S, Fusenig NE. Halting angiogenesis suppresses carcinoma cell invasion. Nat Med 1997; 3:1222-1227.

92. Noda K, Ishida S, Shinoda H et al. Hypoxia induces the expression of membrane-Type 1 matrix metalloproteinase in Retinal Glial Cells. Invest Ophtal Vis Sci 2005; 46:3817-3824.

93. Leppa S, Saarto T, Vehmanen L, Blomqvist C, Elomaa I. A high serum matrix metalloproteinase-2 level is associated with an adverse prognosis in node-positive breast carcinoma. Clin Cancer Res 2004; 10:1057-63.

94. Rao JS, Steck PA, Mohanam S et al. Elevated levels of M(r) 92 000 type IV collagenase in human brain tumors. Cancer Res 1993; 53:2208-2211.

95. Sato H, Seiki M. Regulatory mechanism of 92 KDa type IV collagenase gene expression which is associated invasiveness of tumor cells. Oncogene 1993; 8:39-405.

96. Yao J, Xiong S, Klos K, Nguyen N, Grijalva R, Li P. Multiple signaling pathways involved in activation of matrix metalloproteinase-9 (MMP-9) by heregulin-beta 1 in human breast cancer cells. Oncogene 2001; 20:8066-8074.

97. Amin R, Senga T, Lin OM, Thant AA, Hamaguchi M. Secretion of matrix metalloproteinase-9 by the proinflamatory cytokine, IL-1 beta: a role for a dual signaling pathways, Akt and Erk. Genes Cells 2003; 8:515-523.

98. Klagsbrun M, Baird A. A dual receptor system is required for basic fibroblast growth factor activity. Cell 2000; 67:229-231.

99. Burgess WH, Maciag T. The heparin-binding (fibroblast) growth factor family of proteins. Annu Rev Biochem 1989; 58:575-606.

100. Shin JT, Opalenik SR, Wehby JN et al. Serum starvation induces the extracellular appearance of FGF-1. Biochim Biophys Acta 1996; 1312:27-38.

101. Steele IA, Edmonson RG, Bulmer JN et al. Induction of FGF receptor 2-IIIb expression and response to its ligands in epithelial ovarian cancer. Oncogene 2001; 20:878-5887.

102. Partridge C, Hawker R, Forough R. Overexpression of a secretory form of FGF-1 promotes MMP-1 mediated endothelial cell migration. J Cell Biochem 2000; 78:487-499.

103. Liu JF, Crepin M, Liu JM, Barritault D, Ledoux D. FGF-2 and TPA induce matrix metalloproteinase-9 secretion in MCF-7 cells through PKC activation of the Ras/ERK pathway. Biochem Biophys Res Commun 2000; 293:1174-1182.

104. Eberhardt W, Huwiler A, Beck KF, Walpen S, Pfeilschifter. Amplification of IL-1β-induced matrix metalloproteinase-9 expression by superoxide in rat glomerular mesangial cells is mediated by increased activities of NF-κB and activating protein-1 and involves activation of the mitogen-activated protein kinase pathways. J Immunol 2000; 165:5788-5797.

105. Ding M, Shi X, Dong Z et al. Freshly fractured crystalline silica induces activator-protein-1 activation through ERKs and p38 MAPK. J Biol Chem 1999; 274:30611-30616.

106. Gupta A, Rosenberg SF, Bowden GT. Increased ROS levels contribute to elevated transcription factor and MAP kinase activities in malignantly progressed mouse keratinocyte cell lines. Carcinogenesis 1999; 20:2063-2073.

107. Frigo DE, Tang Y, Beckman SB et al. Mechanism of AP-1-mediated gene expression by select organochlorines through the p38 MAPK pathway. Carcinogenesis 2004; 25:249-261.

108. Shaulian E, Karin M. AP-1 in cell proliferation and survival. Oncogene 2001; 20:2390-2400.

109.Yokoo T, Kitamura M. Dual regulation of IL-1β-mediated matrix metalloproteinase-9 expression in mesangial cells by NF-κB and AP-1. Am J Physiol 1996; 270:F123–F130.

110.Yamamoto Y, Gaynor RB. Therapeutic potential of inhibition of the NF-κB pathway in the treatment of inflammation and cancer. J Clin Invest 2001; 107:135-142.

111. Byrd VM, Wallard BD, Miller GG, Thomas JW. Fibroblast growth factor-1 (FGF-1) enhances IL-2 production and nuclear translocation of NF-κB in FGF receptor bearing Jurkat T cells. J Immunol 1999; 162:5853-5859.

112. Karin M. The regulation of AP-1 activity by mitogen-activated protein kinases. J Biol Chem 1995; 270:16483-16486.

113. Madrid LV, Mayo MW, Reuther JY, Baldwin AS Jr. Akt stimulates the transactivation potential of the RelA/p65 subunit of NF-kappa B through utilization of the Ikappa B kinase and activation of the mitogen-activated protein kinase p38. J Biol Chem 2001; 276:18934-18940.

114. Marshall CJ. Specificity of receptor tyrosine kinase signaling: transient versus sustained extracellular signal-regulated kinase activation. Cell 1995; 80:179-85.

115. Udayakumar TS, Stratton MS, Nagle RB, Bowden TG. Fibroblast growth factor-1 induced promatrilysin expression through the activation of extracellular-regulated kinases and STAT3. Neoplasia 2002; 4:60-67.

116. Lungu GF, Li LM, Xie X, Wang LV, Stoica G. *In vivo* imaging and characterization of hypoxia induced neovasculatization and tumor invasion. Int J Oncol 2007; 30:45-54.

117. Kim HT, Qiang W, Wong PKY, Stoica G. Enhanced proteolysis of IκBα and IκBβ proteins in astrocytes by moloney murine leukemia virus (MoMuLV)-ts1 infection: a potential mechanism of NF-κB activation. J Neuro Virol 2001; 7:466-475.

118.Tamura M, Yanagihara N, Tanaka H. Activation of DNA synthesis and AP- 1 by profilin, an actin-binding protein, via binding to a cell surface receptor in cultured rat mesangial cells. J Am Soc Nephrol 2000; 11:1620-1630.

119. Weylie B, Zhu J, Singh U, Ambrus S, Forough R. Phosphatidylinositide 3 –kinase is important in late-stage fibroblast growth factor-1 mediated angiogenesis in vivo. J Vasc Res 2006; 43:61-69.

120. Thomas KW, Monick MM, Staber MJ et al. Respiratory syncytial virus inhibits apoptosis and induces NF-κB activity through a phosphatidylinositol 3-Kinase-dependent pathway. J Biol Chem 2002; 277:492-501.

121.Tong Q, Zheng L, Lin L et al. VEGF is upregulated by hypoxia-induced mitogenic factor via the PI-3K/Akt- NF-κB signaling pathway. Resp Res 2006; 7:37.

122. Udayakumar TS, Nagle RB, Bowden TG. Fibroblast growth factor-1 transcriptionally induces membrane type-1 matrix metalloproteinase expression in prostate carcinoma cell line. Prostate 2004; 58:66-75.

123. Samuel SK, Hurta RA, Kondaiah P. Autocrine induction of tumor protease production and invasion by a metallothionein-regulated TGF-beta 1. EMBO J 1992; 11:1599-1605.

124. Kondapaka SB, Fridman R, Reddy KB. Epidermal growth factor and amphiregulin up-regulate matrix metalloproteinase-9 (MMP-9) in human breast cancer cells. Int J Cancer 1997; 70:722-726.

125. Esteve PO, Chicoine E, Robledo O et al. Protein kinase C-ς regulates transcription of the matrix metalloproteinase-9 gene induced by IL-1 and TNF-α in glioma cells via NF-κB. J Biol Chem 2002; 277:35150-35155.

126. Penault-Llorca F, Bertucci F, Adelaide J et al. Expression of FGFs and FGF receptor genes in human breast cancer. Int J Cancer 1995; 61:170-176.

127.Yoshimura N, Sano H, Hashiramoto A et al. The expression and localization of fibroblast growth factor-1 (FGF-1) and FGF receptor-1 (FGFR-1) in human breast cancer. Clin Immunol Immunopath 1998; 89:28-34.

128. Kingenberg O, Wiedocha A, Citore L, Olsnes S. Requirement of phosphatidylinositol 3-kinase activity for translocation of exogenous aFGF to the cytosol and nucleus. J Biol Chem 2000; 275:11972-11980.

129. Suyama K, Shapiro M, Guttman M, Hazan RB. A signaling pathway leading metastasis is controlled by N-cadherin and the FGF receptor. Cancer Cell 2002; 2:301-314.

130. Janet T, Labourdette G, Sensenbrenner M, Pettmann B. Mitogenic growth factors regulate differentially early gene mRNA expression: a study on two clones of 3T3 fibroblasts. Exp Cell Res 1992; 198:305-314.

131. Mohan R, Sivak J, Ashton P, Russo LA, Pham BQ, Kasahara N. Curcuminoids inhibit the angiogenic response stimulated by fibroblast growth factor-2, including expression of matrix metalloproteinase gelatinase B. J Biol Chem 2000; 275:10405-10412.

132. Lungu G, Covaleda L, Mendes O, Stoica HM, Stoica G. FGF-1-induced matrix metalloproteinase-9 expression in breast cancer cells is mediated by increased activities of NF-κB and activating protein-1. Molecular Carcinogenesis, In Press 2008.

VITA

Name:	Gina Florentina Lungu
Permanent address:	Texas A&M University, College of Veterinary Medicine, College Station, TX, 77843-4467
Email address:	gina_lungu@yahoo.com
Education:	B.S., Biochemistry, University of Bucharest, 1999
	M.S., Biology, Texas Woman's University, 2004
	Ph.D., Veterinary Microbiology, Texas A&M University, 2008